

Regulation of proteasome granule formation by proteasome shuttle factors

by

Gabrielle Rae Vontz

B.S., Kansas State University, 2018

A THESIS

submitted in partial fulfillment of the requirements for the degree

MASTER OF SCIENCE

Division of Biology  
College of Arts and Sciences

KANSAS STATE UNIVERSITY  
Manhattan, Kansas

2019

Approved by:

Major Professor  
Dr. Jeroen Roelofs

# Copyright

© Gabrielle Vontz 2019.

## Abstract

Protein degradation is crucial for many cellular processes including cell cycle regulation, metabolism, and proteostasis. Proteasomes, essential complexes within cells, degrade short-lived and aberrant proteins that are marked for degradation by ubiquitin chains. Although the proteasome houses three intrinsic ubiquitin receptors, other factors, known as shuttle factors, serve as extrinsic ubiquitin receptors that bind ubiquitinated substrates and deliver them to the proteasome for degradation. In yeast, three shuttle factors exist: Rad23, Dsk2, and Ddi1. These factors play a role in a variety of cellular processes including cell cycle regulation, spindle pole body duplication, and DNA damage response. Additionally, a recent study showed ~90% of substrates are transported to proteasomes by Rad23 or Dsk2 indicating shuttle factors are important contributors to ubiquitin-proteasome system dynamics. While generally considered substrate transporters, it is unknown whether shuttle factors influence proteasome localization. In proliferating cells, proteasomes are largely nuclear; however, in response to certain starvation conditions, proteasomes exit the nucleus and are either degraded in the vacuole through an autophagy pathway (proteaphagy) or sequestered into cytoplasmic granules termed proteasome storage granules (PSGs). Under nitrogen starvation, amino acids become limiting and can be supplemented by the degradation of proteasomes. However, the biological advantage of proteasome sequestration into granules in response to carbon starvation is still unknown. In the mammalian system, shuttle factor homologs are involved in autophagy pathways and form liquid droplets reminiscent of PSGs. Here, in yeast, we test for shuttle factor involvement in proteaphagy and PSG formation using fluorescence microscopy. We show shuttle factors are not important for proteaphagy induced by either nitrogen starvation or proteasome inhibition. However, our data reveal that Rad23 and Dsk2 are important for proteasome localization to granules under certain conditions. Specifically, when carbon is gradually depleted upon cell proliferation or ATP production is blocked by sodium azide treatment, the deletion of *RAD23* or *DSK2* reduces the efficiency of proteasome granule formation. Under these conditions, deletion of both proteins almost completely prevents granules. Interestingly, PSGs induced by abrupt carbon starvation do not depend on Rad23 or Dsk2. This qualitative difference between these granules is corroborated by our observation that active protein translation is required for granule formation under gradual carbon starvation or sodium azide treatment, but not essential for PSGs induced by abrupt

starvation. Finally, we show Ddi1, in direct opposition to Rad23 and Dsk2, prevents premature formation of proteasome granules. Cells deleted for *DDI1* exhibit granules even in the absence of inducing conditions. In sum, we describe a role for Rad23 and Dsk2 in proteasome localization to granules under certain conditions and distinguish Ddi1 as a proteasome granule inhibitor.

## Table of Contents

List of Figures.....	vii
List of Tables.....	ix
Chapter 1 - Introduction.....	1
Two major proteolytic pathways in yeast: autophagy and ubiquitin proteasome system.....	1
Proteasome Structure .....	2
Proteasome Localization .....	3
Proteasome assembly and nuclear import .....	5
Nuclear export (and post-translational modifications).....	7
Proteasome autophagy.....	8
Proteasome storage granules.....	9
Other granule structures .....	11
Proteasome shuttle factors.....	12
Shuttle factor structure and function.....	13
UBA and UBL domains .....	13
Shuttle factor models.....	17
Specific substrates .....	18
Shuttle factors in cellular processes .....	19
Spindle pole body duplication and cell cycle control .....	19
Nucleotide excision repair (NER).....	20
Shuttle factor grouping.....	21
Mammalian homologs.....	22
Rad23 homologs: hHR23A and hHR23B .....	22
Dsk2 homologs: ubiquilins .....	23
Ddi1 homologs: Ddi1 and Ddi2.....	24
Aim of the thesis.....	25
Chapter 2 - Methods and Results.....	27
Introduction .....	27
Materials and Methods.....	29
Yeast strains .....	29

Fluorescence microscopy.....	30
Growth conditions .....	31
Drug treatments.....	31
Canavanine phenotype screen.....	32
Cell lysis & immunoblotting analysis .....	32
Results .....	34
Shuttle factors are not required for proteaphagy.....	34
Rad23 and Dsk2 are required for proteasome granule formation under certain conditions..	36
Different proteasome granules form based on inducing conditions .....	46
Rad23 and Dsk2, but not Ddi1, localize to proteasome granules .....	48
Rad23 and Dsk2 UBL domains alone are not sufficient for wildtype proteasome granule formation .....	54
Chapter 3 - Discussion .....	63
Results Summary .....	63
Potential Models .....	65
Delivery model.....	65
Future experiments.....	66
Degradation signal model.....	67
Future experiments.....	68
Ubiquitin pool model.....	69
Future experiments.....	70
Ddi1: a nonconical shuttle factor .....	72
References .....	76

## List of Figures

Figure 1-1. Proteasome structure.....	3
Figure 1-2. Proteasome targeting events.....	5
Figure 1-3. Yeast shuttle factor domains.....	13
Figure 1-4. Intramolecular and Intermolecular interactions of shuttle factor UBL and UBA domains.....	17
Figure 1-5. Comparison of yeast and mammalian shuttle factor homologs.....	25
Figure 2-1. Generation of truncated shuttle factors with fluorescent tags.....	30
Figure 2-2. Shuttle factor deletions do not affect known proteaphagy pathways.....	36
Figure 2-3. Rad23 and Dsk2 are important for the formation of proteasome granules in rich media.....	38
Figure 2-4. Ubiquitin level and cell cycle arrest do not correlate with defects in PSG formation in shuttle factor mutants.....	39
Figure 2-5. Rad23 and Dsk2 are important for efficient targeting of proteasomes to granules in response to azide exposure.....	40
Figure 2-6. Rad23 and Dsk2 are nonessential for proteasome granules that form upon abrupt glucose starvation.....	41
Figure 2-7. Deletion of both <i>RAD23</i> and <i>DSK2</i> almost completely abrogates proteasome localization to granules under certain conditions.....	42
Figure 2-8. Rad23 and Dsk2 have partially redundant functions in proteasome granule formation under gradual glucose depletion.....	44
Figure 2-9. Deletion of <i>DDI1</i> does not rescue proteasome granule formation in <i>RAD23</i> $\Delta$ <i>DSK2</i> $\Delta$ cells.....	45
Figure 2-10. Cycloheximide sensitivity distinguishes between proteasome granules that form under different conditions.....	47
Figure 2-11. Characterization of proteasome granules induced by different conditions based on disassembly.....	48
Figure 2-12. Rad23 and Dsk2 co-localize with proteasome granules.....	50
Figure 2-13. C-terminal mCherry tags on shuttle factors have do not affect canavanine sensitivity.....	51

Figure 2-14. Rad23 and Dsk2 localize to proteasome granules while Ddi1 localizes to distinct granules.....	53
Figure 2-15. Ddil granules are distinct from proteasome granules. ....	54
Figure 2-16. Schematic representations of generated shuttle factor truncations.....	55
Figure 2-17. Shuttle factors UBL truncations exhibit similar defects in proteasome granule formation as deletions. ....	58
Figure 2-18. Relief of competitive proteasomal binding does not promote detectable co-localization between UBL truncations and proteasomes.....	60
Figure 2-19. $\Delta$ UBL shuttle factor truncations are not detectable under experimental parameters. ....	61
Figure 3-1. Delivery model. ....	67
Figure 3-2. Degradation signal model. ....	69
Figure 3-3. Ubiquitin pool model. ....	72
Figure 3-4. Deletion of <i>DDII</i> rescues defects in proteasome granule formation in <i>MPK1</i> $\Delta$ cells. ....	74

## List of Tables

Table 2-1. Strains used.....	33
Table 2-2. Truncation amino acid ranges.....	34

# Chapter 1 - Introduction

## **Two major proteolytic pathways in yeast: autophagy and ubiquitin proteasome system**

In cells, proteins have major structural, biochemical, and metabolic functions. Therefore, adjustments in protein levels allow cells to respond to changes in the environment. This process of proteostasis depends not only on the synthesis of proteins, but also on protein turnover. Two major protein degradation pathways are responsible for protein turnover: 1) ubiquitin-proteasome system (UPS) and 2) autophagy. Autophagy involves the formation of an autophagosome, a double membraned structure, around cargo that is delivered to the vacuole (in yeast and plants) or lysosome (in animals) for degradation<sup>1</sup>. Autophagy substrates range in size from individual proteins to large complexes and even entire organelles. While basal level autophagy has a homeostatic role, a dramatic upregulation of autophagy occurs in response to various stresses such as nutrient starvation. Unlike autophagy, the UPS is responsible for degradation of short-lived or aberrant proteins. Proteasomes are molecular proteases that directly recognize, unfold, and degrade individual polypeptides. In addition to proteostasis, proteasomal degradation is important for many cellular processes including cell cycle regulation, protein quality control, and stress responses<sup>2</sup>.

Coordinated protein turnover is important to prevent harmful protein accumulation as well as excessive degradation. Ubiquitination of substrates, as a prerequisite for both proteasomal and autophagic clearance, regulates which proteins are susceptible to proteolysis. Ubiquitin, a small regulatory protein, is covalently attached to lysine residues via an enzymatic cascade. E1 enzymes activate ubiquitin and transfer activated ubiquitin to E2 enzymes, also known as ubiquitin conjugating enzymes. Each E2 enzyme interacts with a subset of specific E3 enzymes that are responsible for ligating ubiquitin to a target substrate. E3 enzymes provide substrate specificity for the ubiquitination reaction, so unsurprisingly, they are the most variable and have a high degree of domain diversity. In yeast, around 11 E2 enzymes exist, while 60-100 putative E3 enzymes have been identified<sup>2</sup>. In humans, over 600 E3 enzymes are responsible for targeting specific proteins within the ubiquitination process<sup>3</sup>.

Ubiquitin, which has several lysine residues itself, is often ligated to other ubiquitin molecules forming polyubiquitin chains on substrates. The variety of ubiquitin chain lengths and linkages, which can be homogeneous or mixed, contributes to the complexity and functionality of ubiquitin

signaling. For example, ubiquitin K63 linkages are often important for endocytic trafficking while K48 linkages normally signal proteasomal degradation. However, exceptions to these generalizations exist and understanding the impact of different modifications remains an area of active research. Although distinct pathways, autophagy and the UPS both rely on ubiquitination as a signal for substrate degradation.

As the major pathways of protein degradation, autophagy and the UPS are vital for human health. Dysfunction within either system can cause accumulation of toxic protein aggregates and lead to diseases including amyloid lateral sclerosis (ALS), Huntington's, Parkinson's, and Alzheimer's<sup>4</sup>. Within these proteinopathies, genetic or spontaneous mutations cause proteins to misfold, accumulate, and aggregate. These large protein deposits can induce neuronal death through coordinated pathways like apoptosis or autophagy induced cell death (ACD) as well as unregulated mechanisms like necrosis<sup>5</sup>.

In addition to neurodegeneration, defects in protein degradation are also linked to cancer. For example, inefficient clearance of oncoproteins or excess degradation of tumor suppressor proteins can cause uncontrolled cell proliferation<sup>4</sup>. Consequently, the therapeutic potential of UPS components and autophagy machinery is an active area of translational research. In fact, Bortezomib is an FDA-approved proteasome inhibitor used to treat multiple myeloma. Specifically, these cancer cells synthesize a large amount of immunoglobulin, rely heavily on proteasomal protein quality control, and, thus, are extremely sensitive to drug induced proteasome inhibition<sup>4</sup>.

## **Proteasome Structure**

Proteasomes are large molecular complexes that recognize, unfold, and degrade ubiquitinated substrates. Proteasomal degradation requires substrate entry into a proteolytic barrel-shaped subcomplex, the core particle (CP). The CP consists of four heptameric rings—two inner rings of  $\beta$  subunits ( $\beta$ 1-7) and two outer rings of  $\alpha$  subunits ( $\alpha$ 1-7). The  $\alpha$  rings prevent nonspecific degradation of substrates by forming a “gate” that restricts access to the catalytic  $\beta$  subunits ( $\beta$ 1,  $\beta$ 2,  $\beta$ 5). Opening of this gate is facilitated by a second subcomplex, the regulatory particle (RP). Specifically, docking of the RP base (Rpt1-6, Rpn1, Rpn2, Rpn10, Rpn13) on an  $\alpha$  ring opens the CP gate. Rpn10, Rpn13, and Rpn1 all contain ubiquitin receptors that bind ubiquitinated substrates, while the Rpt base subunits are ATPases responsible for unfolding substrates in an ATP

dependent fashion. The remaining RP subunits compose the RP lid (Rpn3, Rpn5-9, Rpn11, Rpn12, Rpn15). The lid is responsible for substrate deubiquitination prior to degradation. Together, RP and CP form a proteolytically active protease: ubiquitinated substrates are deubiquitinated at the RP lid, unfolded at the RP base, and degraded within the CP. The process of substrate preparation at the RP and translocation through the CP involves a series of conformational changes in the proteasome. In recent years, numerous high resolution cryo-EM structures of the proteasome have provided structural insight into this process<sup>6-9</sup>. The symmetry of the CP allows RP subcomplexes to bind on each face forming RP-CP-RP complexes, or 26S proteasomes (Figure 1.1).

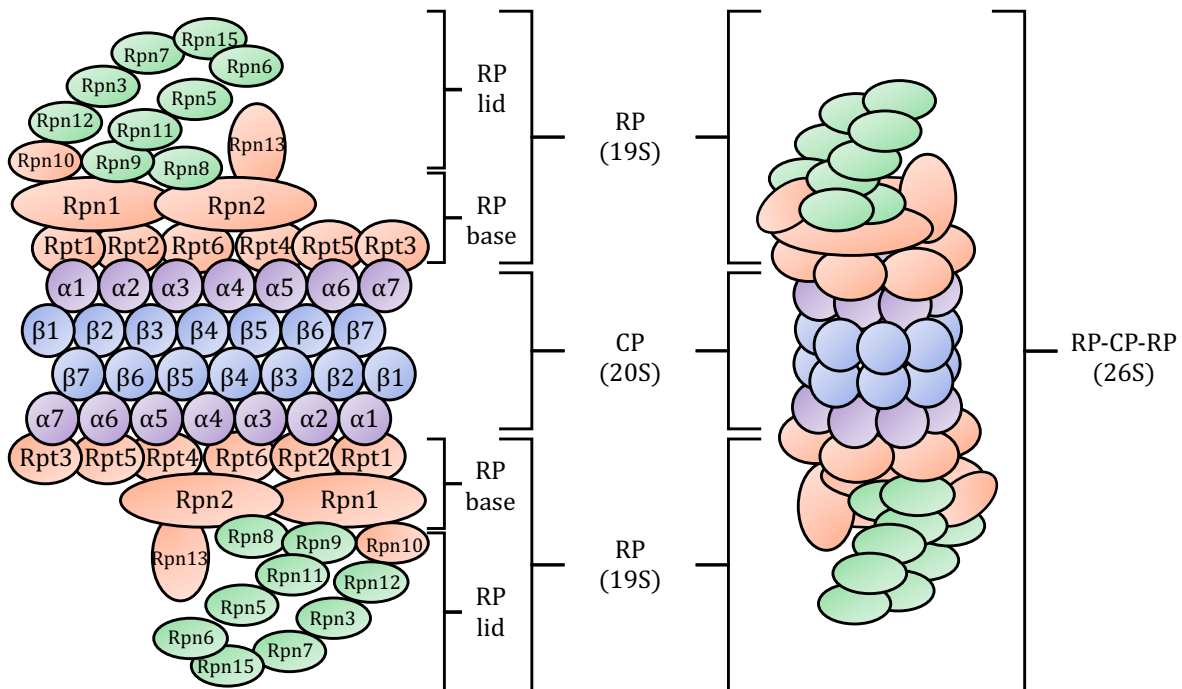


**Figure 1-1. Proteasome structure.**

*Proteolytically active proteasomes are made up of two subcomplexes: a core particle (CP) and one or two regulatory particles (RPs). The CP consists of four heptameric rings: two inner rings of  $\beta$  subunits and two outer rings of  $\alpha$  subunits. Three of the seven  $\beta$  subunits contain active sites responsible for peptide cleavage. Substrate entry into the CP requires bound RP at an outer  $\alpha$ -ring surface. RP is divided into two structures: RP base (Rpt1-6, Rpn1, Rpn2, Rpn10, Rpn13) and RP lid (Rpn3, Rpn5-9, Rpn11, Rpn12, Rpn15). Together, RP base and lid recognize, deubiquitinate, and unfold substrates in an ATP-dependent process. CPs bound by RP at both faces form canonical 26S proteasomes.*

## Proteasome Localization

Proteasomes are abundant complexes that localize to a variety of cellular locations: freely in the cytosol, associated with certain membrane structures including the ER, as well as in the

nucleus<sup>10,11</sup>. In logarithmically growing yeast cells, a majority of proteasomes are nuclear<sup>12</sup>. Similarly, in proliferating mammalian cells, an abundance of nuclear proteasomes has been reported<sup>13</sup>. Nuclear localization might not be surprising considering many proteasomal substrates such as transcription factors and cyclins reside in the nucleus<sup>14</sup>. However, proteasome localization is not static, and, under certain conditions, proteasomes exit the nucleus and localize to granules in the cytoplasm. Proteasome granules that form specifically upon carbon source depletion or during quiescence are defined as proteasome storage granules (PSGs)<sup>15,16</sup>. Previous research has characterized PSGs as reversible membrane-less protein droplets: upon carbon replenishment, they quickly disassemble and proteasomes return to the nucleus<sup>15</sup>. PSG formation involves nuclear-to-cytoplasmic targeting of proteasomes; in other words, proteasomes undergo nuclear export.

As opposed to carbon starvation, nitrogen starvation in yeast targets proteasomes to the vacuole for degradation<sup>17</sup>. Similar to vacuolar degradation of other large complexes, proteasome degradation requires autophagy machinery. However, some factors required for proteasome degradation are nonessential for general autophagy<sup>18–20</sup>. Thus, proteasome autophagy, or proteaphagy, is considered a distinct and specific autophagy pathway.

Proteasome localization events, under different conditions, can be distinguished into four processes:

1. Proteasome assembly and nuclear import
2. Nuclear export
3. Proteaphagy
4. PSG formation and disassembly

In this study, we aim to model a pathway for proteasome targeting to PSGs under certain conditions. Here, to provide context, we summarize what is currently known about proteasome localization and targeting events (Figure 1.2).

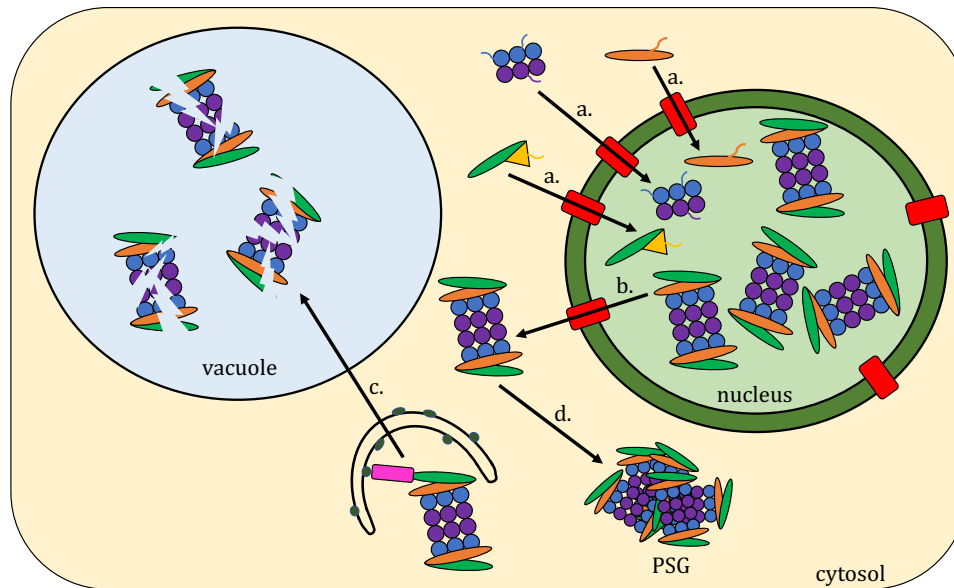


**Figure 1-2. Proteasome targeting events.**

*Proteasomes are found in various cellular compartments, and proteasome localization changes in response to physiological conditions. (A) Proteasomes are imported into the nucleus as immature complexes via canonical NLS signaling (nuclear pore complexes shown in red, Sts1 protein shown in yellow). (B) Proteasomes exit the nucleus prior to degradation (in C) or PSG formation (in D)), however, the mechanism of nuclear export of proteasomes is largely unknown. Proteasomes contain many post-translational modification sites which may contribute to the nuclear export of either 26S proteasomes or individual proteasome subcomplexes. (C) Proteasomes are degraded upon nitrogen starvation or proteasome inhibitor treatment through a specific autophagy pathway that involves proteaphagy adaptor proteins (adaptor proteins shown in pink). (D) Proteasomes are sequestered into PSGs under certain conditions like glucose starvation; the mechanism of PSG formation is largely unknown but seems to require acetylation as it depends on the N-terminal acetyltransferase NatB.*

### **Proteasome assembly and nuclear import**

Proteins synthesized in the cytosol enter the nucleus through nuclear pore complexes (NPCs). NPCs are selective protein channels that penetrate the nuclear envelope; fusion of the inner and outer nuclear membrane creates a protein lined pore which allows nuclear-cytoplasmic exchange. Molecules and small proteins diffuse through NPCs, but larger complexes require active transport. In the canonical pathway, proteins targeted for active nuclear import contain a specific amino acid sequence known as an NLS (nuclear localization signal). Karyopherin  $\alpha\beta$  (spr1/Kap95 in yeast), an importin protein, recognizes NLSs and facilitates protein transport from the cytoplasm, through an NPC, and into the nucleus. Based on physical size and some experimental evidence, mature 26S proteasomes are capable of import through NPCs; however, a majority of studies agree that,

instead, proteasomes are transported into the nucleus as precursor complexes via canonical NLS signaling.

Proteasome assembly involves 1) translation of individual subunits, 2) chaperone-mediated assembly of precursor complexes, 3) nuclear import, and 4) activation. Assembly of the core particle subcomplex (CP or 20S) begins with assembly of immature half-CPs: specific chaperones guide  $\alpha$  ring formation, while a complete  $\alpha$  ring provides a foundation for  $\beta$  subunit binding<sup>21</sup>. Ump1, a CP-specific chaperone, binds intermediate complexes and recruits  $\beta$  subunits. Recruitment of  $\beta 7$  allows half-CP dimerization to form a full, immature CP<sup>22,23</sup>. Autocatalytic cleavage of propeptides on specific  $\beta$  subunits completes CP maturation and allows activator complexes to bind. Therefore, CP maturity can be monitored by 1) identifying bound chaperones, and 2) assessing propeptide cleavage.

Studies suggest nuclear import of CP intermediates occurs before maturation. Specifically, Ump1 localization in the nucleus indicates immature half-CPs are imported prior to dimerization<sup>24</sup>. Additionally, unprocessed  $\beta$  subunits co-immunoprecipitate with nuclear import machinery suggesting immature CPs are transported across the nuclear envelope. Finally, NPC mutations that compromise import cause cytoplasmic accumulation of CP subcomplexes as opposed to fully assembled CPs<sup>24</sup>. Therefore, the current model for CP nuclear import involves recognition of NLS sequences on half-CPs followed by dimerization and maturation within the nucleus. Many  $\alpha$  proteasome subunits contain NLS sequences, which are presumably functionally redundant in individual complexes.

Regulatory particle (RP or 19S) nuclear import is analogous to CP: immature subcomplexes are imported through NPCs by NLS-mediated transport. In short, RP base and lid are separately assembled in the cytosol, transported across the nuclear membrane, and bound together to form mature RP subcomplexes in nucleus. For the RP base, the NLS on Rpn2 is required for import; Rpn2 NLS deletion not only prevents nuclear import of RP base but also causes cell cycle arrest most likely due to impaired degradation of nuclear proteasomal substrates<sup>25</sup>. Interestingly, the RP lid subcomplex does not contain any putative NLS sequences. Instead, nuclear import of RP lid requires Rpn11 interaction with NLS harboring protein, Sts1<sup>26</sup>. Deletion of the NLS of Sts1 not only impacts RP lid localization but causes an accumulation of assembled 26S proteasomes in the cytoplasm. Therefore, Sts1 may have an uncharacterized role in nuclear import of other proteasome subcomplexes or proteasome associated proteins<sup>26</sup>.

In summary, nuclear transport of proteasomes relies on NLS targeting of immature proteasome complexes. Specifically, half-CPs, RP base, and RP lid are assembled separately in the cytosol and imported into the nucleus prior to maturation and 26S assembly.

### **Nuclear export (and post-translational modifications)**

The specific mechanism of proteasome nuclear export is unknown. However, post-translational modifications including acetylation and N-myristoylation influence proteasome distribution between the cytoplasm, nucleus, and nuclear envelope.

In yeast, three complexes are largely responsible for N-terminal acetylation: NatA, NatB, and NatC. Each acetyltransferase recognizes and modifies specific N-terminal sequences. Deletions of NatB or NatC subunits both influence proteasome localization. Specifically, deletion of critical subunits from each acetyltransferase causes nuclear enrichment of proteasomes that is not attributed to biogenesis<sup>27</sup>. This indicates NatB and NatC activity are both required for efficient nuclear export of proteasomes. However, only a NatB deletion displays a defect in PSG formation upon starvation; NatC mutants form granules comparable to wildtype<sup>27</sup>. The different acetylation requirements of nuclear export and PSG formation suggest that these two processes can be uncoupled. Specific acetylation sites that control proteasome targeting have yet to be identified. Therefore, whether or not acetylation of a single subunit or a combination of subunits regulates nuclear-cytoplasmic distribution remains unknown.

As cells are starved of a carbon source, proteasomes exit the nucleus and accumulate at the nuclear periphery prior to proteasome granule formation. Studies examining interactors of NPCs found nuclear periphery localization of proteasomes may be due to direct interactions with proteins in the basket of the NPC, specifically, Esc1<sup>28</sup>. The NPC basket consists of filamentous proteins that protrude from the NPC into the nucleus. Currently, the function of the NPC basket is accepted as mostly structural: basket proteins prevent chromatin blockage at the NPC opening, provide a docking site for messenger ribonucleoprotein complexes prior to export, and contribute to equal NPC distribution throughout the nuclear envelope<sup>29</sup>. The nature of proteasome interaction with the NPC basket—whether it is functional (proteasomes are involved in NE-located processes like chromatin remodeling) or is a step in nuclear export of proteasomes—is unclear.

In addition to acetylation and NPC interaction, N-myristoylation also influences proteasome localization. N-myristoylation is a post-translational modification that mediates interactions with membrane lipids or hydrophobic proteins. Rpt2, a subunit of the RP base, contains the only N-myristoylation site on the 26S proteasome. Mutation or deletion of this site does not affect proteasome assembly, activity, or nuclear import, but does cause increased cytoplasmic distribution of proteasomes<sup>30</sup>. In a proposed model, N-myristoylation of Rpt2 mediates nuclear retention of proteasomes via anchoring to the nuclear envelope. Therefore, proteasome localization at the nuclear periphery may be due to 1) interactions with NPC basket proteins, 2) N-myristoylation anchoring, or 3) a combination of both.

Although post-translational modifications influence proteasome localization, the precise molecular mechanism as well as nutrient-driven regulation of nuclear-to-cytoplasm targeting of proteasomes is not well characterized. In addition to acetylation and N-myristoylation, many post-translational modifications on the proteasome have been identified, but only a few are functionally understood and none are known to impact localization<sup>31</sup>. Phosphorylation of specific subunits impacts complex stability, protease activity, as well as ATPase activity. Ubiquitination of specific proteasome subunits indirectly modulates proteasome activity by blocking substrate binding. Other post translational modification sites—including methylation, SUMOylation, and succinylation—have been identified, but functionally, remain ambiguous<sup>31</sup>. As such, nuclear export may or may not be regulated by additional post-translational modifications.

It is important to note that the UPS is regulated by changing the ratio of different proteasome populations. As cells enter stationary phase, proteasome configurations shift from 26S into dissociated RP and CP subcomplexes<sup>16,32</sup>. This shift aligns with the re-localization of proteasomes from the nucleus to cytoplasmic PSGs. However, it is unknown whether or not this dissociation precludes nuclear export. Dissociation may be a limiting step during nuclear export, a result of unbound ATPase subunits, or a characteristic of PSG architecture.

### **Proteasome autophagy**

Autophagy pathways have a wide range of specificity; bulk autophagy involves the formation of autophagosomes around non-specific cytosolic material, while other autophagic pathways target specific complexes or entire organelles. Although all autophagic degradation requires core

machinery, selective autophagy requires substrate-specific factors. Cargo adaptors bind specific ubiquitinated substrates and the autophagosome membrane to facilitate selective delivery to the lysosome/vacuole. Selective autophagy allows coordinated degradation of complexes and organelles in response to different conditions.

Many starvation conditions induce an upregulation of protein degradation. Although the UPS is a major contributor to proteostasis, as a large molecular complex, the proteasome itself is a suitable target for degradation. Nitrogen starvation and proteasome-inhibitor inactivation both induce selective autophagic degradation of proteasomes, or proteaphagy. As an autophagy pathway, proteaphagy in response to nitrogen starvation is induced by the inactivation of the mTOR kinase, a central regulator of cell growth and autophagy. TOR inactivation and signaling, the core of autophagy upregulation, is well characterized. Proteaphagy specific events are less clear. In *Arabidopsis* and yeast, cargo adaptors for proteasome-inhibitor induced proteaphagy have been identified as Rpn10 and Cue5, respectively<sup>18,19</sup>. However, neither protein is required for starvation induced proteaphagy. Interestingly, proteaphagy in mammalian cells does not involve homologs of either identified adaptor, and instead requires the autophagy receptor p62<sup>20</sup>. Identification of other proteaphagy specific factors and signaling events remain an active area of investigation.

### **Proteasome storage granules**

Unlike nitrogen starvation, carbon starvation does not induce proteaphagy, but instead induces the sequestration of proteasomes in cytoplasmic aggregates termed proteasome storage granules (PSGs)<sup>15,16</sup>. The function of PSGs remains poorly understood. Consistent with its name, one model suggests that proteasome storage granules store a pool of proteasomes that are readily accessible upon nutrient availability. Within this model, as cells enter quiescence (or are starved of carbon), nutrients are depleted, protein synthesis drops, and the demand for proteasomal degradation of short-lived nuclear proteins decreases. Consistent with this model, proteasome dissociation over time (and consequent reduced proteasomal activity) correlates with proteasome granule formation<sup>16,32</sup>. Here, monoubiquitin level may regulate PSG formation as an indicator of proteasomal demand. Mutations that lower free monoubiquitin such as *UBP6Δ* and *UBI4Δ* almost completely abrogate PSG formation<sup>16</sup>.

An alternative model suggests granular aggregation protects proteasomes from autophagic degradation induced by carbon starvation<sup>33</sup>. Consistent with this model, deletion of an N-terminal acetyltransferase, namely, NatB, which prevents PSG formation upon carbon starvation, induces proteaphagy<sup>33</sup>. In other words, when proteasome granule formation is blocked, proteaphagy occurs more quickly than when proteasome granule formation is functional. While both models are supported by some data, the biological advantage of proteasome sequestration into granules remains unclear. For example, proteasomal degradation depends on ubiquitination, so presumably, altering the ubiquitin landscape within the nucleus could directly modulate proteasomal activity without proteasome re-localization. In addition, some of our preliminary data suggests nuclear proteasomes are protected from autophagy. Thus, nuclear retention of proteasomes, as opposed to granular targeting, is apparently sufficient for prevention of autophagic degradation.

While the function of PSGs remains debated, previous research has described PSG composition and properties. Mass spectrometry analysis identified the major components of PSGs as proteasome subcomplexes and free ubiquitin<sup>16</sup>. PSG reversibility prompted the storage model: when nutrients are replenished and cell proliferation begins, PSGs readily disassemble, and proteasomes re-enter the nucleus (within a few minutes)<sup>15,16</sup>. Besides ubiquitin levels, intracellular pH is a proposed signaling mechanism between carbon source availability and proteasome sequestration. Mutations in vacuolar ATPases that constitutively lower intracellular pH also induce PSG formation in the absence of carbon starvation<sup>34</sup>. Vacuolar ATPases are important for pH homeostasis—when glucose is abundant, V-ATPases pump protons from the cytoplasm into the vacuole. Glucose depletion lowers intracellular pH, V-ATPase complexes disassemble, and acidification of the cytoplasm intensifies. Thus, pH may link nutrient availability to PSG formation. pH directly modulates biophysical properties, affinities, and interactions of proteins, and therefore, sensitivity to pH suggests proteasome granules may form via a biophysical mechanism like liquid-liquid phase separation. In addition to pH sensitivity, reversibility is also a shared property between PSGs and liquid droplets.

Although low pH may signal proteasome granule formation, a precise mechanism for PSG assembly has yet to be described. In large scale knockout screens, several factors required for RP and CP sequestration into granules upon quiescence have been identified<sup>16</sup>. These comprise proteins involved in a variety of cellular processes including phosphorylation, DNA repair, ubiquitination, and metabolism. However, few of the identified factors co-localize with

proteasome granules, and therefore the role of many of these factors in PSG formation remains ambiguous<sup>16</sup>.

Interestingly, of 45 factors required for CP sequestration into granules, only 21 are important for RP localization to PSGs, suggesting that CP and RP, at least partially, are targeted to PSGs in separate pathways<sup>16</sup>. For example, CP-specific interactor, Blm10, has been reported to be required for granular targeting of CP only. However, Blm10 dependence might be condition specific as our lab has not observed a requirement of Blm10 for CP localization to PSGs<sup>16,35</sup>. For RP subcomplexes, Spg5, an RP-specific interactor important for proteasome assembly in stationary phase, impacts RP, but not CP, sequestration into granules<sup>33</sup>. Since CP and RP require partially different factors for granular targeting, it appears proteasomes are sequestered as separate RP and CP subcomplexes into granules. However, the sequestration of 26S complexes has not been excluded. It should be noted that certain deletions may prevent delivery of one subcomplex due to defects independent of PSG formation. For example, *SPG5* deletion may destabilize RP subcomplexes which indirectly affects RP ability to localize to granules.

## **Other granule structures**

In addition to proteasomes, other cellular components form granular deposits. JUNQs (Juxtannuclear Quality Control Compartment) and IPODs (Insoluble Protein Deposit) are both evolutionarily conserved sites of protein aggregation that form in response to proteotoxic stress. Normally, misfolded proteins are destroyed by proteasomal degradation. However, misfolded proteins accumulate under certain conditions like heat stress or proteasome dysfunction. Under such conditions, JUNQs and IPODs isolate misfolded proteins to prevent their potentially harmful or toxic effects. Misfolded proteins that are ubiquitinated are sorted into the JUNQ, while non-ubiquitinated aberrant proteins are targeted to the IPOD<sup>36</sup>. Protein sequestration into JUNQs is reversible upon re-folding, while IPOD inclusions are less dynamic<sup>36</sup>. JUNQs are considered perinuclear sites of protein re-folding and proteasomal degradation. While IPOD function is less clear, one hypothesis suggests IPOD aggregation promotes autophagic degradation, however, little evidence exists to support this model<sup>37</sup>. Interestingly, some evidence suggests early PSGs transiently interact with the IPOD before maturation<sup>38</sup>. Dysfunctional proteasomes remain co-localized with IPOD compartments, fail to form independent PSGs, and are eventually degraded

by proteophagy<sup>38</sup>. Thus, the IPOD may serve as a site that determines proteasome fate upon stress: sorting into specific compartments promotes storage, while retention increases susceptibility to degradation. JUNQs directly recruit proteasomes via ubiquitinated substrates; however, JUNQs and proteasome storage granules are distinct cellular structures. The formation of JUNQs and IPODs depends on functional actin cytoskeleton dynamics and most likely requires molecular chaperones; however, a specific mechanism for the assembly of either protein deposit has yet to be described<sup>37,39,40</sup>.

While IPODs and JUNQs sequester potentially toxic protein aggregates, processing bodies (P bodies) and stress granules contain RNA and translation machinery. P bodies and stress granules both form around non-translating mRNAs and have overlapping roles in the mRNA Cycle. Under normal conditions, P bodies are sites of mRNA decay, but upon stress, P bodies can mature into stress granules<sup>41</sup>. Stress granules inhibit translation and allow mRNA to cycle to translation machinery as conditions become conducive for protein synthesis. The formation of both foci involves the recruitment of specific factors which phase separate into soluble protein droplets in a process known as liquid-liquid phase separation<sup>42,43</sup>. Both P bodies and stress granules are sensitive to cycloheximide treatment<sup>41,44,45</sup>. Cycloheximide, an inhibitor of translation elongation, traps mRNAs in polysomes which prevents recruitment of phase separating factors. Therefore, cycloheximide sensitivity provides a potential readout to differentiate between P-bodies/stress granules and other granular structures.

In addition to defined granules, many kinases and proteins involved in metabolism localize to reversible cytoplasmic puncta that do not co-localize with one another or with known granular structures<sup>46</sup>. Many identified granules share some universal properties including 1) lack of a cellular membrane, 2) reversibility, and 3) conditional formation. However, little is known about how or why certain granules form. Consequently, cytoplasmic granules, including PSGs, represent a largely unexplored cellular space.

## **Proteasome shuttle factors**

Proteasomal degradation requires recognition of ubiquitinated substrates. Three proteasome subunits, Rpn10, Rpn13, and Rpn1, contain integral ubiquitin receptors. Thus, proteasomes alone bind and degrade ubiquitinated proteins. However, in addition to these RP subunits, shuttle factors

serve as extrinsic ubiquitin receptors. Shuttle factors bind ubiquitinated substrates as well as proteasomes and, as such, transport ubiquitinated material to proteasomes for degradation. Each shuttle factor contains a C-terminal UBA domain that interacts with ubiquitinated substrates, a flexible region, and a N-terminal UBL domain that interacts with proteasomes. In yeast, three such factors exist: Dsk2, Rad23, and Ddi1. Previous research shows shuttle factors provide an additional tier of regulation within the UPS: each shuttle factor exhibits substrate selectivity and is involved in specific cellular processes. In other words, no proteasomal ubiquitin receptors (intrinsic or extrinsic) show complete redundancy. Rad23 and Ddi1 are important for DNA damage response while Rad23 and Dsk2 participate in spindle pole body duplication<sup>47-49</sup>. Recent work shows ~90% of substrates are delivered to proteasomes by Dsk2 or Rad23 suggesting shuttle factors are also important for overall UPS function<sup>50</sup>. Therefore, how shuttle factors influence proteasome dynamics is an emerging, relevant, and unanswered question.

## Shuttle factor structure and function

### UBA and UBL domains

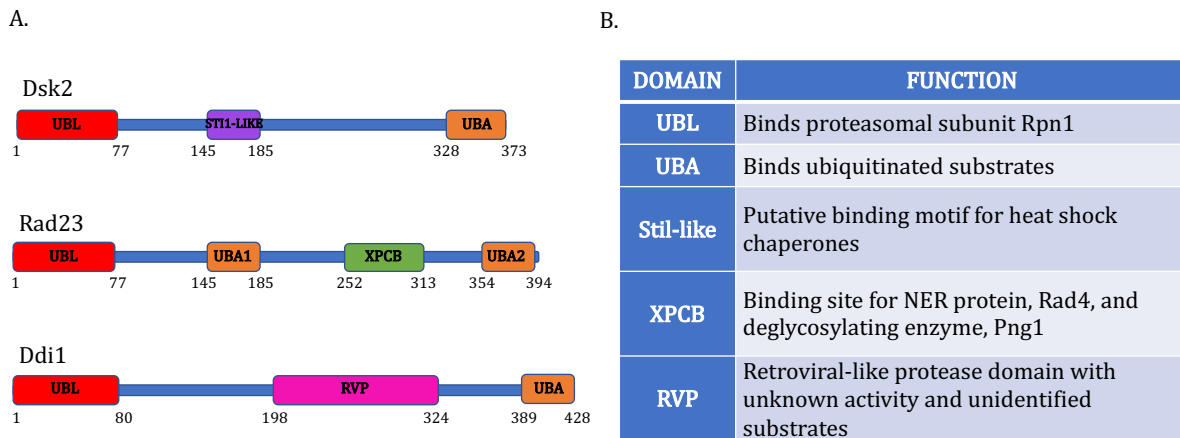


**Figure 1-3. Yeast shuttle factor domains.**

Yeast shuttle factors contain an N-terminal UBL domain which binds the proteasome and a C-terminal UBA domain responsible for interacting with ubiquitinated substrates. In addition to UBA and UBL domains, each shuttle factor has unique domains that serve specific functions. (A) Schematic representation of yeast Dsk2, Rad23, and Ddi1. Numbers indicate the AA range which defines each domain<sup>47,51-56</sup>. (B) Functional description of each domain within yeast shuttle factors. (Note: In other proteins, the same domains may serve alternative functions).

Although ubiquitination requirements vary among substrates, K48 ubiquitin linkages are considered the major signal for proteasomal degradation. Proteasomes recognize and bind multiubiquitinated substrates at three subunits: Rpn10, Rpn13, and Rpn1. Each subunit interacts with multiubiquitin through different domains: Rpn10 contains ubiquitin interacting motifs (UIMs), Rpn13 has a Pleckstrin-like receptor for ubiquitin (Pru) domain, and a site within Rpn1, T1, preferentially binds specific ubiquitin chains<sup>57-60</sup>. Shuttle factors, unlike any intrinsic ubiquitin receptors, interact with ubiquitinated proteins through yet another domain: ubiquitin associated domain (UBA). Canonical UBA domains consist of a three-helix bundle with a conserved hydrophobic patch responsible for ubiquitin interaction<sup>61</sup>. Even though ubiquitin receptors share a common ligand, they are sequentially and structurally variable.

Rad23, Dsk2, and Ddi1 all contain a UBA domain on the C-terminus (Figure 1.3). Consistent with canonical UBA domains, NMR data on the human homolog of yeast Rad23, hHR23A, revealed that ubiquitin binding is mediated by residues within the first helix, a conserved loop, and the third helix that form a hydrophobic patch<sup>62</sup>. The UBA domain of Dsk2 forms an analogous interface with ubiquitin, but with a markedly higher affinity than other UBA domains ( $K_d = 14.8 \mu\text{M}$  compared to  $K_d = 250\text{--}600 \mu\text{M}$ )<sup>62-64</sup>. In addition to a higher affinity for ubiquitin, Dsk2 UBA also exhibits less selectivity for specific ubiquitin linkages. *In vitro*, Rad23 UBA preferentially binds K48 linkages while Dsk2 UBA shows no preference among K48, K63, and artificial K6 and K29 ubiquitin polymers<sup>65</sup>. In contrast, recent *in vivo* experiments suggest, under normal physiological conditions, Dsk2 and Rad23 both preferentially interact with K48 ubiquitin linkages<sup>50</sup>. Nevertheless, the high affinity of Dsk2 UBA for monoubiquitin as well as across different ubiquitin linkages suggests Dsk2 may have undiscovered roles in other cellular processes involving non-proteolytic ubiquitin signaling. Compared to Dsk2 and Rad23, Ddi1 exhibits markedly weaker binding to ubiquitinated substrates *in vivo*<sup>50</sup>.

In addition to interacting with ubiquitinated substrates, the UBA domain is also important for protection from proteasomal degradation<sup>66</sup>. As proteins that interact with both ubiquitin and the proteasome, shuttle factors are ideal proteasomal substrates. However, the UBA domain protects these proteins from degradation through 1) a conserved motif and 2) C-terminality. Although the functional differences between UBA1 and UBA2 in Rad23 remain a mystery, only the C-terminal UBA2 contains the protective motif (Figure 1.3a). When UBA2 is mutated, replaced with UBA1,

or placed in front of the C-terminus, the half-life of Rad23 is considerably shortened<sup>66</sup>. Thus, protection from proteasomal degradation is a direct result of C-terminal UBA domain properties.

Each shuttle factor also has an N-terminal ubiquitin-like domain (UBL) that is responsible for interacting with the proteasome. As implied by the name, the ubiquitin like domain is structurally similar to ubiquitin and consequently, capable of binding ubiquitin interactors. Specifically, proteins with UBL domains associate with proteasomal ubiquitin receptors and are often considered “proteasome interacting proteins.” For example, some ubiquitin ligases and deubiquitinases (DUBs) contain UBL domains that bind the proteasome and compete for substrate modification. The competition between ligases and DUBs regulates substrate degradation directly at the site of proteolysis.

Shuttle factor UBL domains bind Rpn1, one of the three intrinsic ubiquitin receptors on the proteasome<sup>57,67,68</sup>. In the mammalian system, shuttle factors also interact with the other proteasomal ubiquitin receptors, Rpn10 and Rpn13<sup>60,69</sup>. However, in yeast, whether or not shuttle factors are capable of binding Rpn10 and Rpn13 in addition to Rpn1 remains unresolved<sup>57,67</sup>. Interestingly, a portion of Rpn10 is found in an extraproteasomal pool indicating it serves as both as an intrinsic and extrinsic proteasomal ubiquitin receptor<sup>70</sup>. A direct interaction between Rpn10 and Dsk2 has been reported; however, as opposed to acting as a proteasomal binding site for Dsk2, extraproteasomal Rpn10 actually attenuates Dsk2-proteasome interaction<sup>11</sup>. Evidence suggests monoubiquitination of Rpn10 reduces its association with both Dsk2 and the proteasome, and correspondingly, increases the population of Dsk2-bound proteasomes<sup>71</sup>. Thus, dynamic interactions between extraproteasomal ubiquitin receptors, competition for proteasomal binding sites as well as post-translational modifications all influence substrate delivery.

Although more research is necessary to determine extraproteasomal ubiquitin receptor dynamics, currently, Rpn1 is considered the major shuttle factor docking site in yeast. Rad23UBL-Rpn1 interaction has been studied with NMR. Unsurprisingly, the Rad23UBL-Rpn1 interaction mimics Rpn1 interaction with ubiquitin: hydrophobic residues within the UBL interact with the Helix28/Helix30 at the T1 ubiquitin binding site<sup>72</sup>. Surprisingly, although all three shuttle factors interact with Rpn1, there is evidence that they may bind unique surfaces; a mutation in the LRR domain of Rpn1 completely abrogates Ddi1 interaction, only partially influences Dsk2 binding, and has no effect on Rad23 affinity<sup>68</sup>. Consistently, shuttle factors exhibit different affinities for proteasomal receptors. Rad23 has the strongest affinity for the proteasome, while Ddi1 has the

weakest<sup>67,73,74</sup>. Post-translational modifications on UBL domains may modulate affinity for proteasomal receptors. For example, phosphorylation of Rad23UBL inhibits interaction with the proteasome, while ubiquitination of Dsk2UBL is important for efficient substrate delivery<sup>75,76</sup>. Unlike Rad23 and Dsk2, the UBL domain of Ddi1 interacts with ubiquitin itself<sup>55</sup>. The nature of this uncharacteristic UBL-ubiquitin interaction remains obscure.

Even though shuttle factors specifically bind an RP base subunit, there is evidence that shuttle factors preferentially interact with 26S proteasomes. Mutations that prevent 26S assembly cause accumulation of substrate-bound shuttle factors<sup>77</sup>. This accumulation was shown to be independent of proteasomal activity. Instead, inhibition of proteasomes causes an accumulation of substrate-bound proteasomes indicating efficient substrate shuttling<sup>77</sup>. Thus, shuttle factor-mediated delivery does not depend on proteasome activity, but rather 26S configuration.

In addition to interacting with ubiquitin and the 26S proteasome, UBA and UBL domains also interact with one another. When unoccupied by substrates, intramolecular interactions between the UBA, a ubiquitin receptor, and UBL, a ubiquitin analog, cause shuttles to adopt a “folded” state<sup>51,64,78</sup> (Figure 1.4a). Additionally, Rad23 and Dsk2 both exist as homodimers (Figure 1.4b). Counterintuitively, dimerization is not mediated by UBA-UBL intermolecular interactions. Instead, only the UBA domains of Rad23 and Dsk2 are involved in dimerization in yeast while mammalian homologs require neither the UBA or UBL, but the central region to dimerize<sup>79–81</sup>. Nonetheless, an accepted model involves ubiquitinated substrates interrupting either “folded” or dimerized shuttles via ubiquitin-UBA binding, which “frees” the UBL domain for interaction with the proteasome (Figure 1.4d).

Ddi1 also forms homodimers, but neither the UBA or UBL domain is required. Instead, Ddi1 dimerization requires the retroviral-like aspartyl protease (RVP) domain located in the center portion of the protein<sup>82</sup> (Figure 1.4c). Of all shuttle factor domains, the RVP domain in Ddi1 is the only site of enzymatic activity. However, the function of this domain in Ddi1 is obscure. In human homologs, the Ddi1 RVP domain is conserved, while the UBA domain is not, suggesting Ddi1 may serve as a protease itself rather than a proteolytic adaptor (Figure 1.5c). In addition to homodimers, heterodimers between different shuttles also exist, but these interactions are less characterized<sup>79,83</sup>.

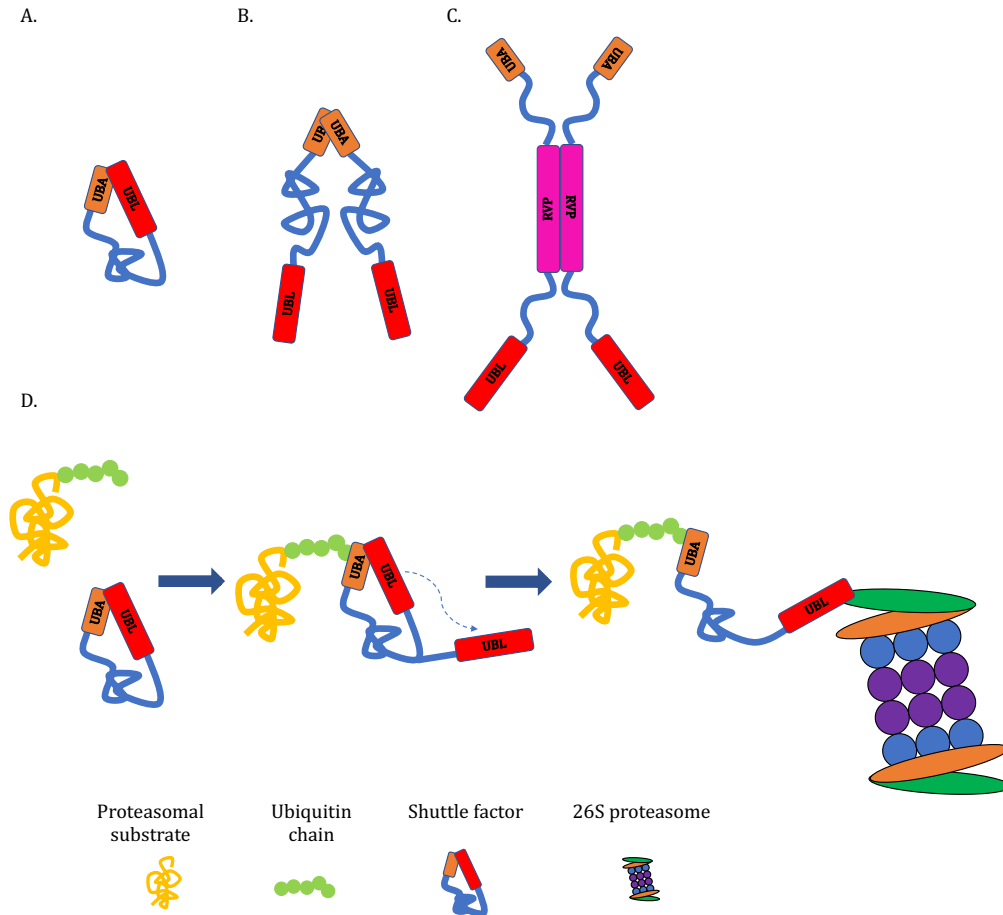


**Figure 1-4. Intramolecular and Intermolecular interactions of shuttle factor UBL and UBA domains.**

*In addition to interacting with proteasomes and substrates, shuttle factor UBL and UBA domains interact with one another resulting in different conformations. (A) Individual shuttle factors adopt a “folded state” due to intramolecular interaction between UBL and UBA domains. (B) In yeast, intermolecular binding between UBA domains results in homodimerization of Rad23 and Dsk2. (C) Unlike Rad23 and Dsk2, Ddi1 homodimerization does not involve the UBA domain but is instead facilitated by the conserved RVP domain. (D) Ubiquitinated substrates interrupt intramolecular interactions between shuttle factor domains to promote delivery to proteasome.*

### Shuttle factor models

Shuttle factors are considered proteasome adaptors: they link ubiquitinated substrates to proteasomes through 1) UBA interaction with substrates, and 2) UBL interaction with proteasomes<sup>84</sup>. A proteolytic role for Rad23 and Dsk2 was first observed by the stabilization of an artificial proteasomal substrates upon either *RAD23* or *DSK2* deletion<sup>85,86</sup>. Additional work has shown that shuttle factors are required for degradation of physiological substrates<sup>87–89</sup>. Thus, an

accepted model involves shuttle delivery of substrates to the proteasome for degradation (Figure 1.4d).

Interestingly, some evidence suggests that proteasome shuttles serve an opposite function. That is, instead of promoting degradation, shuttle factor binding actually prevents degradation by blocking ubiquitin chain extension<sup>90</sup>. Consistent with a role in substrate stabilization, overexpression of Rad23 or Dsk2 causes an accumulation of ubiquitinated substrates<sup>91</sup>. However, it is important to recognize shuttle factor binding to the proteasome is competitive—overexpression could saturate proteasomal ubiquitin receptors and cause inefficient proteolysis. Additionally, although shuttle factor binding prevents ubiquitin chain extension, it also prevents deubiquitination<sup>91,92</sup>. Therefore, an additional proposed function of shuttle factors is not protection of substrates from proteasomal degradation, but protection of the degradation signals themselves; shuttle factor binding may prevent deubiquitination of substrates in transit to proteasomes. Stabilization of ubiquitinated substrates upon Rad23 or Dsk2 overexpression may be due to inefficient deubiquitination, a prerequisite for proteasomal degradation. Regardless of protective roles, shuttle factors have the ability to suppress both ubiquitin chain extension and disassembly, and therefore, contribute to ubiquitin chain dynamics.

### **Specific substrates**

Although all shuttle factors participate in the general delivery of ubiquitinated material to proteasomes, each factor exhibits some degree of substrate specificity. For example, Ddi1 is required for the degradation of Ho endonuclease, an enzyme responsible for mating-type switching<sup>87</sup>. The double knockout of *RAD23* and *DSK2* interrupts a variety of cellular processes including cell cycle regulation, spindle pole body duplication, and DNA repair<sup>88</sup>. Kre22, a protein of unknown function, specifically requires Dsk2 for degradation<sup>88</sup>. In concert with Rpn10, Rad23 is important for the turnover of cell cycle regulators, Far1 and Sic1<sup>89</sup>.

One potential mechanism for substrate selectivity relies on shuttle factor ability to interact with ubiquitin ligases. Within this model, substrate ubiquitination and shuttle factor binding are coupled. Thus, a shuttle factor which preferentially interacts with a specific ligase will exhibit similar substrate selectivity. Some evidence exists for this model. For example, Rad23 and Dsk2 both interact with Ufd2, an E4 ligase responsible for ubiquitin chain extension, while Ddi1 selectively interacts with Ufo1, an F-box protein that regulates substrates for the SCF E3 ubiquitin

ligase complex<sup>93-96</sup>. Although many ligases exist, only few ligase-shuttle factor interactions have been identified. Additionally, shuttle factor interaction with ubiquitinated substrates does not require ligase mediation. Thus, additional mechanisms of substrate selectivity likely exist.

Rad23 and Dsk2 interaction with Ufd2 ligase suggests these shuttle factors selectively deliver ER-associated degradation (ERAD) substrates. ERAD is responsible for degradation of erroneous ER-translated proteins before they reach final destinations. Misfolded proteins (and protein intermediates) are recognized, ubiquitinated, and retro-translocated out of the ER where they are subject to degradation by cytosolic proteasomes. The core ERAD machinery includes Cdc48, an essential ATPase that provides energy for disassembly of protein complexes and translocation out of the ER. Ufd2, Rad23/Dsk2-interacting ligase, requires Cdc48 binding for activity<sup>97</sup>. Presumably, Ufd2 is responsible for ubiquitinating ERAD substrates which are delivered to proteasomes by Rad23 and Dsk2. However, not all ERAD substrates depend on Rad23 or Dsk2 for effective clearance, so how ubiquitin receptors distinguish among ERAD targeted proteins remains an area of active investigation. There is evidence that Rad23 may selectively target glycosylated ERAD substrates for degradation. The XPCB domain of Rad23 binds Pgn1, a deglycosylating enzyme, and this interaction is important for effective ERAD clearance of glycosylated protein ricin A chain<sup>98</sup>. Whether or not glycosylation is a requirement for Rad23-dependent ERAD has not been shown.

Confusingly, Rad23 and Ddi1 are both capable of interacting with Cdc48 directly. Evidence suggests Cdc48-Rad23 interaction serves a function in ERAD substrate delivery: Cdc48 binding to Rad23 destabilizes Rad23-Ufd2 ligase complexes and allows the UBL domain of Rad23 to interact with proteasomes<sup>99</sup>. On the other hand, Ddi1 interaction with Cdc48 does not serve a proteolytic role. Recent work revealed Cdc48-Ddi1 complexes are involved in selective anterograde protein sorting. Specifically, Cdc48-Ddi1 mutants are defective for delivery of Cps1, a membranal vacuolar hydrolase, to the vacuole<sup>100</sup>. Shuttle factor delivery of non-proteasomal substrates is an interesting hypothesis for future work.

## **Shuttle factors in cellular processes**

### **Spindle pole body duplication and cell cycle control**

Although complete sets of shuttle factor substrates remain undefined, it has been shown shuttle factors are involved in multiple cellular processes including spindle pole body duplication, cell cycle regulation, and DNA damage response. In most circumstances, the involvement of shuttle factors in cell processes is ambiguous. For example, a double knockout of *DSK2* and *RAD23* prevents spindle pole body duplication, but the mechanism is not understood<sup>49</sup>.

The link between shuttle factors and cell cycle progression is limited to observed phenotypes of shuttle factor mutants. Cell cycle progression requires the coordinated degradation of specific signaling factors. Presumably, shuttle factors deliver specific substrates to proteasomes to promote normal cell cycle progression. Different knockout combinations of Rad23, Dsk2, and Ddi1 cause cell cycle arrest at the G2/M transition. Rad23 has overlapping roles with both Dsk2 and Ddi1 in cell cycle control, but these roles are not redundant with one another. That is, deletion of *RAD23* in *DSK2Δ* or *DDI1Δ* strains causes a slight accumulation of arrested cells, but deletion of all three shuttles causes arrest in the majority (70%) of cells<sup>101</sup>. Additionally, Rad23 and Ddi1 are important for S-phase checkpoint control; when synchronized with hydroxyurea, cells deleted for the UBA domains of both proteins prematurely enter anaphase<sup>82,102</sup>. Although the mechanism is not well understood, there is speculation that Rad23 and Ddi1 contribute to Pds1 stability, an anaphase inhibitor<sup>102</sup>. The only concrete support for a proteolytic role of shuttle factors in cell cycle control is Rad23-mediated degradation of Sic1 and Far1, both cyclin dependent kinase inhibitors that block cell cycle progression<sup>89</sup>.

### **Nucleotide excision repair (NER)**

The most well studied example of shuttle factor involvement in a cellular process is the role of Rad23 in nucleotide excision repair (NER). In fact, Rad23 nomenclature, RADiation sensitive, is based on the phenotype of Rad23 mutants and reflects its importance in UV protection. Interestingly, Rad23 involvement in NER is not proteolytic. Instead, Rad23 actually prevents degradation of NER protein, Rad4. NER removes UV-damaged DNA through 1) recognition of a photolesion, 2) DNA unwinding, 3) excision of single stranded DNA segment, and 4) DNA synthesis using complementary strand as a template. Rad4 is involved in DNA damage recognition; Rad4, in complex with Rad23, binds damaged DNA, destabilizes the double helix, and facilitates damaged bases to “flip” outward of the helix<sup>103</sup>. Deletion of *RAD23* causes Rad4 destabilization, and consequently, impaired NER<sup>54</sup>. Although protective roles of shuttle factors

have been proposed, Rad23 protection of Rad4 does not depend on its “shuttling” domains. Instead, Rad23 interacts with Rad4 through the XPCB domain, and this domain alone rescues Rad4 destabilization observed upon Rad23 deletion<sup>54</sup>. Therefore, Rad23 probably influences Rad4 stability not through proteasomal regulation, but through biochemical interactions.

Recent work has shown that beyond stabilization, Rad23 binding actually increases Rad4 affinity for DNA<sup>104</sup>. In fact, in the absence of UV-damage, Rad4-Rad23 complexes bind promoters of DNA damage response genes to block transcription<sup>105</sup>. The coordinated release of these complexes from promoters and subsequent affinity for photolesions is facilitated by Rad4 ubiquitination<sup>105</sup>.

Beyond Rad4 stability and affinity, there is also evidence that Rad23 links the proteasome to NER regulation. However, conflicting studies report different requirements of proteasome activity for efficient NER<sup>106107</sup>. Therefore, Rad23 and proteasomal involvement in NER is an ongoing area of research.

Similar to Rad23, Ddi1 may be involved in DNA repair. In response to genotoxic stress, Ddi1 is transcriptionally upregulated; however, the specific role of Ddi1 in DNA repair processes (if any) is unknown<sup>108</sup>.

### **Shuttle factor grouping**

Ddi1 is often considered separately from Rad23 and Dsk2 for multiple reasons: 1) the UBA and UBL domains show uncharacteristic affinities; Ddi1 UBL interacts with ubiquitin, neither UBL or UBA domain is required for dimerization, and Ddi1 associates with a different ligase from Rad23 and Dsk2. 2) Ddi1 contains an enzymatic protease domain. And 3) Ddi1 shows weak binding to ubiquitin chains<sup>50</sup>. Consistent with noncanonical biochemistry, Ddi1 is involved in unique cellular processes. Ddi1 was originally named “Vsm1,” v-SNARE-master 1, due to its discovery as a negative regulator of SNARE assembly during exocytosis<sup>109</sup>. Specifically, amino acid residues directly upstream of the UBA domain bind Sso1, an exocytotic t-SNARE, and prevent Sso1 association with its t-SNARE partner<sup>82</sup>. The deletion of *DDI1* relieves competition for t-SNARE binding, and therefore, results in a slight increase in protein secretion<sup>109</sup>. In addition to exocytosis, Ddi1, in complex with Cdc48, also mediates anterograde protein sorting<sup>100</sup>. In both processes, Ddi1 function does not involve substrate delivery to proteasomes. Thus, even though

Rad23, Dsk2, and Ddi1 have similar architecture, the distinction between Ddi1 and other shuttles is an emerging pattern worth more investigation.

### **Mammalian homologs**

From yeast to human, sequence homology between shuttle factors is low. For example, ubiquilin-1, a Dsk2 mammalian homolog, shares only 19% sequence homology with Dsk2<sup>81</sup>. Nonetheless, mammalian and yeast shuttle factors exhibit highly conserved structural domains. With the exception of Ddi1 homologs, mammalian shuttle factors all contain terminal UBA and UBL domains similar to yeast (Figure 1.5). Evidence also suggests that, like yeast, shuttle factors are a part of the UPS. In addition to sequence variation, evolution from yeast to mammal also involved genetic duplication events which resulted in multiple mammalian homologs of each protein. Interestingly, some homologs of the same yeast shuttle factor do not share completely redundant functions. For example, hHR23A and hHR23B, both homologs of Rad23, have different roles in embryogenesis. Mammalian shuttle factors are involved in a wide range of biological functions, and consequently, implicated in many diseases.

### **Rad23 homologs: hHR23A and hHR23B**

Similar to yeast, both mammalian homologs of Rad23 contribute to nucleotide excision repair through complex formation with DNA binding proteins<sup>110</sup>. However, hHR23A and hHR23B exhibit non-redundant roles in other cellular processes most likely due to different proteasomal substrate specificities. For example, hHR23B, but not hHR23A, is required for the degradation of Pax3, a critical regulator of fetal development<sup>111</sup>. Mouse embryos lacking hHR23B have poor vascularization and low blood cell counts, and consequently, exhibit an extremely low survival rate<sup>112,113</sup>. hHR23A knockout mice, on the other hand, progress through embryogenesis normally<sup>114</sup>.

At the cellular level, Rad23 homologs influence cell cycle regulation and apoptosis. Interestingly, Rad23 homologs are important for stabilization as opposed to degradation of specific cell cycle factors. For example, both hHR23A and hHR23B have been shown to stabilize p53, a transcription factor responsible for cell cycle arrest and gene stability in response to stress<sup>115,116</sup>. The deletion of either Rad23 homolog induces rapid p53 turnover and, consequently, prevents

normal apoptotic signaling in response to genotoxic stress<sup>117</sup>. As proteins that influence cell cycle regulation, Rad23 homologs are associated with tumorigenesis. Specifically, hHR23A has been shown to stabilize a ubiquitin ligase that promotes cell proliferation in certain breast cancers, and downregulation of hHR23B is associated with breast cancer invasiveness<sup>118,119</sup>.

In addition to cancer, Rad23 homologs, like other components of the UPS, are associated with neurodegenerative diseases. Both homologs interact directly with ataxin-3, the causative agent of spinocerebellar ataxia-3<sup>120</sup>. Similar to p53, the interaction of Rad23 homologs with ataxin-3 promotes stabilization as opposed to deletion<sup>121</sup>. Thus, as opposed to functioning as proteolytic facilitators, shuttle factors may have a broader contribution to degradation kinetics. How Rad23 homologs specifically influence disease—through substrate stabilization, substrate destabilization, NER, or an unidentified function—remains an area of active research.

### **Dsk2 homologs: ubiquilins**

Dsk2 is related to a family of mammalian proteins called ubiquilins. All four mammalian ubiquilins (ubiquilin1-4) contain terminal UBL and UBA domains; however, ubiquilin-1 and 2 are usually grouped together and considered the closest homologs of Dsk2<sup>122</sup> (Figure 1.5b). Like Dsk2, ubiquilin-1 and 2 shuttle substrates to proteasomes for degradation<sup>123</sup>. Beyond proteasomal shuttling, however, ubiquilin-1 and 2 also contribute to other degradative pathways including inclusion body (IB) formation and autophagy<sup>124–126</sup>. In short, ubiquitinated proteins recognized by ubiquilin 1 or 2 can meet one of three fates: 1) delivery to the proteasome, 2) aggregation into IB, or 3) autophagic clearance. What mediates ubiquilin shuttling between the proteasome, IB, or autophagy machinery remains a mystery; regulation of ubiquilin shuttling could be susceptible to metabolic, spatial, or client-specific regulation. For example, opposite of its role in IB formation, in the nucleus, ubiquilin-2 associates with disaggregase complexes to facilitate proteasomal degradation of aggregated proteins<sup>127</sup>. The relationship between aggregation status and degradation pathway as well as the involvement of ubiquilins in both processes provide an interesting connection for future investigation.

As proteins involved in multiple degradative pathways, ubiquilin-1 and 2 are both associated with proteotoxic diseases. Ubiquilin-1 is specifically linked to Brown-Vialetto-Van Laere syndrome, an infantile onset motor neuron disease<sup>128</sup>. Mutations in ubiquilin-2 are associated with familial amyloid lateral sclerosis (ALS)<sup>129</sup>. ALS-associated mutations in ubiquilin-2 are not

located within either shuttling domain, but instead in the PRR (proline rich repeat) region<sup>129</sup> (Figure 1.5b). A study in *Drosophila* proposes ALS-linked ubiquilin-2 mutations induce ubiquilin aggregates through biochemical changes in ubiquilin solubility<sup>130</sup>. Current research focuses on ubiquilins as potential mediators for autophagy-UPS crosstalk as well as potential targets for disease treatment.

### **Ddi1 homologs: Ddi1 and Ddi2**

Two mammalian Ddi1 homologs exist: Ddi1 and Ddi2. Unlike yeast Ddi1, mammalian homologs do not contain UBA domains (Figure 1.5c). Instead, there is evidence that Ddi1/2 weakly interacts with ubiquitin via UIM (ubiquitin interacting motif) on the C-terminus<sup>131</sup>. Mammalian Ddi1 and Ddi2 are required for replication stress recovery; Ddi1/2-dependent removal of a replisome component allows stalled replication forks to restart<sup>132</sup>. However, whether or not this process involves proteasomal shuttling is unknown. In *C. elegans*, the RVP domain of Ddi1 is important for upregulation of proteasome transcription in response to proteasome dysfunction. In short, defective proteasomal degradation stabilizes an ERAD substrate which is cleaved by Ddi1, and following Ddi1 processing, acts as a transcription factor for proteasome genes<sup>133</sup>. In *Drosophila*, Rngo, Ddi1/2 homolog, has been identified as a substrate for ubiquitination by Ube3a, the single gene associated with neurodevelopmental disorder, Angelman syndrome<sup>134</sup>. Whether or not Ddi1 homologs serve as proteasomal shuttles as well as the significance of the conserved Ddi1 protease domain are questions for future research.

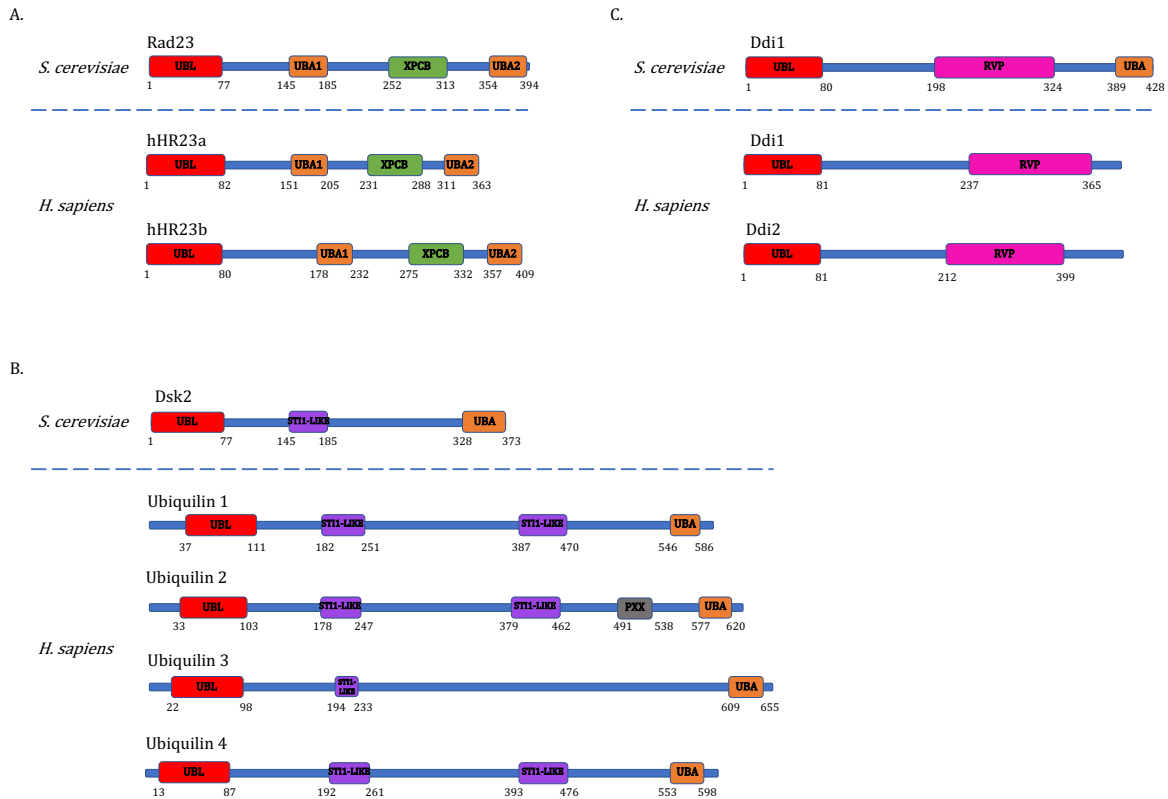


**Figure 1-5. Comparison of yeast and mammalian shuttle factor homologs.**

The structural domains between yeast and mammalian shuttle factors are highly conserved. (A) – (C) show schematic representations of mammalian homologs of Rad23, Dsk2, and Ddi1, respectively. Numbers indicate AA range of specific domains. Curiously, the UBA domain of Ddi1 is not conserved in mammals.

## Aim of the thesis

The purpose of this work is to identify the relationship between shuttle factors and proteasome localization. Recent work shows ~90% of substrates are delivered to proteasomes by shuttle factors<sup>50</sup>. Consequently, proteasome-shuttle factor interactions are more prominent than previously assumed. Some proteasomal targeting events, like nuclear-to-cytoplasmic transport, depend on post-translational modifications including acetylation and N-myristoylation. With 19 ubiquitinated sites on the proteasome spanning 12 subunits, ubiquitination is likely a regulator of proteasome distribution<sup>31</sup>. Additionally, both proteophagy and proteasome granule formation involve ubiquitin signaling—autophagy pathways recognize ubiquitinated cargo and free ubiquitin is a major PSG component. Shuttle factors, with an identified role in protein delivery, interact with proteasomes directly as well as ubiquitin, and thus, are likely to influence proteasome targeting

within these processes. Identified proteaphagy adaptors including Rpn10 (*Arabidopsis*) and p62 (mammals) are functionally similar to shuttle factors—both proteins participate in substrate delivery to proteasomes<sup>71,135</sup>. In addition, ubiquilin-2, a Dsk2 homolog, forms membrane-less droplets reminiscent of proteasome storage granules. Similar to PSGs, ubiquilin-2 droplets are also modulated by ubiquitin; ubiquitin binding to ubiquilin-2 eliminates multivalent interactions required for phase separation<sup>136</sup>. As proteins involved in 1) protein transport, 2) proteasome binding, 3) ubiquitin dynamics, and 4) phase separation, shuttle factors are strong potential mediators of proteasome re-localization. Therefore, this thesis aims to identify the role of proteasome shuttle factors in proteasome targeting events including proteaphagy and PSG formation.

## Chapter 2 - Methods and Results

### Introduction

Coordinated protein degradation is crucial for cell survival. Cells employ two major protein degradation systems: autophagy and the ubiquitin proteasome system (UPS). While autophagy involves the delivery of cargo to the vacuole (in plants and yeast) or lysosome (in mammals) in bulk, proteasomes degrade individual polypeptides. Proteasomes are molecular proteases made up of two subcomplexes, the core particle (CP) and the regulatory particle (RP); together, RP and CP recognize, unfold, and degrade proteasomal substrates. Autophagy pathways play a major role in response to certain stresses, however, during cell proliferation, the UPS is responsible for 80%-90% of homeostatic protein degradation<sup>137</sup>. As part of the major protein degradation pathway, proteasomes participate in a variety of cellular processes including signal transduction, cell cycle regulation, and protein quality control<sup>2</sup>. Proteasome involvement in diverse processes indicates protein turnover is finely tuned. Indeed, both the UPS and autophagy rely on ubiquitination for substrate recognition. Ubiquitination involves an enzyme cascade that activates and transfers ubiquitin molecules to lysine residues on target proteins. As a marker for degradation, ubiquitination of specific substrates allows coordinated protein turnover. The human genome encodes over 600 genes dedicated to ubiquitination and substrate specificity indicating the importance of selective degradation<sup>3</sup>.

While not all ubiquitination events result in degradation, ubiquitin conjugation is generally considered a prerequisite for substrate recognition and degradation by the proteasome. The proteasome contains three subunits that bind polyubiquitinated substrates, namely RP subunits Rpn1, Rpn10, and Rpn13<sup>57-60</sup>. Thus, proteasomes alone recognize and degrade ubiquitinated proteins. However, in addition to intrinsic receptors, other proteins called shuttle factors act as extrinsic ubiquitin receptors that transport ubiquitinated material to proteasomes for degradation. In yeast, three shuttle factors exist: Dsk2, Rad23, and Ddi1<sup>138</sup>. Each shuttle factor has a Ubiquitin-Associated (UBA) domain that interacts with ubiquitinated substrates and a ubiquitin-like domain (UBL) domain that binds proteasomes. Specifically, shuttle factor UBL domains, with structural and sequence homology to ubiquitin, interact with proteasomal ubiquitin receptors<sup>57</sup>. Although shuttle factors have overlapping roles within the UPS, each factor exhibits some degree of substrate

specificity<sup>87-89</sup>. Previous work has shown shuttle factors are involved in a variety of cellular processes including cell cycle progression, spindle pole body duplication, and DNA damage response<sup>82,88,101,102</sup>. Recent work shows ~90% of proteasomal substrates are delivered to proteasomes by Dsk2 or Rad23 suggesting shuttle factors are prominent contributors to overall UPS function<sup>50</sup>. Therefore, how shuttle factors influence proteasome dynamics is an emerging and important question.

Proteasomes are largely nuclear in proliferating cells. However, under certain starvation conditions, proteasomes exit the nucleus and are either degraded in the vacuole through an autophagy pathway (proteaphagy) or sequestered into cytoplasmic granules. Proteasome granules that form specifically upon carbon source depletion or quiescence are referred to as proteasome storage granules (PSGs)<sup>15,16</sup>. Mass spectrometry analysis of cross-linked PSGs induced by quiescence identified the main PSG components as CP and RP proteasome subcomplexes as well as monoubiquitin and lower levels of some proteasome interacting proteins<sup>16</sup>. Previous research has characterized PSGs as reversible membrane-less protein deposits that quickly dissociate upon carbon source replenishment<sup>15</sup>. The biological advantage of proteasome sequestration into reversible cytoplasmic granules is debated. One model suggests PSGs store a pool of proteasomes that are readily accessible upon conducive nutrient conditions. Consistent with this model, a correlation between proteasome downregulation and PSG formation has been observed<sup>32</sup>. A second model suggests granular sequestration protects proteasomes from autophagic degradation in response to carbon starvation<sup>33</sup>. When proteasome granule formation is blocked by deletion of NatB, an N-terminal acetyltransferase important for PSG targeting, proteaphagy occurs more quickly than when proteasome granule formation is functional<sup>33</sup>.

Although some factors like pH and ubiquitin level have been shown to influence PSG formation, a precise mechanism of proteasome granule assembly has yet to be described<sup>32,34</sup>. Here, we investigate the involvement of shuttle factors in proteasome localization in *Saccharomyces cerevisiae*. We show shuttle factors are important for proteasome localization to PSGs under certain conditions. Specifically, Rad23 and Dsk2, but not Ddi1, are required for proteasome targeting to granules as glucose levels gradually deplete or ATP production is blocked by sodium azide. Under these conditions, deletion of both proteins almost completely prevents proteasome granules. Co-localization experiments show Rad23 and Dsk2 are PSG components suggesting these proteins likely have a direct role in PSG assembly. Mutants with truncated versions of Rad23

and Dsk2 reveal that the C-terminal portion of each protein is required for its respective role in proteasome localization to granules. Interestingly, Rad23 and Dsk2 are not required for proteasome granules induced by abrupt carbon starvation. Based on differences in Rad23/Dsk2-dependency as well as cycloheximide sensitivity, we propose at least two different types of proteasome granules form in response to different metabolic states. Finally, we distinguish Ddi1 from Rad23 and Dsk2 as a negative regulator of proteasome granule formation. Even in the absence of inducing conditions, *DDI1Δ* cells exhibit granular localization of proteasomes. Thus, we propose a model in which Rad23 and Dsk2 are important for proteasome localization to granules, while Ddi1, in direct opposition to Rad23 and Dsk2, inhibits PSG formation.

## **Materials and Methods**

### *Yeast strains*

Strains used in this work are reported in Table 2.1. Strains with C-terminal GFP or mCherry fusions on proteasome subunits or shuttle factors were generated using standard PCR-based procedures<sup>139,140</sup>. Endogenous mCherry tagged UBL truncations were generated by transformation with a DNA construct that contained the mCherry open reading frame (ORF) and a selection cassette flanked by 40 bp of homologous sequence to the targeted region within the yeast genome. Homologous sequences were designed to delete the C-terminal portion of a shuttle factor and continue the mCherry ORF with the gene's ORF (Figure 2.1a). Endogenous UBLΔ truncations with N-terminal mCherry tags were generated using a Cre-Lox recombinase system to allow for expression of the truncation by the endogenous promoter at the original genomic locus. The background strain, sJR1255, which encodes for the GFP-tagged proteasome subunit Rpn1, was transformed with the DNA construct outlined in Figure 2.1b. Homologous sequences were designed so integration of the construct resulted in UBL domain deletion. Proper integration was confirmed by PCR and resulted in clones containing an excisable hygromycin selection cassette followed by an N-terminal mCherry tag on the C-terminal portion of the protein. Next, these clones were transformed with a plasmid encoding inducible Cre-Lox recombinase (-URA selection), and Cre-Lox expression was induced by growth in galactose media. Desired strains were isolated by screening for the loss of hygromycin resistance. Finally, growth on 5-FOA plates was used to counter-select for the inducible Cre-Lox plasmid. 5-FOA is converted into a toxic product (5-

fluorouracil) by the URA3 gene product, orotidine 5'-phosphate decarboxylase, allowing for selection of clones without the URA3-containing Cre-Lox plasmid. Finally, strains with fluorescently tagged truncations were confirmed by microscopy, PCR, and sequencing of PCR amplifications of manipulated genomic regions to ensure the absence of mutations at the gene-tag transition. The range of amino acids for each truncation are listed in Table 2.2.

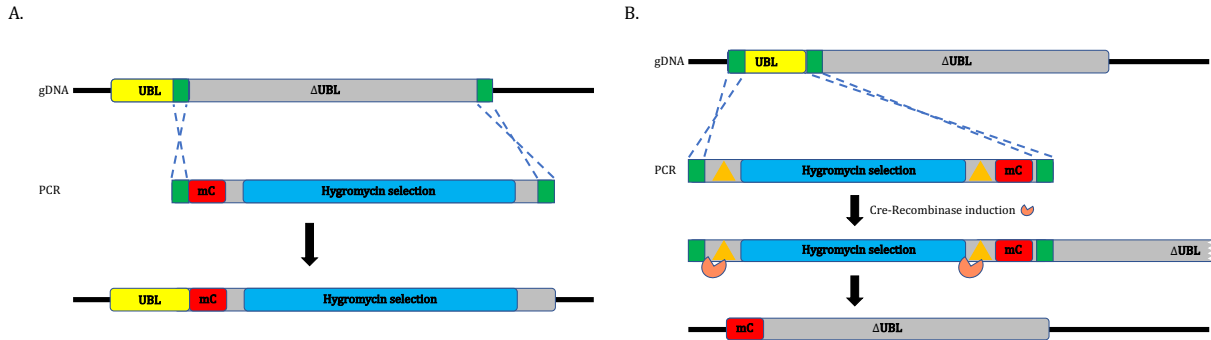


**Figure 2-1. Generation of truncated shuttle factors with fluorescent tags.**

Endogenous *mCherry* fusions were incorporated at the C-terminal end of UBL domains and the N-termini of  $\Delta$ UBL shuttle factors to create two truncations: 1) UBL-*mCherry* (A) and 2) *mCherry*-UBL $\Delta$  (B). Green regions represent sequences of homology; dashed lines indicate homologous recombination events; and orange triangles denote Cre-Lox specific sites. (A) UBL truncations were generated by PCR amplification of DNA encoding an *mCherry* protein followed by a hygromycin selection cassette and flanked by sequences homologous to the targeted region within the yeast genome (surrounding the non-UBL encoding portion of the shuttle factor ORF). Upon transformation, strains contained a UBL-only truncation with a C-terminal *mCherry* fusion at the endogenous shuttle factor locus. (B) A Cre-Lox recombinase system was used to generate UBL $\Delta$  truncations with N-terminal *mCherry* tags. First, a PCR product was generated which encoded a hygromycin selection cassette flanked by Cre-Lox sites followed by a *mCherry* protein; this construct was flanked by homologous sequences to regions surrounding the genomic UBL domain. Thus, upon transformation, strains exhibit an excisable hygromycin cassette and *mCherry* fusion in place of the UBL domain. Cre-Lox induction followed by selection for loss of hygromycin resistance allowed isolation of strains with an endogenous  $\Delta$ UBL truncation fused with *mCherry* at the N-terminus.

### ***Fluorescence microscopy***

Live yeast cells were spun down and resuspended in water, PBS buffer, or a small volume of supernatant. Cells were immobilized on a microscopy slide using a 1% agarose pad supplemented with PBS buffer (modified from <https://www.youtube.com/watch?v=ZrZVbFg9NE8>, 2019). Images were acquired at room temperature on a Nikon Eclipse TE2000-S microscope at  $\times 600$  magnification using a Plan Apo  $\times 60/1.40$  objective and R3 Retiga camera. For GFP images, Sedat Quad filter set (Chroma 86000v2, Bellows Falls, VT) was set to an excitation wavelength of 490/20 nm and emission wavelength of 528/38 nm. *mCherry* images were obtained using

excitation and emission wavelengths of 555/28 nm and 685/40 nm, respectively. Images were collected using Metamorph (Molecular Devices) within 10 minutes of cell immobilization on microscopy slides. Fluorescent signal was analyzed and measured using Fiji (SciJava)<sup>141,142</sup>. For proteasome granule quantification, over 200 cells per experiment were counted and scored (granules/no granules). mCherry signal intensity was quantified by measuring average fluorescence intensity in 3 cells per image in 2 images and subtracting the average fluorescent intensity from 3 independent background measurements per image; graphs show signal normalized to autofluorescence.

### ***Growth conditions***

For all experiments, yeast cultures were grown in either YPD medium or synthetic defined (SD) medium (0.17% yeast nitrogen base, 0.5% (NH<sub>4</sub>)<sub>2</sub>SO<sub>4</sub>, 2% dextrose, and amino acids) and incubated at 30 °C with constant shaking. For nitrogen starvation, SD media was prepared without nitrogen base or amino acids (SD -N). For abrupt glucose starvation, SD media was prepared without dextrose (SD -G). To starve cells of either nitrogen or glucose, overnight cultures grown in YPD were diluted to an  $A_{600}$  of 0.5 in fresh media and allowed to grow to an  $A_{600}$  between 1 and 2. Cells were spun down, washed with appropriate starvation media, and inoculated to an  $A_{600}$  of 1.5 (0 hr. time point). To test gradual glucose depletion, overnight cultures grown in YPD were diluted to an  $A_{600}$  of 0.5 and allowed to grow to indicated time points. For nutrient replenishment experiments, cultures grown to the indicated time points were pelleted, washed with respective fresh media (SD complete for glucose starved cultures and YPD for cultures grown in YPD with or without azide), and re-inoculated in respective fresh media at the same  $A_{600}$  as original cultures.

### ***Drug treatments***

For proteasome inhibitor and sodium azide treatments, overnight cultures grown in YPD were diluted to an  $A_{600}$  of 0.5 in fresh media, allowed to grow to a  $A_{600}$  between 1 and 2, and drugs were added at proper concentrations: 40 mM proteasome inhibitor PS-341 (also known as Bortezomib or Velcade) was added to a final concentration of 100  $\mu$ M; 1 M sodium azide stock solution was added to a final concentration of 0.5 mM. For cycloheximide treatment, cells were first pre-treated with cycloheximide for ~20 min. before inoculation in final growth condition: overnight cultures

were diluted in fresh YPD, allowed to growth to a  $A_{600}$  between 1 and 2, and 50 mg/mL cycloheximide solution was added to a final concentration of 50  $\mu\text{g}/\text{mL}$  and cultures were incubated for  $\sim 20$  min. Next, cells were washed with respective media, inoculated at an  $A_{600}$  of 1.5 in respective media with 50  $\mu\text{g}/\text{mL}$  cycloheximide, and allowed to grow to indicated time points. Cell cycle synchronization was achieved by hydroxyurea treatment. Cultures were grown overnight in YPD, diluted to an  $A_{600}$  of 0.3, allowed to grow for 1.5 hrs. (to an  $A_{600} \sim 0.5$ ), and 1 M of hydroxyurea was added to a final concentration of 0.2 M. Light microscopy was used observe cell morphology and confirm cell cycle arrest.

### ***Canavanine phenotype screen***

Overnight cultures grown in YPD were diluted to an  $A_{600}$  of 0.5 and allowed to grow to an  $A_{600}$  between 1 and 1.5. For each strain, the equivalent volume to 1  $A_{600}$  of culture was pelleted, washed with sterile water, and resuspended in 133  $\mu\text{L}$  of sterile water. 1:4 serial dilutions of cell suspensions were made across a 96 well plate, and cells were spotted on SD -Arg plates with or without 2.5  $\mu\text{g}/\text{mL}$  canavanine. To confirm observed growth phenotypes were not caused by unequal cell concentrations, control plates (SD -Arg) were incubated at 30  $^{\circ}\text{C}$  and imaged after 2 days. +Canavanine plates were incubated up to 6 days at 30  $^{\circ}\text{C}$  before imaging.

### ***Cell lysis & immunoblotting analysis***

At indicated time points, for each strain, an  $A_{600}$  of 2 was harvested by centrifugation and immediately lysed or stored at -80  $^{\circ}\text{C}$ . Cells were lysed using a previously reported mild alkali treatment method<sup>143</sup>. In short, pellets were resuspended in 100  $\mu\text{L}$  distilled water, 100  $\mu\text{L}$  200 mM NaOH was added to cell suspensions, and samples were incubated at room temperature for 5 min. Cell suspensions were pelleted, resuspended in 50  $\mu\text{L}$  SDS-PAGE sample buffer (0.06 M Tris-HCl, pH 6.8, 5% glycerol, 2% SDS, 4%  $\beta$ -mercaptoethanol, 0.0025% bromophenol blue), boiled at 96  $^{\circ}\text{C}$  for 5 min, and supernatant was collected. 10  $\mu\text{L}$  samples were loaded and ran on 12% acrylamide SDS-PAGE gels at  $\sim 120$  V in Tris-Glycine running buffer (25 mM Tris, 192 mM glycine, 0.1% SDS), and gels were transferred onto PVDF membranes overnight at 4  $^{\circ}\text{C}$  and  $\sim 30$  V in transfer buffer (12.5 mM Tris, 100 mM glycine). Membranes were analyzed by immunoblotting using antibodies against GFP (Roche Applied Science, catalog no.11814460001),

Pgk1 (Invitrogen, catalog no.459250), and ubiquitin (LifeSensors, catalog no. VU101). Images were acquired using a Gbox imaging system (Syngene) and captured with GeneSnap software.

**Table 2-1. Strains used**

All strains were generated using one of two genetic backgrounds from a *S. cerevisiae* knockout library (BY4742)<sup>144</sup>:

- a) MAT $\alpha$  his3 $\Delta$ 1 leu2 $\Delta$ 0 lys $\Delta$ 0 ura2 $\Delta$ 0
- b) MATa can1 $\Delta$ ::STE2pr-Sp\_his5 lyp1 $\Delta$  his3 $\Delta$ 1 leu2 $\Delta$ 0 ura3 $\Delta$ 0 met15 $\Delta$ 0

Strain	Background	Genotype	Figure(s)
sJR1255	a	<i>RPNI::RPNI-GFP</i> (HIS3)	2.3, 2.5, 2.6, 2.7, 2.9, 2.11, 2.13, 2.17d
sJR1123	a	<i>RPNI::RPNI-GFP</i> (HIS3) <i>DSK2<math>\Delta</math>::KAN</i>	2.2, 2.3, 2.4, 2.5, 2.6, 2.8, 2.13
sJR1124	a	<i>RPNI::RPNI-GFP</i> (HIS3) <i>DDI1<math>\Delta</math>::KAN</i>	2.2, 2.3, 2.4, 2.5, 2.6, 2.8
sJR1127	a	<i>RPNI::RPNI-GFP</i> (HIS3) <i>RAD23<math>\Delta</math>::KAN</i>	2.2, 2.3, 2.4, 2.5, 2.6, 2.8, 2.13
sJR1203	a	<i>RPNI::RPNI-GFP</i> (HIS3) <i>RAD23<math>\Delta</math>::KAN DSK2<math>\Delta</math>::cloNAT</i>	2.7, 2.8, 2.13
sJR1220	a	<i>RPNI::RPNI-GFP</i> (HIS3) <i>RAD23<math>\Delta</math>::KAN DSK2::DSK2-MCHERRY</i> (HYG)	2.13
sJR1230	a	<i>RPNI::RPNI-GFP</i> (HIS3) <i>DSK2<math>\Delta</math>::KAN RAD23::RAD23-MCHERRY</i> (HYG)	2.13
sJR1263	a	<i>RPNI::RPNI-GFP</i> (HIS3) <i>RAD23<math>\Delta</math>::KAN DSK2<math>\Delta</math>::cloNAT DDI1<math>\Delta</math>::HYG</i>	2.9
sJR1296	a	<i>RPNI::RPNI-GFP</i> (HIS3) <i>DSK2::DSK2<math>\Delta</math>78-373-MCHERRY</i> (HYG)	2.17d
sJR1300	a	<i>RPNI::RPNI-GFP</i> (HIS3) <i>RAD23::RAD23<math>\Delta</math>79-398-MCHERRY</i> (HYG)	2.17d
sJR1334	a	<i>RPNI::RPNI-GFP</i> (HIS3) <i>DSK2<math>\Delta</math>::KAN RAD23::RAD23<math>\Delta</math>79-398-MCHERRY</i> (HYG)	2.18
sJR1335	a	<i>RPNI::RPNI-GFP</i> (HIS3) <i>RAD23<math>\Delta</math>::KAN DSK2::DSK2<math>\Delta</math>78-373-MCHERRY</i> (HYG)	2.18
sJR1313	a	<i>RPNI::RPNI-GFP</i> (HIS3) <i>DSK2::MCHERRY-DSK2<math>\Delta</math>1-77</i> (HYG)	2.19
sJR1314	a	<i>RPNI::RPNI-GFP</i> (HIS3) <i>RAD23::MCHERRY-RAD23<math>\Delta</math>1-78</i> (HYG)	2.19
sJR1359	a	<i>RPNI::RPNI-GFP</i> (HIS3) <i>DDI1::MCHERRY-DDI1<math>\Delta</math>1-80</i> (HYG)	2.19
sJR1322	a	<i>SCL1::SCL1-MCHERRY</i> (HYG) <i>RAD23::RAD23-GFP</i> (HIS)	2.14, 2.15
sJR1323	a	<i>SCL1::SCL1-MCHERRY</i> (HYG) <i>DSK2::DSK2-GFP</i> (HIS3)	2.14, 2.15
sJR1324	a	<i>SCL1::SCL1-MCHERRY</i> (HYG) <i>DDI1::DDI1-GFP</i> (HIS3)	2.14, 2.15
sJR1052	b	<i>RPNI::RPNI-GFP</i> (cloNAT)	2.2, 2.3, 2.4, 2.5, 2.6, 2.7, 2.8, 2.10, 2.17

sJR1208	b	<i>RPNI::RPNI-GFP</i> (cloNAT) <i>DSK2::DSK2-MCHERRY</i> (HYG)	2.12
sJR1210	b	<i>RPNI::RPNI-GFP</i> (cloNAT) <i>DDI1::DDI1-MCHERRY</i> (HYG)	2.12
sJR1222	b	<i>RPNI::RPNI-GFP</i> (cloNAT) <i>RAD23::RAD23-MCHERRY</i> (HYG)	2.12
sJR1228	b	<i>RPNI::RPNI-GFP</i> (cloNAT) <i>DSK2::DSK2Δ78–373-MCHERRY</i> (HYG)	2.17
sJR1229	b	<i>RPNI::RPNI-GFP</i> (cloNAT) <i>DDI1::DDI1Δ81–428-MCHERRY</i> (HYG)	2.17
sJR1234	b	<i>RPNI::RPNI-GFP</i> (cloNAT) <i>RAD23::RAD23Δ79–398-MCHERRY</i> (HYG)	2.17

**Table 2-2. Truncation amino acid ranges**

Protein	Truncation	AA range
Rad23	UBL	1-78
	UBLΔ	79-398
Dsk2	UBL	1-77
	UBLΔ	78-373
Ddi1	UBL	1-80
	UBLΔ	81-428

## Results

### Shuttle factors are not required for proteaphagy

Under nitrogen starvation, proteasomes are susceptible to autophagic degradation. Like other large molecular complexes and organelles, proteaphagy involves specific factors in addition to core autophagy machinery. In *Arabidopsis*, Rpn10, an RP subunit harboring an ubiquitin receptor, is important for proteaphagy<sup>18</sup>. RP is found both incorporated into 26S proteasomes as well as in an extraproteasomal pool<sup>71</sup>. Similar to shuttle factors, unincorporated Rpn10 has the capacity to interact with polyubiquitinated substrates as well as proteasomes. In mammalian cells, p62 has been identified as a proteaphagy adaptor—p62 links proteasomes to autophagosome components<sup>20</sup>. Although a p62 homolog does not exist in yeast, yeast shuttle factors and p62 share structural and functional similarities—both p62 and yeast shuttle factors interact with polyubiquitinated proteins via UBA domains and deliver them to proteasomes<sup>135</sup>. Additionally, in the mammalian system, ubiquilins, which are the mammalian homologs of yeast Dsk2, are important for general autophagy<sup>145</sup>. Therefore, as proteins that 1) directly interact with

proteasomes and 2) share homologs involved in autophagy, we hypothesized shuttle factors may serve as proteaphagy adaptors in yeast.

To test this hypothesis, we monitored autophagic degradation of proteasomes in strains deleted for each shuttle factor using a GFP cleavage assay. In addition to localization studies, GFP tags are useful for monitoring vacuolar degradation of fusion proteins. The beta barrel structure of GFP is fairly resistant to vacuolar hydrolases, while the linker between GFP and a tagged protein is extremely susceptible to hydrolytic cleavage. Therefore, upon delivery to the vacuole, GFP is cleaved from a tagged protein resulting in a “free GFP” species. To monitor proteasome autophagy within strains deleted for each shuttle factor, an endogenous GFP tag was incorporated on the C-terminus of proteasomal subunit Rpn1. Rpn1-GFP is a common proteasomal tag which exhibits normal incorporation into proteasomes and does not influence proteasome activity or localization<sup>25,35,146</sup>. Within these strains, vacuolar degradation of proteasomes was monitored by measuring the disappearance of a Rpn1-GFP band (~136 kDa) and a corresponding accumulation of free GFP (~27 kDa) on a Western blot.

We tested the effect of shuttle factor deletions on two conditions that induce proteaphagy: 1) nitrogen starvation, and 2) proteasome inhibitor treatment. To test if Rad23, Dsk2, or Ddi1 are important for either proteaphagy pathway, shuttle factor knockout strains with Rpn1-GFP tags were exposed to both nitrogen starvation conditions as well as proteasome inhibitor treatment. Samples were collected before and after treatments, lysed, and analyzed via Western blot against GFP. Under both conditions, the accumulation of free GFP in each mutant strain was comparable to WT (Figure 2.2). This indicates that, in yeast, none of the three shuttle factors are required for efficient starvation or inhibitor induced proteaphagy.

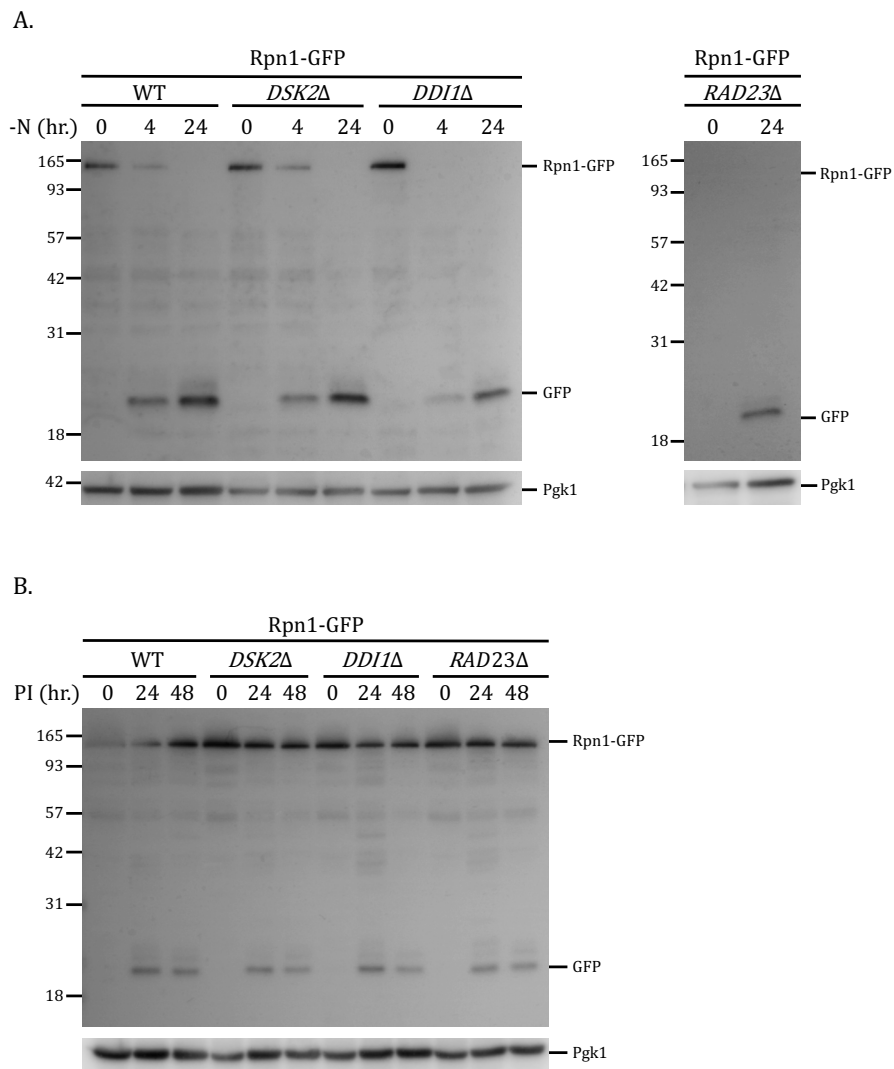


**Figure 2-2. Shuttle factor deletions do not affect known proteaphagy pathways.**

*Autophagic degradation of proteasomes was monitored using a GFP cleavage assay. (A + B) The indicated strains were grown to log phase and either inoculated in SD-N media (A) or treated with proteasome inhibitor PS-341 (B). Cells were collected at indicated time points and lysed. Whole cell lysates were resolved on an SDS-PAGE gel and immunoblotted against GFP. Pgk1 was used as a loading control. The comparable accumulation of a free GFP band (~27 kDa) between mutant strains and WT under both conditions indicates shuttle factors are not essential for proteaphagy induced by either nitrogen starvation or proteasome inhibition.*

### **Rad23 and Dsk2 are required for proteasome granule formation under certain conditions**

In the mammalian system, ubiquilin-2, a Dsk2 homolog, is capable of liquid-liquid phase separation and localizes to foci reminiscent of proteasome granules under certain conditions<sup>136</sup>. Additionally, shuttle factors link proteasomes to ubiquitin which has been identified as a major

PSG component<sup>16</sup>. Thus, we hypothesized shuttle factors may be involved in PSG formation via phase separation or direct transport of proteasomes. To test this hypothesis, we monitored PSG formation in shuttle factor knockout strains with Rpn1-GFP tags (used above) using fluorescence microscopy. In short, proteasome granules were induced by specific growth conditions and proteasome localization was visualized in live cells. PSG formation was induced using three different conditions: 1) growth in rich media (YPD) over an extended period of time, 2) exposure to sodium azide, a novel PSG inducer identified by our lab, and 3) overnight growth in media without a carbon source (SD -G). Examination of these three conditions allowed us to test granules that form under varying metabolic states. Prolonged growth in YPD is a mild starvation condition—glucose is gradually depleted from the media as cells proliferate. Overnight growth in SD -G media, conversely, is an immediate and intense starvation condition. Logarithmically growing cells are transferred to media without a carbon source leading to abrupt changes in cell signaling. Finally, sodium azide inhibits cytochrome oxidase, the final enzyme in the electron transport chain. Inhibition of cytochrome oxidase blocks aerobic respiration and limits ATP production similar starvation conditions.

To test if shuttle factors are important for PSG formation after gradual glucose depletion, Rpn1-GFP tagged strains were grown in YPD for 48 hr. and analyzed by fluorescence microscopy. The fraction of cells with PSGs in each knockout strain was compared to wildtype. About ~10% of WT cells exhibited proteasome localization to granules after 24 hr. growth, and this percentage increased to ~40% after 48 hr. (Figure 2.3a & b). The deletion of either *DSK2* or *RAD23* reduced the fraction of cells with PSGs by ~65-75% at both time points (Figure 2.3a & c). This suggests Dsk2 and Rad23 both contribute to proteasome localization to granules under conditions of slow nutrient depletion. Interestingly, in contrast to Rad23 and Dsk2, deletion of *DDI1* substantially increased the fraction of cells with granules at both 24 hr. and 48 hr. time points. (Figure 2.3a & c). Additionally, logarithmically growing *DDI1*Δ cells exhibited granular localization of proteasomes in the absence of starvation (Figure 2.3a). The early formation of granules in *DDI1*Δ cells indicates a role for Ddi1 in the prevention of premature proteasome granule localization when glucose is abundant. In sum, when glucose is gradually depleted, Rad23 and Dsk2 are important for efficient proteasome granule formation, and when glucose is readily available, Ddi1 has a role in PSG prevention.

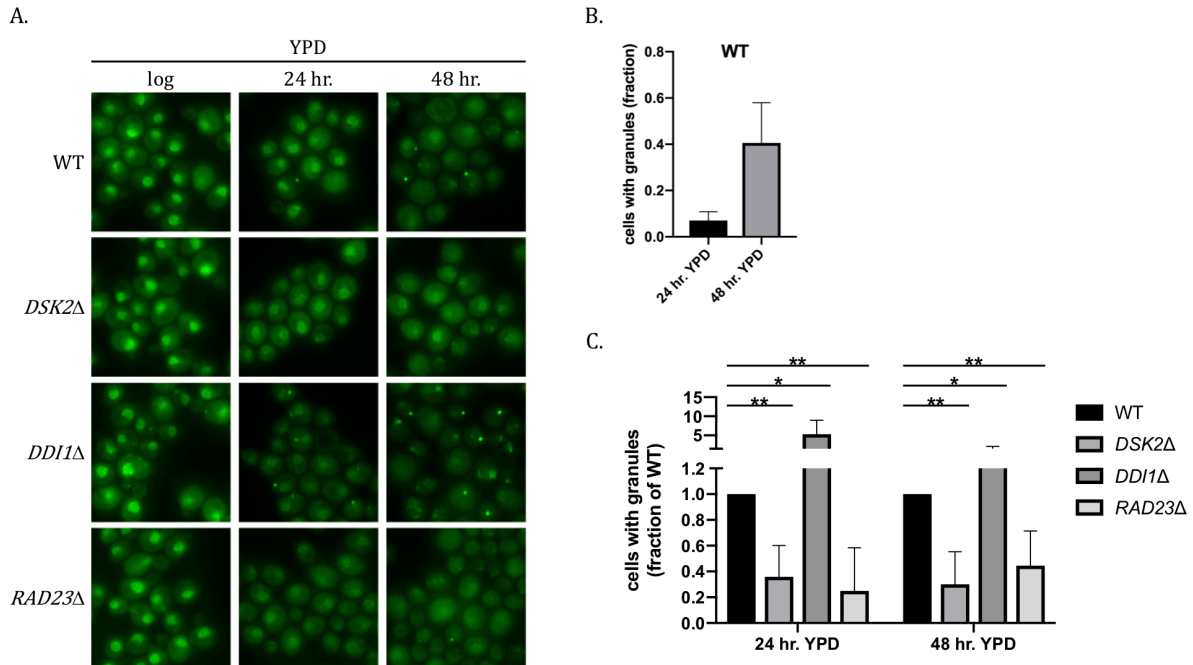


**Figure 2-3. Rad23 and Dsk2 are important for the formation of proteasome granules in rich media.**

The indicated *Rpn1-GFP* strains were grown in YPD and proteasome localization was visualized at indicated time points in live cells using fluorescence microscopy. (A) After 48 hr. growth in YPD, WT and *DDI1Δ* cells exhibited proteasome granules while granular localization of proteasomes was observably reduced in *RAD23Δ* and *DSK2Δ* mutants. Additionally, *DDI1Δ* cells showed uncharacteristic proteasome granules during logarithmic growth. (B) In WT cells, the fraction of cells with proteasome granules after growth in YPD at indicated time points was quantified. (C) The fraction of cells with proteasome granules after growth in YPD at indicated time points in mutant strains was quantified and normalized to WT. A single asterisk (\*) indicates a *p*-value < 0.05, and a double asterisk (\*\*) denotes a *p*-value < 0.005.

It has been shown that individual shuttle factor deletions can influence ubiquitin levels and cell cycle progression based on impaired substrate delivery to the proteasome<sup>50,101</sup>. To test if ubiquitin accumulation correlated with the observed defects in PSG formation, polyubiquitin levels in knockout and WT cells were monitored by Western blot under the same growth conditions. Ubiquitin levels in shuttle factor mutants were comparable to WT over 48 hr. growth in YPD (Figure 2.4a). Additionally, hydroxyurea treatment, which arrests cells in early S phase, did not influence deletion-specific effects on proteasome granules observed after 24 hr. growth. Similar to non-synchronized cultures, arrested *DDI1Δ* cells exhibited granules during logarithmic growth while *DSK2Δ* and *RAD23Δ* mutants showed inefficient PSG formation (Figure 2.4b). Thus, the deletions of shuttle factors do not appear to impair proteasome localization to PSGs through

ubiquitin level or cell cycle defects. Rather, these knockouts likely have direct effect on proteasome localization after prolonged growth in YPD.

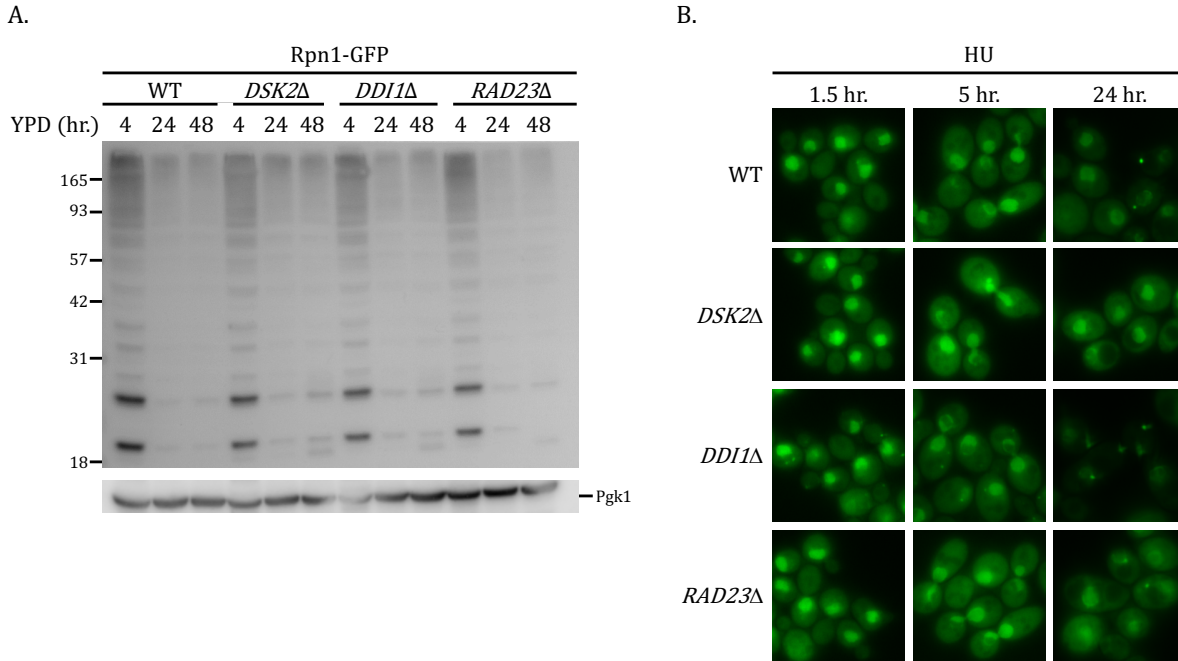


**Figure 2-4. Ubiquitin level and cell cycle arrest do not correlate with defects in PSG formation in shuttle factor mutants.**

(A) Cells were grown in YPD, collected at indicated time points, and lysed. Whole cell lysates were resolved on an SDS-PAGE gel and immunoblotted with an anti-ubiquitin antibody that recognizes poly- and mono-ubiquitinated proteins. Pgf1 was used as a loading control. Levels of ubiquitinated material (visible as a high molecular weight smear) were comparable between WT and mutant strains. (B) Logarithmically growing Rpn1-GFP tagged cells were treated with hydroxyurea and proteasome localization was visualized in live cells at indicated time points using fluorescence microscopy. Mutant strains exhibited similar defects in proteasome granule localization to non-arrested cells in Figure 2.3a.

Similar to prolonged growth, granule formation induced by sodium azide treatment was also impaired by DSK2 or RAD23 deletion. After 24 hr. of exposure to sodium azide, about ~65% of WT cells exhibit proteasome granules (Figure 2.5a & b). Unlike YPD conditions where the fraction of cells with granules increased with time, the fraction of cells with granules after azide treatment remained the same between 24 hr. and 48 hrs. (Figure 2.5b). This is most likely due to the fact that azide is a more potent inducer of proteasome granules than prolonged growth. We speculate, upon exposure to sodium azide, granule formation in WT cells reaches an equilibrium prior to the 24 hr. time point. In response to azide exposure, the DSK2 and RAD23 deletions reduced the fraction of cells with proteasome granules although less dramatically than after growth

in YPD (Figure 2.5a & c). While the reduction in granule formation for *RAD23Δ* cells was consistent over time (~50% at both time points), the defect in proteasome granule formation observed in *DSK2Δ* cells lessened over time. After 48 hrs. of azide exposure, *DSK2Δ* cells only showed a ~20% reduction in the fraction of granule-harboring cells compared to WT. This indicates deletion of *DSK2* delays granule formation in azide-treated cells. Thus, Dsk2 might facilitate early steps of granule formation while Rad23 may contribute to both PSG formation and maintenance.

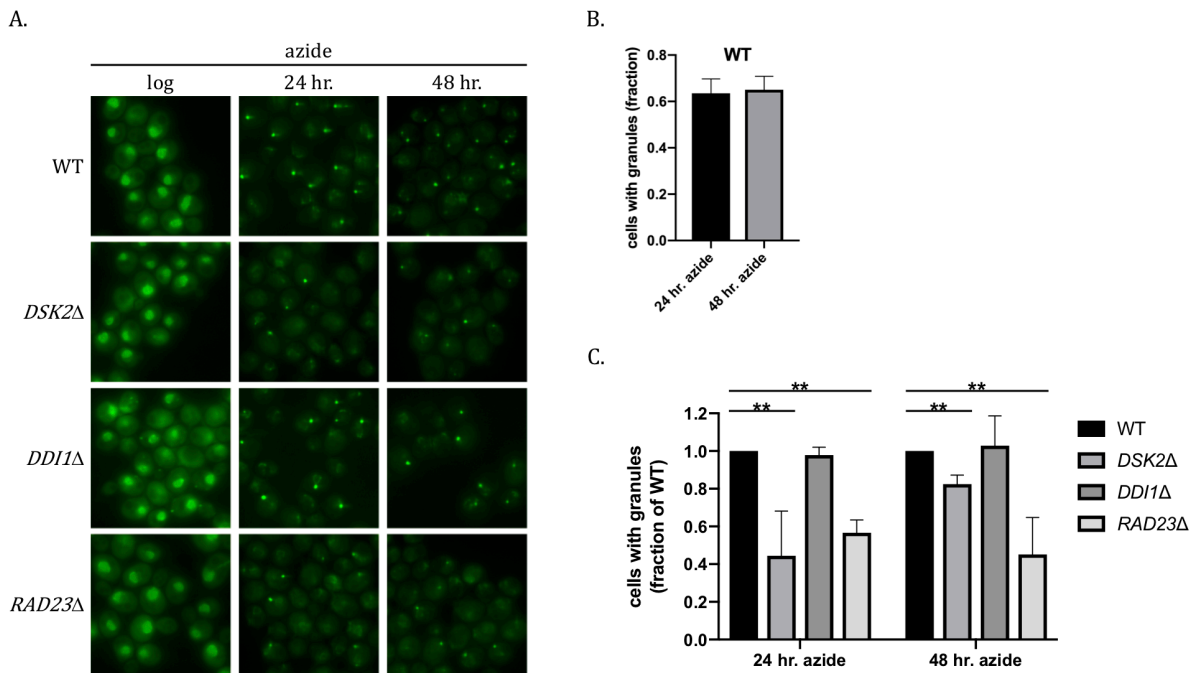


**Figure 2-5. Rad23 and Dsk2 are important for efficient targeting of proteasomes to granules in response to azide exposure.**

Logarithmically growing *Rpn1-GFP* strains were treated with sodium azide and proteasome localization was visualized at indicated times points in live cells using fluorescence microscopy. (A) All strains showed proteasome granules after sodium azide treatment; however, compared to WT, the fraction of cells with granules was reduced in *RAD23Δ* and *DSK2Δ* mutants. (B) In WT cells, the fraction of cells with proteasome granules after growth in the presence of sodium azide at indicated time points was quantified. (C) The fraction of cells with proteasome granules upon sodium azide treatment in mutant strains was quantified and normalized to WT. A single asterisk (\*) indicates a *p*-value < 0.05, and a double asterisk (\*\*) denotes a *p*-value < 0.005.

Finally, shuttle factor mutants were tested for ability to form PSGs under commonly used abrupt glucose starvation conditions. Logarithmically growing cells were transferred to SD media without carbon and allowed to grow overnight. No significant differences between WT and shuttle

factor knockouts were observed; all strains showed PSGs in ~60% of cells after starvation (Figure 2.6). In summary, the requirements of Dsk2 and Rad23 for PSG formation vary by condition: Dsk2 and Rad23 play an important role in proteasome localization to granules upon gradual glucose depletion as well as sodium azide exposure; however, their role is not crucial, if they play a role at all, in the formation of PSGs upon abrupt glucose starvation.

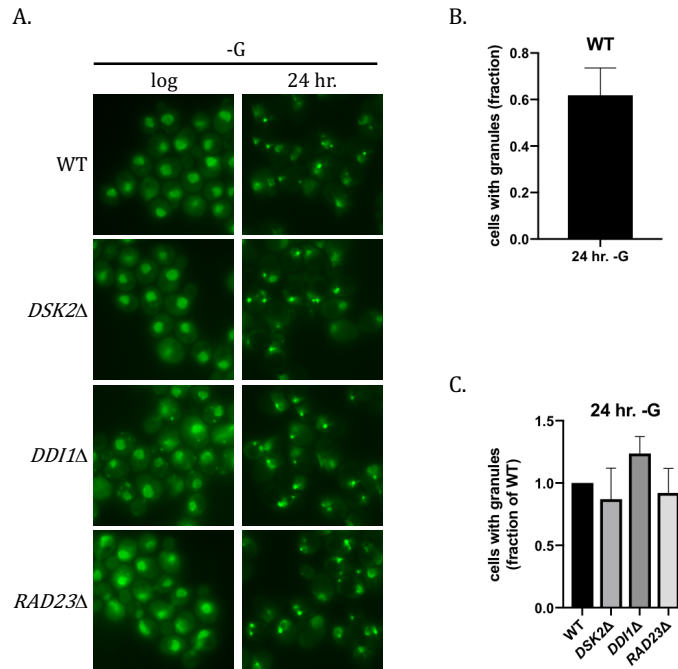


**Figure 2-6. Rad23 and Dsk2 are nonessential for proteasome granules that form upon abrupt glucose starvation.**

*Logarithmically growing Rpn1-GFP strains were transferred to SD -G media and grown overnight. Proteasome localization was observed in live cells by fluorescence microscopy at the indicated time point. (A) Proteasome shuttle factor mutants exhibited comparable PSG formation to WT in response to abrupt glucose starvation. (B) The fraction of WT cells with proteasomes granules after glucose starvation was quantified. (C) The fraction of cells with proteasome granules upon glucose starvation in mutant strains was quantified and normalized to WT.*

Deletion of *RAD23* or *DSK2* greatly reduced granule formation in YPD, showed a moderate defect in azide-induced granules, and did not significantly influence PSG formation after glucose starvation. However, Rad23 and Dsk2 have been reported to have redundant functions including their shared proteolytic role in the general delivery of substrates to the proteasome<sup>50,84</sup>. Therefore, we hypothesized deletions of *RAD23* or *DSK2* may produce varying degrees of PSG defects across conditions due to Rad23 and Dsk2 redundancy in granule formation. In other words,

the defect in proteasome granule formation observed in single knockout strains may be limited (under gradual starvation/azide treatment) or nonexistent (under abrupt glucose starvation) due to Rad23 and Dsk2 redundancy. To test this possibility, we generated a double knockout strain of Dsk2 and Rad23 (*RAD23Δ DSK2Δ*) with an endogenous Rpn1-GFP tag. If Rad23 and Dsk2 have a redundant function in granule formation, we would expect the double knockout to completely prevent granules. This strain was exposed to granule inducing conditions and analyzed by fluorescence microscopy. Granules induced by prolonged growth and azide exposure were almost completely prevented by the double knockout of *DSK2* and *RAD23* (Figure 2.7). However, after abrupt glucose starvation, granule formation in the double knockout strain was comparable to WT (Figure 2.7). Thus, Dsk2 and Rad23 share a partially redundant role in proteasome granule formation upon prolonged growth and azide treatment; however, neither factor is required for proteasome localization to granules in response to abrupt glucose depletion.

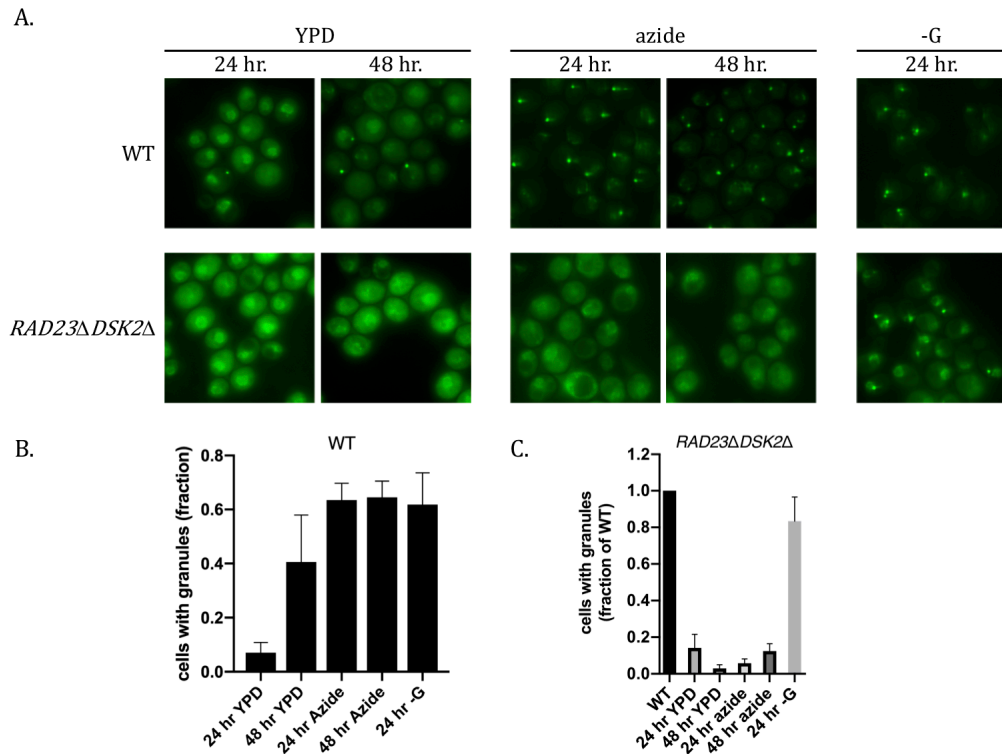


**Figure 2-7. Deletion of both *RAD23* and *DSK2* almost completely abrogates proteasome localization to granules under certain conditions.**

*Proteasome granules were induced by indicated treatments in Rpn1-tagged WT and RAD23ΔDSK2Δ cells. Fluorescence microscopy was used to monitor proteasome localization in live cells at indicated time points. (A) Compared to WT, RAD23ΔDSK2Δ cells showed a reduction in proteasome granules after growth in YPD and*

exposure to azide. However, granule formation upon glucose starvation was comparable between WT and *RAD23ΔDSK2Δ* cells. (B) The fraction of WT cells with proteasome granules was quantified under indicated conditions. (C) Under each condition, the fraction of cells with proteasome granules in a *RAD23Δ DSK2Δ* mutant was quantified and normalized to WT.

Granules were not detected in *RAD23Δ DSK2Δ* cells grown in YPD. However, at the latest time point analyzed (48 hr.), we speculate granule formation has not reached an equilibrium and cells are actively forming PSGs (Figure 2.7b). Thus, one explanation for the different requirements of Dsk2 and Rad23 under different conditions is that the double knockout of *DSK2* and *RAD23* delays granule formation upon mild starvation conditions, but this delay is not observed under extreme starvation conditions like glucose starvation. To test if Rad23 and Dsk2 are essential for granule formation in YPD, we analyzed proteasome granule formation over the course of five days. As cells proliferate, glucose is readily metabolized and depleted from the media. Therefore, if the double knockout of *DSK2* and *RAD23* delays granule formation in YPD, we would reasonably expect PSGs to be visible after five days of growth when glucose availability is extremely low. Single mutants and a double knockout strain were grown in YPD and analyzed by fluorescence microscopy at several time points. Single deletions of *RAD23* and *DSK2* delayed granule formation, while a double knockout of *RAD23* and *DSK2* completely prevented PSG formation even after five days of growth (Figure 2.8). This indicates that the defects in proteasome granules observed in *RAD23ΔDSK2Δ* cells were not due to delayed granule formation, but rather, Rad23 and Dsk2 are essential for granules induced by YPD or azide. Conversely, PSGs induced by glucose starvation do not depend on Rad23 or Dsk2 (Figure 2.7a & c). Therefore, we predict at least two different types of proteasome granules form in response to different conditions.

While the deletion of both *RAD23* and *DSK2* completely prevented proteasome granule formation in YPD, single knockout strains showed a delay in granule formation over time (Figure 2.8). Additionally, granules that form in single knockout cells at later times were less intense than WT indicative of inefficient PSG targeting. Together, these results suggest Rad23 and Dsk2 exhibit partial redundancy in granule formation. In other words, Rad23 and Dsk2 can partially compensate for one another in single deletion strains, and PSGs still form albeit delayed and inefficiently. However, the deletion of both factors completely prevents PSG formation in rich media. In sum, Rad23 and Dsk2 are required for granule formation under gradual starvation as well as azide treatment. However, neither factor is essential for proteasome targeting to PSGs in response to

abrupt glucose starvation. This indicates proteasomes can be targeted to granules in two distinct pathways: Rad23/Dsk2-dependent and Rad23/Dsk2-independent.

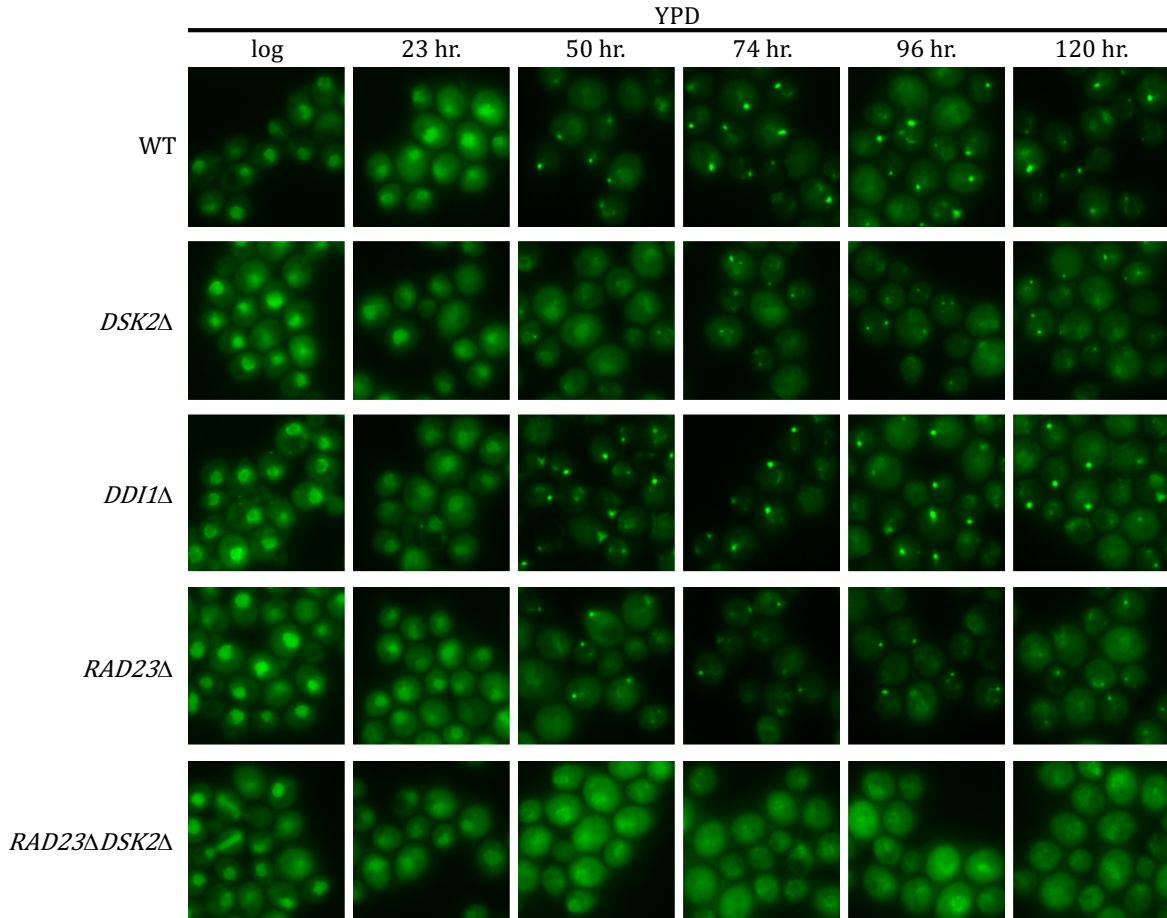


**Figure 2-8. Rad23 and Dsk2 have partially redundant functions in proteasome granule formation under gradual glucose depletion.**

*Indicated Rpn1-GFP tagged strains were grown in YPD, and proteasome localization in live cells was visualized using fluorescence microscopy at indicated time points. While RAD23 and DSK2 single knockouts exhibited a delay in granule formation, deletion of both proteins completely prevented proteasome granules even after five days of growth. Deletion of DDI1, on the other hand, caused proteasome granules to form more quickly than WT.*

Interestingly, unlike Rad23 and Dsk2 mutants, strains deleted for *DDI1* showed a dramatic increase in the fraction of cells with PSGs after growth in rich media (Figure 2.3a & c). *DDI1Δ* cells also exhibited earlier granule formation compared to WT when cells were grown in YPD (Figure 2.8). This suggests Ddi1 acts as an inhibitor of granule formation when nutrients are abundant, presumably by binding proteasomes or controlling the stability of specific substrates

that impact the process. If direct binding of Ddi1 to proteasomes is involved in granule inhibition, it could imply proteasome localization to granules is controlled by competition for proteasome binding amongst shuttle factors. Therefore, a double knockout of *RAD23* and *DSK2* could reduce competition for proteasomal binding and promote Ddi1-mediated granule inhibition. To test if Ddi1-mediated inhibition is responsible for the PSG defect observed in *RAD23ΔDSK2Δ* cells, we generated a triple knockout strain (*RAD23ΔDSK2ΔDDI1Δ*) and analyzed granule formation after prolonged growth, azide treatment, and glucose starvation. If Ddi1 inhibition prevents granules in *RAD23Δ DSK2Δ* cells, we would expect deletion of *DDI1* to rescue granule formation. The triple knockout strain, like the *RAD23Δ DSK2Δ* double knockout, showed impaired granule formation after prolonged growth and azide treatment, but not glucose starvation (Figure 2.9). In other words, deletion of *DDI1* did not rescue proteasome granule formation in *RAD23ΔDSK2Δ* cells. This indicates proteasome granules are not solely regulated by Ddi1 binding. Instead, Rad23 and Dsk2 likely have direct roles in PSG assembly. In an inverse model, the higher occurrence of PSGs in *DDI1Δ* cells might result from increased Rad23/Dsk2 binding to proteasomes. Within this model, deletion of *DDI1* relieves competition for proteasomal binding, and direct interactions between Rad23/Dsk2 and proteasomes promote granule formation.

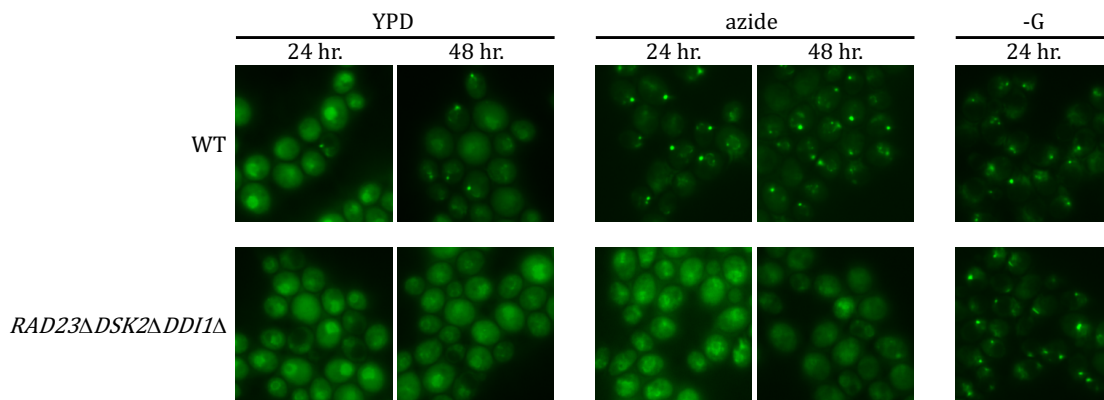


**Figure 2-9. Deletion of *DDI1* does not rescue proteasome granule formation in *RAD23ΔDSK2Δ* cells.**

*Proteasome granules were induced by indicated treatments in Rpn1-GFP tagged WT and *RAD23ΔDSK2ΔDDI1Δ* cells. Fluorescence microscopy was used to monitor proteasome localization in live cells at indicated time points. (A) Similar to *RAD23ΔDSK2Δ* cells in Figure 2.7, triple KO cells showed a significant reduction in proteasome granules compared to WT after growth in YPD and exposure to sodium azide.*

## **Different proteasome granules form based on inducing conditions**

Rad23 and Dsk2 are required for proteasome localization to granules induced by prolonged growth or azide treatment, but not abrupt carbon starvation. Overnight glucose starvation and growth in YPD for five days are both strong starvation conditions. Yet, Rad23 and Dsk2 are only required for proteasome granule formation in YPD. Therefore, we predicted at least two different types of proteasome granules form in response to different cellular energy states. We wanted to test if additional properties distinguished these two types of proteasome granules from one another. One readout used to distinguish between stress granules/P bodies and other granular structures is cycloheximide sensitivity. Cycloheximide blocks protein synthesis by interfering with tRNA-mRNA translocation during translation. It has been shown that stress granules and P bodies, which require mRNA and protein translation sites, do not form in the presence of cycloheximide<sup>41,44,45,147</sup>. To test if proteasome granules require active protein translation sites, Rpn1-GFP tagged WT cells were exposed to granule inducing conditions in the presence or absence of cycloheximide. Cycloheximide prevented proteasome granules induced by azide and prolonged growth in YPD but did not affect PSG formation upon glucose starvation (Figure 2.10). Thus, in addition to Dsk2 and Rad23 requirements, cycloheximide sensitivity further distinguishes between granules induced by abrupt carbon starvation and granules induced by prolonged growth or azide treatment. Rad23/Dsk2-dependent granules require active protein translation, while Rad23/Dsk2-independent granules form even when translation is blocked. Therefore, we propose at least two different types of proteasome granules exist and form in response to varying carbon availability.

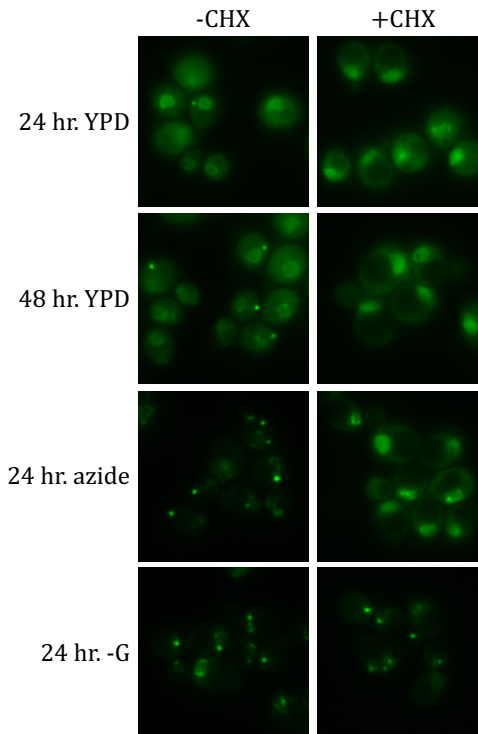


**Figure 2-10. Cycloheximide sensitivity distinguishes between proteasome granules that form under different conditions.**

*Rpn1-GFP tagged WT cells were exposed to granule inducing conditions in the presence or absence of cycloheximide. Proteasome localization in live cells was visualized using fluorescence microscopy at indicated time points. Cycloheximide treatment prevented proteasome granule formation when cells were grown in YPD or exposed to sodium azide but did not influence PSG formation during glucose starvation.*

In addition to cycloheximide sensitivity, we also tested how long it took different granules to disassemble upon nutrient replenishment. Rpn1-GFP tagged WT cells grown in YPD or treated with azide were spun down and re-inoculated in fresh YPD, while carbon starved cells were spun down and re-inoculated in SD complete media. Samples were collected at 5 min. and 15 min. after re-inoculation and examined under the microscope. Consistent with previous reports, granules induced by all three conditions disassembled within 15 min. upon carbon replenishment<sup>15,16</sup>. However, granules induced by prolonged growth in YPD (after 48 hr. and 6 days) as well as azide treatment were already dissolved after 5 min. of replenishment while granules in glucose starved cells remained intact at this time point (Figure 2.11). Therefore, granules that form under abrupt carbon starvation may be slightly more resistant to nutritional changes. Consistently, 15 min. after re-inoculation, glucose starved cells showed proteasome localization at the nuclear periphery while cells treated with azide or grown in YPD exhibited diffuse proteasomal signal in the nucleus

(Figure 2.11). This indicates cytoplasmic-to-nuclear targeting of proteasomes in PSGs induced by glucose starvation may be slower than (and distinct from) other proteasome granule disassembly pathways. Then again, SD complete media is less rich than YPD and, consequently, may produce weaker signaling events that induce proteasome re-localization from PSGs to the nucleus. Thus, additional experiments are required to consider granule disassembly time a true distinguishing characteristic among proteasome granules.

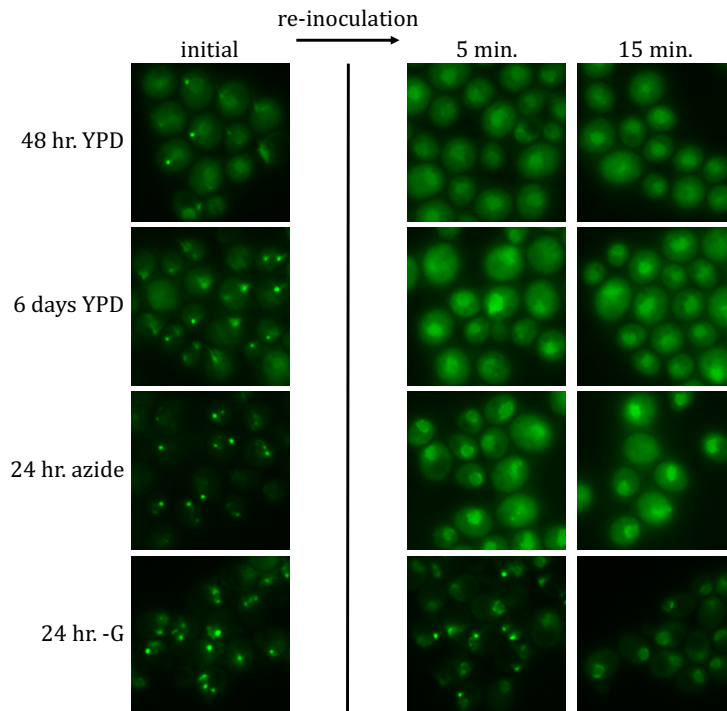


**Figure 2-11. Characterization of proteasome granules induced by different conditions based on disassembly.**

*Rnp1-GFP tagged WT cells were grown under the indicated conditions (“initial”), spun down, and re-inoculated in nutrient rich media; cells grown in YPD with or without azide were re-inoculated in YPD while cells grown in SD – G were re-inoculated in SD complete media. Proteasome granule disassembly was monitored at the indicated time points in live cells using fluorescence microscopy. All proteasome granules were dissolved within 15 min. of re-inoculation. However, after 5 min. following re-inoculation, PSGs induced by glucose starvation remained intact while granules induced by other conditions were already disassembled.*

### **Rad23 and Dsk2, but not Ddi1, localize to proteasome granules**

Rad23 and Dsk2 are both important for proteasome localization to granules under certain conditions, specifically, after prolonged growth or azide treatment. As proteins that have an

established protein delivery role as well as proteasomal binding sites, we hypothesized Rad23 and Dsk2 may directly deliver proteasomes to granules under these conditions. Within this model, we would expect Rad23 and Dsk2 to localize to proteasome granules which form upon gradual glucose depletion or azide exposure. Additionally, we would not expect Ddi1, as a proteasome granule inhibitor, to co-localize with proteasome granules under this hypothesis. To test our model, we generated strains with endogenous C-terminal mCherry tags on each shuttle factor in a Rpn1-GFP background strain. Thus, shuttle factor localization as well as proteasome localization could be monitored by fluorescence microscopy within the same strain.

Doubly tagged strains were exposed to granule inducing conditions and analyzed under the microscope. As predicted, Rad23 and Dsk2 co-localized with proteasome granules after 48 hr. growth in YPD as well as after azide treatment (Figure 2.12). Interestingly, although neither protein is required for proteasome localization to granules upon glucose starvation, Rad23 and Dsk2 also co-localized with proteasome granules under this condition. Since neither protein is important for PSGs induced by glucose starvation, we speculate Rad23 and Dsk2 co-localization with these granules is due to proteasomal binding and does not represent a role in granule formation. Ddi1, consistent with our predication, did not co-localize with proteasome granules under any condition.

Confusingly, in addition to granular localization, shuttle factors exhibited localization to non-nuclear compartments that align with vacuoles (vacuoles are devoid of proteasome signal under these conditions) (Figure 2.12). This phenomenon was especially apparent in Dsk2 and Ddi1 tagged strains after growth in YPD. Additionally, the doubly tagged Dsk2/Rpn1 strain showed delayed granule formation in YPD compared to a Rpn1-GFP tag alone (Figure 2.3, Figure 2.12). Previous experiments carried out by our lab revealed vacuolar autofluorescence produces a similar non-nuclear compartmental signal. Therefore, we predicted either 1) due to low expression of the tagged shuttle factors, mCherry autofluorescence may interfere with detection or 2) a C-terminal mCherry tag may interrupt shuttle factor function and cause vacuolar degradation.

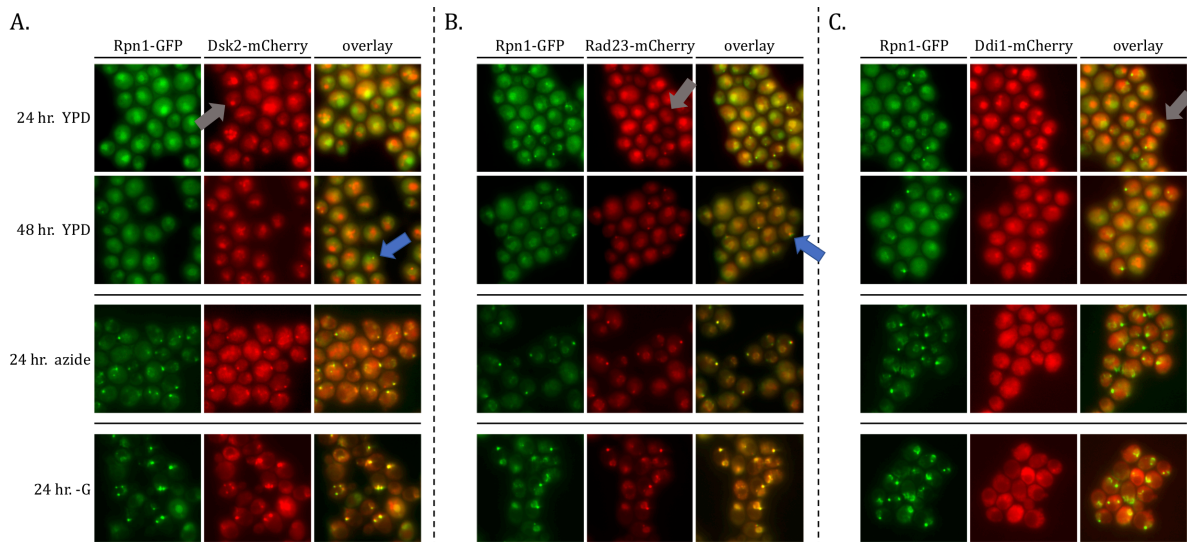


**Figure 2-12. Rad23 and Dsk2 co-localize with proteasome granules.**

Shuttle factor and proteasome localization were visualized in doubly tagged strains using fluorescence microscopy. Blue arrows indicate cells with co-localized granules while gray arrows specify cells which exhibit vacuolar mCherry signal. (A + B) Dsk2-mCherry and Rad23-mCherry co-localized with proteasome granules under all tested conditions. (C) Ddi1-mCherry did not co-localize with proteasome granules under any tested conditions. (A + B + C) All shuttle factor-mCherry fusions produced vacuolar signal.

To test whether or not mCherry tags influence shuttle factor function, we used a canavanine phenotype screen. Canavanine is an arginine analog that causes protein misfolding. Sensitivity to canavanine can therefore indicate protein quality control defects including inefficient substrate shuttling. We tested several mutants for canavanine sensitivity and found, consistent with previous reports, a double knockout of *DSK2* and *RAD23* displays a strong phenotype, while single deletions of either protein do not<sup>93</sup> (Figure 2.13). To determine if mCherry tags influence shuttle factor function, we compared strains with an mCherry tag on one shuttle and deletion of the other to single and double deletion strains. Our logic was as follows: if a *RAD23*Δ Dsk2-mCherry strain (or *DSK2*Δ Rad23-mCherry) shows canavanine sensitivity similar to a double knockout, then mCherry tags likely interrupt shuttle-factor mediated proteolysis; conversely, similar sensitivity to a single knockout indicates a C-terminal tag has little to no influence on shuttling capacity. Our screen showed that both strains (*RAD23*Δ Dsk2-mCherry and *DSK2*Δ Rad23-mCherry) display a phenotype similar to respective single deletions. (Figure 2.13). Thus, the proteolytic function of shuttle factors, at least in response to canavanine stress, is likely maintained in C-terminal mCherry

fusions. However, this result offers little explanation for the observed vacuolar localization of Dsk2 and Ddi1.

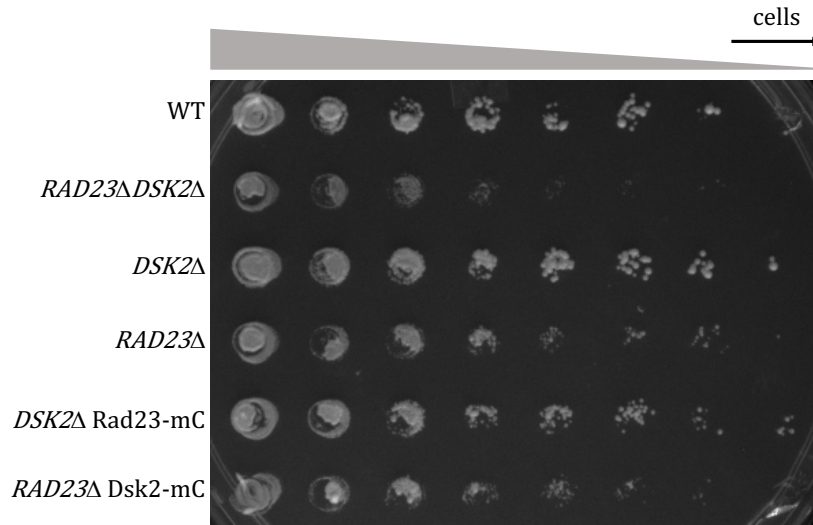


**Figure 2-13. C-terminal mCherry tags on shuttle factors have do not affect canavanine sensitivity.**

*Functionality of mCherry tagged shuttle factors was assayed using a canavanine phenotype screen. Equal cells from logarithmically growing cultures were harvested and four-fold dilutions were spotted onto +canavanine plates. Strains with both an mCherry tag and shuttle factor deletion exhibited a phenotype similar to respective single knockout strains.*

Next, we sought to determine if the mCherry signal observed in the vacuole was true shuttle factor localization or autofluorescence. One way to determine if shuttle factors are, indeed, susceptible to vacuolar degradation (as suggested by the mCherry signal) would be to monitor shuttle factor degradation by Western blot against mCherry; accumulation of a free mCherry species that corresponds with vacuolar localization would indicate cleavage of the exposed linker between mCherry and the fused shuttle protein. Vacuolar degradation can also be confirmed by deletion of *PEP4*, an important vacuolar hydrolase, and testing for stabilization of the mCherry fused shuttle factor. However, preliminary Western blots were difficult to interpret due to high background signal produced by the mCherry antibody. Additionally, deletion of *PEP4* can influence other cellular conditions including pH, a reported regulator of proteasome granules, which may affect shuttle factor localization<sup>34</sup>. Thus, to avoid such complications, we instead generated C-terminally GFP-tagged shuttle factor strains. Previous experiments in our lab indicated microscope settings for GFP imaging produce less autofluorescence than mCherry

settings. Indeed, GFP-tagged shuttle factors did not display vacuolar localization indicating the vacuolar signal observed in the mCherry tagged strains represents autofluorescence (Figure 2.14). Instead, in proliferating cells, shuttle factors largely localized to the nucleus and cytoplasm consistent with current literature<sup>148</sup>. Within these strains, an  $\alpha$ 1-mCherry tag was used to monitor proteasome localization. Due to high proteasomal expression, the previously problematic autofluorescence produced by the mCherry channel does not influence interpretation of proteasome localization within these strains.

Consistent with our mCherry data, GFP-tagged strains showed Rad23 and Dsk2 localize to proteasome granules after both prolonged growth and azide treatment (Figure 2.14). In cells without granules, Rad23 exhibited co-localization with proteasomal signal in the nucleus while Dsk2 signal was more diffuse throughout the cytoplasm (Figure 2.14). Surprisingly, Ddi1-GFP showed localization to granules that were previously undetected in a Ddi1-mCherry tagged strain. Specifically, after 48 hr. growth in YPD as well as after azide treatment, Ddi1 exhibited localization in cytoplasmic puncta—some Ddi1-GFP granules co-localized with proteasome granules, while some Ddi1 granules did not (Figure 2.14). To determine if these Ddi1 granules were distinct cellular structures from proteasome granules, we tested granule disassembly time upon removal of azide. Unlike proteasome granules which generally disassemble within 5 min., Ddi1-GFP granules persisted up to 35 min. after azide removal (Figure 2.15). Thus, Ddi1 granules are likely distinct from proteasome granules. Moreover, Rad23 and Dsk2 puncta dissolved from granules at the same rate as proteasomes further supporting a model in which Rad23 and Dsk2, but not Ddi1, are PSG components. Whether or not Ddi1 granules are sites of degradation for a specific substrate as well as how Ddi1 granules influence proteasome granule formation are questions for future investigation.

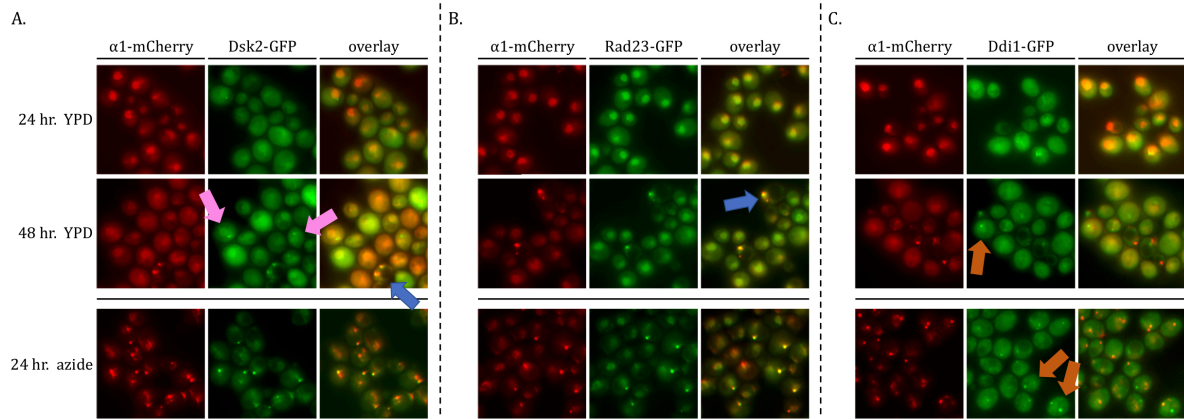


**Figure 2-14. Rad23 and Dsk2 localize to proteasome granules while Ddi1 localizes to distinct granules.**

*Shuttle factor and proteasome localization were visualized in doubly tagged strains using fluorescence microscopy. Blue arrows indicate cells with co-localized granules while pink arrows and orange arrows designate cells with Dsk2-only granules and Ddi1-only granules, respectively. (A + B) Dsk2-GFP and Rad23-GFP co-localized with proteasome after growth in YPD and exposure to azide. (C) Ddi1-GFP did not co-localize with proteasome granules under any tested conditions. Ddi1-GFP granules were observed after growth in YPD and exposure to azide.*

At earlier time points after growth in rich media, some cells exhibited Dsk2 localization to granules while proteasomal signal remained nuclear (Figure 2.14a). Thus, we hypothesized Dsk2 may function as a nucleation factor that forms an initial aggregate in response to certain environmental conditions. These Dsk2 granules would then serve as sites for proteasome delivery by Rad23. If this hypothesis is correct, then over a time course, we would expect an observable population of cells with Dsk2-only granules followed by a majority of cells with co-localized Dsk2 granules and proteasome granules. We tried looking at several time points within 72 hrs. of growth in YPD to see if there was an observable fraction of cells with Dsk2-only granules. However, we were not successful in isolating a specific time point in which a significant population of cells exhibited Dsk2 granules distinct from proteasome granules (data not shown). This is most likely due to the heterogenous population created by a logarithmically growing culture.

Another way to test this hypothesis that does not involve population statistics would be to monitor both Dsk2 and proteasome localization by fluorescent microscopy over a time course in single cells. This experiment requires a fixed position for a microscopy slide with the same frame (and therefore, same cells) for all time points. However, leaving cells on a microscope slide changes several conditions including temperature, nutrient availability, oxygen availability, pH, etc. All of these factors may contribute to signaling events that influence proteasome granule

formation. Therefore, we propose using a confocal microscope that allows control of such variables as well as fluorescence imaging of a set field of cells over a time course to determine if Dsk2, Rad23, and proteasomes are recruited to granules in a temporal fashion.

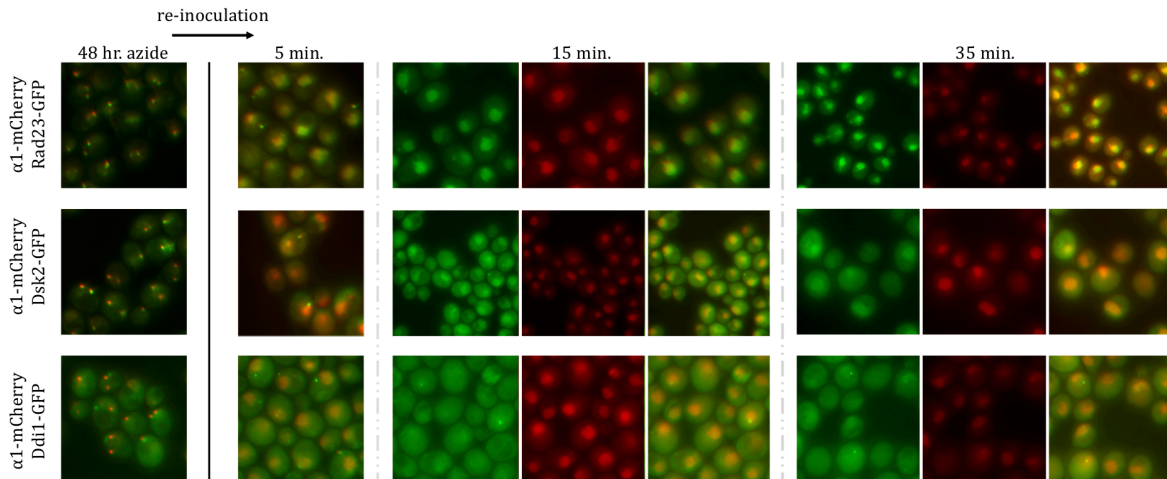


**Figure 2-15. Ddi1 granules are distinct from proteasome granules.**

*Granule disassembly was monitored in indicated strains following the removal of azide. Cells were exposed to sodium azide for 48 hr., washed, and re-inoculated in media without azide. Localization of shuttle factors and proteasomes in live cells was analyzed at the indicated time points by fluorescence microscopy. While Dsk2, Rad23, and proteasomes all disassemble from co-localized granules within 5 min. of azide removal, Ddi1-GFP granules are still observed after 35 min.*

### **Rad23 and Dsk2 UBL domains alone are not sufficient for wildtype proteasome granule formation**

Under certain conditions, Rad23 and Dsk2 are 1) required for proteasome granules to form efficiently and 2) co-localize with proteasome granules. Taken together, these data support our shuttle transport hypothesis in which proteasomes are delivered to granules by Rad23 and Dsk2. To test this model, we generated two shuttle factor truncations: 1) UBL domain alone and (<sup>UBL</sup>) and 2) UBL deletion (<sup>UBLΔ</sup>). We monitored truncation localization as well as PSG formation within these strains using fluorescence microscopy. Within our hypothesis, the UBL domain of Rad23/Dsk2 interacts with the proteasome, while the UBA domain is responsible for granular targeting. Therefore, we expected Rad23/Dsk2 UBL-only truncations to co-localize with proteasomes, but also cause inefficient granule formation. Conversely, we predicted truncations

with UBL deletions would localize to granules, but be unable to transport (and thus, not co-localize with) proteasomes.

Each shuttle factor has a N-terminal UBL domain and C-terminal UBA domain. An endogenous mCherry tag on the UBL domain was incorporated into a Rpn1-GFP background strain by generating a DNA construct with homologous regions surrounding the desired C-terminal deletion. Thus, confirmed recombinant strains contained an mCherry tag on the C-terminus of the UBL domain with the rest of the protein truncated (Figure 2.16a). For UBL $\Delta$  truncations, we were concerned that a C-terminal tag on the UBA domain would interrupt UBA interactions. Therefore, to both preserve UBA binding capacity as well as maintain the endogenous promoter, a Cre-Lox recombinase system was utilized to produce strains with an N-terminal mCherry tag in place of the endogenous UBL domain. In short, a DNA construct was generated that contained 1) a selection cassette surrounded by Cre-Lox sites, 2) mCherry open reading frame, and 3) homologous regions surrounding the endogenous UBL domain. Upon transformation, confirmed strains contained the constructs outlined in Figure 2.1b in place of the UBL domain. Recombinant strains were then transformed with an inducible Cre-Lox expressing plasmid, and Cre-Lox induction caused excision of the selection cassette. Thus, negative selection allowed isolation of desired strains expressing endogenous C-terminal truncations with N-terminal mCherry tags (Figure 2.16b).

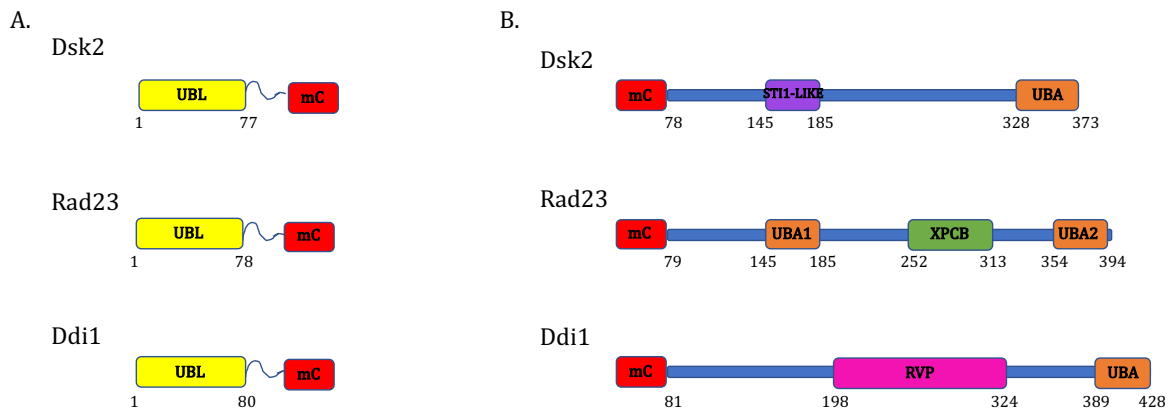


**Figure 2-16. Schematic representations of generated shuttle factor truncations.**

*Numbers indicate AA ranges of domains. (A) UBL-only truncated shuttle factors were fused with mCherry at the C-terminal end of the UBL domain. (B) UBL $\Delta$  shuttle factor truncations were generated with mCherry tags on the N terminus.*

Shuttle factor truncation strains were exposed to granule inducing conditions and proteasome localization as well as truncated shuttle factor localization was visualized using fluorescence microscopy. Compared to WT, Rad23<sup>UBL</sup> and Dsk2<sup>UBL</sup> truncations reduced proteasome granules after prolonged growth and azide treatment but had no effect on granules formed upon glucose starvation (Figure 2.17). In other words, Rad23<sup>UBL</sup> and Dsk2<sup>UBL</sup> truncations exhibited defects in proteasome granule formation similar to cells deleted for these proteins. This indicates that the UBL domain alone is not sufficient for the role of Rad23 or Dsk2 in granule formation. This is consistent with our shuttle-mediated transport model in which UBL domains mediate proteasome interaction and are thus indispensable for efficient granule formation.

Ddi1<sup>UBL</sup>, similar to a Ddi1 knockout, promoted earlier granule formation in rich media (Figure 2.17c & d). Presumably, Ddi1<sup>UBL</sup> maintains its ability to interact with proteasomes. If Ddi1-mediated inhibition of proteasome granules was mediated by competitive proteasomal binding alone, we would expect the Ddi1<sup>UBL</sup> to behave similar to WT. However, truncated strains exhibited premature proteasome granules indicating UBL domains alone are not sufficient for normal granule inhibition. Thus, it is unlikely that Ddi1 inhibits granules through competition with Rad23 and Dsk2 for proteasomal binding. Instead, Ddi1 prevents proteasome granules through an unidentified mechanism that requires either the full protein or the N-terminal portion. Therefore, inhibition of granule formation by Ddi1 may require either substrate delivery, RVP domain activity, or interaction with ubiquitinated material. To determine the mechanism of granule inhibition of Ddi1, future experiments involve analyzing Ddi1 mutants for variations in proteasome granule dynamics.

Although the effect of UBL-only truncations on proteasome localization was clear, the localization of these truncations was difficult to interpret. Once again, under certain conditions, mCherry signal was prevalent in a non-nuclear compartment that resembled vacuolar autofluorescence. This signal was especially apparent for Dsk2<sup>UBL</sup> (Figure 2.17a). Rad23<sup>UBL</sup>, on the other hand, clearly co-localized with proteasome granules after azide treatment and glucose starvation (Figure 2.17b). Because Rad23<sup>UBL</sup> and *RAD23Δ* cells exhibit similar defects in proteasome granule formation, we speculate Dsk2 redundancy is important for granule formation in both strains. Therefore, under our hypothesis in which Rad23 and Dsk2 act as proteasome transporters, Rad23<sup>UBL</sup> co-localization with proteasome granules is not due to a functional role in

proteasome transport, but rather indicates Rad23<sup>UBL</sup> interaction with proteasomes that have been delivered to granules in a Dsk2-mediated process.

Unlike Rad23, Dsk2<sup>UBL</sup> and Ddi1<sup>UBL</sup> did not appear to co-localize with proteasomes, but instead exhibited mCherry signal resembling vacuolar autofluorescence (Figure 2.17a & c). To make sure these truncations were, in fact, being expressed, we compared average cellular signal intensity produced by UBL-only truncations to autofluorescence. Under all conditions, with the exception of 48 hr. azide treatment, all mCherry fusion strains exhibited statistically higher mCherry signal than background (Figure 2.17e). Low expression could still account for the appearance of autofluorescent vacuolar signal—average cellular signal produced by tagged Dsk2<sup>UBL</sup> and Ddi1<sup>UBL</sup> truncations is markedly lower than Rad23<sup>UBL</sup> (Figure 2.17e). Thus, Dsk2<sup>UBL</sup> and Ddi1<sup>UBL</sup> levels may not produce mCherry intensity above a certain detection threshold. However, the fluorescent signal produced by mCherry fused truncations was statistically significant, and therefore, indicates expression. Additionally, previous reports have shown that truncated Dsk2 consisting of the UBL domain alone are stable *in vivo*<sup>76</sup>. Thus, although we cannot accurately assess the localization of truncated shuttle factors, we are confident that the effect on proteasome localization within these strains is not simply a result of no protein. Rather, observed defects in proteasome granule formation resulted from specific truncations. In conclusion, the C-terminal domains of Dsk2 and Rad23 are important for proteasome granule formation after prolonged growth and azide treatment, while Ddi1 C-terminal domains are required for prevention of premature proteasome granules.

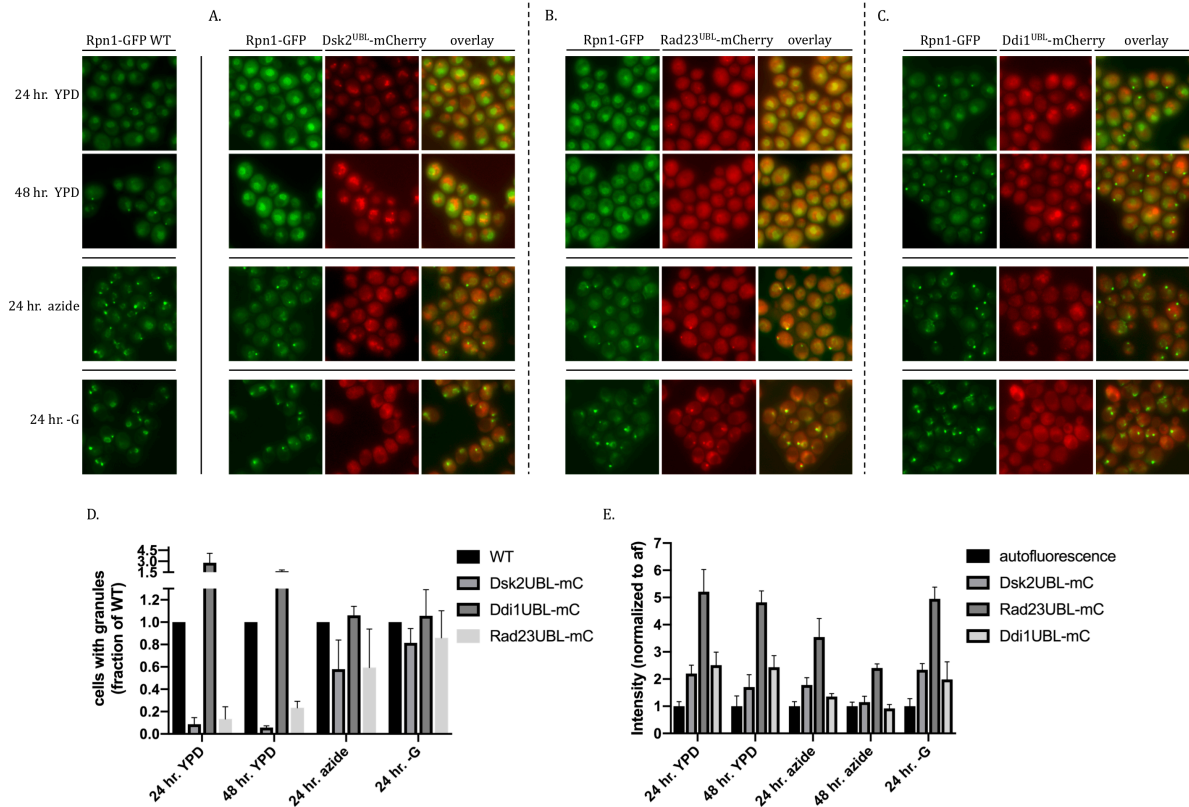


**Figure 2-17. Shuttle factors UBL truncations exhibit similar defects in proteasome granule formation as deletions.**

Localization of proteasomes and UBL-only shuttle factor truncations were visualized in doubly tagged strains using fluorescence microscopy under indicated conditions. (A + B + C) Truncated Rad23<sup>UBL</sup> and Dsk2<sup>UBL</sup> caused defects in proteasome granule formation after growth in YPD and exposure to azide while a Ddi1<sup>UBL</sup> truncation promotes earlier granule formation in YPD. (D) Fraction of cells with proteasome granules in UBL-only truncation strains were quantified and normalized to WT. (E) Average cellular mCherry signal in truncation strains was quantified and normalized to autofluorescence (af). With the exception of 48 hr. azide, all strains produced signal significantly higher than autofluorescence under all tested conditions ( $p < 0.05$ ).

Within our hypothesis, we expected Rad23<sup>UBL</sup> and Dsk2<sup>UBL</sup> truncations to co-localize with proteasomes, but we could not easily assess truncation localization under some conditions due to vacuolar autofluorescence. Because full length tagged shuttle factors exhibit co-localization with proteasomes (Figure 2.12), we speculated UBL-only truncations may exhibit a reduced affinity for proteasomes. Within truncated strains, full length shuttle factors may outcompete UBL-only truncations for proteasomal binding and prevent co-localization. To test this hypothesis, we generated strains with a truncated version of Rad23 or Dsk2 and a deletion of the other. We speculated deletion of *RAD23* in a Dsk2<sup>UBL</sup> strain (and vice versa) would relieve competition for proteasomal binding and potentially allow for visualization of co-localization between UBL-only

truncations and proteasomes. However, compared to respective truncation strains, these double mutants did not exhibit a detectable increase in co-localization between UBLs and proteasomes (Figure 2.18a & b). Additionally, the deletion of either *RAD23* or *DSK2* did not significantly increase the fluorescent signal intensity produced by corresponding UBL-only truncations (Figure 2.18c). Thus, under tested conditions, stability of UBL-only truncations is not likely influenced by competitive binding by other full length shuttle factors. Future experiments include pull downs assays that allow comparison of proteasomal binding between UBL-only truncations and full length shuttle factors. In addition, we also plan to generate GFP-tagged truncations in an  $\alpha 1$ -mCherry strain to more accurately monitor localization via fluorescence microscopy.

In addition to testing for co-localization, we also monitored PSG formation within these strains. The deletion of *DSK2* or *RAD23* in respective truncation strains prevented proteasome granules after growth in YPD or azide treatment (Figure 2.18). This is consistent with our model in which Rad23 and Dsk2 directly transport proteasomes to granules—in *DSK2* $\Delta$ *Rad23*<sup>UBL</sup> or *RAD23* $\Delta$ *DSK2*<sup>UBL</sup> cells, neither protein is a functional transporter and proteasome localization to granules is prevented. Consistent with our knockout data, neither double mutant strain showed a defect in granule formation induced by glucose starvation (Figure 2.18).

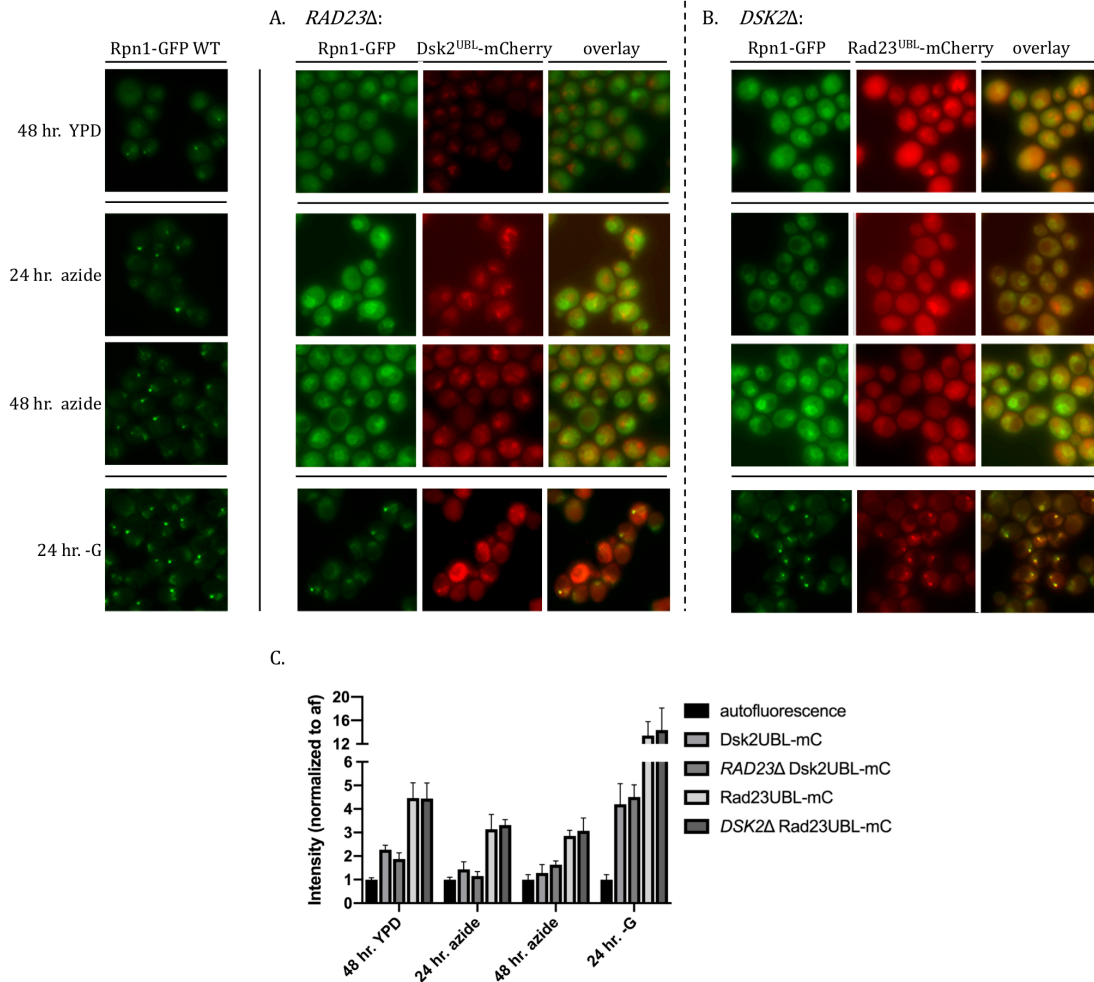


**Figure 2-18. Relief of competitive proteasomal binding does not promote detectable co-localization between UBL truncations and proteasomes.**

Under indicated conditions, localization of proteasomes and UBL-only shuttle factor truncations was visualized in doubly tagged strains using fluorescence microscopy. (A + B) *Rad23<sup>UBL</sup>* and *Dsk2<sup>UBL</sup>* in *DSK2Δ* and *RAD23Δ* cells, respectively, did not exhibit an observable increase in co-localization with proteasomes compared to strains in Figure 2.17a & b. (C) Average cellular mCherry signal in truncation strains was quantified and normalized to autofluorescence (af).

Next, we tested the localization of mCherry-tagged UBL $\Delta$  truncations for defects in proteasome granule formation. Within our model, UBL $\Delta$  truncations are targeted to granules via UBA domains but are unable to interact with proteasomes. Therefore, we expected *Rad23<sup>UBLΔ</sup>* and *Dsk2<sup>UBLΔ</sup>* truncations to localize to granules as well as reduce proteasome localization to granules. Like UBL-only truncations, mCherry-tagged UBL $\Delta$  truncations of each shuttle factor produced signal resembling autofluorescence (data not shown). We compared average cellular signal

intensity produced by UBL $\Delta$  truncations to autofluorescence and found no significant difference (Figure 2.19a). Thus, if these truncations are present, they are undetectable using our experimental parameters. Although we did observe defects in proteasome granule formation in Dsk2<sup>UBL $\Delta$</sup>  and Rad23<sup>UBL $\Delta$</sup>  strains (data not shown), we cannot attribute these defects to shuttle factor mutations because Dsk2<sup>UBL $\Delta$</sup>  and Rad23<sup>UBL $\Delta$</sup>  levels were undetectable.

We hypothesized UBL $\Delta$  truncations may be undetectable because they are proteasomal substrates. To test this hypothesis, we treated UBL $\Delta$  truncation strains with proteasome inhibitor and compared average cellular mCherry signal between treated and untreated cultures. However, proteasome inhibitor had no significant effect on fluorescent signal indicating degradation of Dsk2<sup>UBL $\Delta$</sup>  and Rad23<sup>UBL $\Delta$</sup>  by proteasomes is not responsible for their inability to be detected (Figure 2.19b). Future experiments intend to use full length shuttle factors with “inactive” UBL domains. Mutations at amino acid residues critical for proteasome interaction will be introduced, and strains will be tested for defects in proteasome granule formation using fluorescence microscopy. Results will reveal if interaction between shuttle factor UBL domains and proteasomes is important for observed shuttle factor roles in proteasome granule regulation. In sum, although UBL-only truncations are consistent with our model in which Rad23 and Dsk2 directly transport proteasome to granules, more experiments are necessary to analyze if shuttle factor-proteasome interactions are important for granule formation.

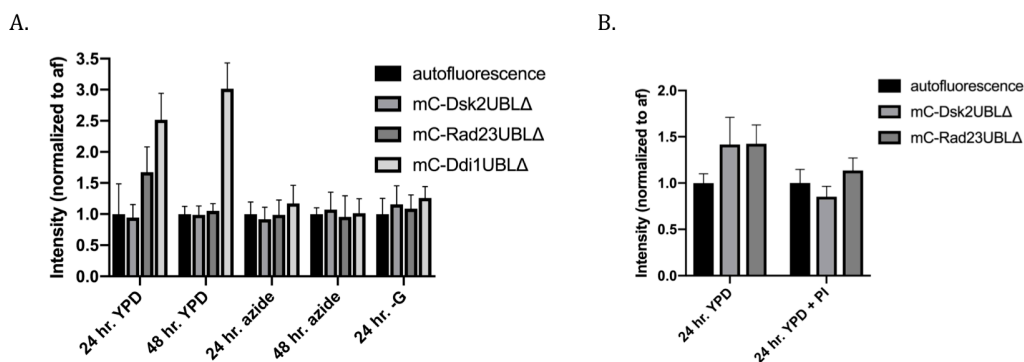


**Figure 2-19.  $\Delta$ UBL shuttle factor truncations are not detectable under experimental parameters.**

(A) In  $\Delta$ UBL truncation strains, average cellular signal intensity was quantified under indicated conditions and normalized to autofluorescence. (B) Cells were grown for 24 hr. in YPD with or without proteasome inhibitor and average cellular signal in  $\Delta$ UBL truncation strains was quantified and normalized to autofluorescence (af). Average

*cellular signal intensity produced by Dsk2<sup>UBLΔ</sup> and Rad23<sup>UBLΔ</sup> was comparable to autofluorescence even after treatment with proteasome inhibitor.*

## Chapter 3 - Discussion

### Results Summary

The ubiquitin proteasome system is crucial for many cellular processes including homeostasis, cell cycle progression, and elimination of harmful protein aggregates. Hence, much research has been devoted over the years to understanding proteasomal degradation. More recently, work from our lab and several others has described proteasome re-localization in response to nutritional changes. The factors and mechanisms involved, however, are not well characterized. Carbon starvation induces proteasome transport from the nucleus to cytoplasmic storage granules (PSGs), while nitrogen starvation causes vacuolar degradation of proteasomes through a specific autophagy pathway (proteaphagy)<sup>15,17</sup>. We hypothesized shuttle factors may be involved in proteasome re-localization events. Shuttle factors deliver substrates to proteasomes through two terminal domains: a N-terminal UBL domain interacts with ubiquitin receptors on the proteasome while a C-terminal UBA domain binds polyubiquitin chains on substrates. Thus, shuttle factors act as adaptor proteins for substrate-proteasome interactions. Evidence suggests proteins related to shuttle factors are important for autophagic processes as well as protein sequestration. For example, mammalian shuttle factor ubiquilin-2 is involved both in autophagy pathways as well as liquid-liquid phase separation which forms droplets reminiscent of PSGs<sup>125,126,136</sup>. Therefore, we hypothesized shuttle factors in yeast are important for proteasome targeting events including proteaphagy and PSG formation.

To test this hypothesis, we monitored the effects of shuttle factor deletions on proteasome localization in yeast using fluorescence microscopy. We found that none of the three yeast shuttle factors—Rad23, Dsk2, or Ddi1—are required for proteasome autophagy in response to nitrogen starvation or proteasome inhibition. However, under certain conditions, Dsk2 and Rad23 are important for proteasome granule formation. Specifically, when carbon is gradually depleted from rich media due to cell proliferation or when cells are treated with mitochondrial inhibitor sodium azide, *DSK2* or *RAD23* knockouts show a defect in proteasome localization to granules. Rad23 and Dsk2 exhibit partial redundancy in granule formation; that is, when both *DSK2* and *RAD23* are deleted, proteasome granules are almost completely prevented. This suggests that Rad23 and Dsk2 do not act in a linear pathway, but rather share a common function in PSG formation.

Surprisingly, neither knockout influences proteasome granules induced by abrupt glucose starvation. Metabolic differences between inducing conditions correlate with Rad23/Dsk2 dependency for granule formation. Specifically, cells grown in YPD or exposed to azide participate in fermentation and require Rad23/Dsk2 for proteasome granules, while cells starved of glucose largely rely on aerobic respiration and do not depend on either protein for PSG formation. Thus, we predict proteasome granules have different properties and require different factors based on metabolic state.

To further distinguish between granules that form under gradual and abrupt carbon starvation, we tested proteasome granule sensitivity to cycloheximide treatment. Cycloheximide blocks protein synthesis and has been shown to prevent the formation of other biological granules including stress granules<sup>147</sup>. To test if proteasome granules require active protein translation, cells were exposed to granule inducing conditions in the presence or absence of cycloheximide. Interestingly, granules that form in response to abrupt glucose starvation are able to form in the presence of cycloheximide. However, Rad23/Dsk2-dependent granules do not form after cycloheximide treatment. Thus, we conclude that abrupt and gradual carbon starvation conditions induce proteasome granules that, at least in part, exhibit different properties. Transferring cells from a fermentable carbon source to glucose starvation media induces dramatic physiological changes including an immediate and significant drop in intracellular ATP, translation inhibition, and a decrease in intracellular pH<sup>149,150</sup>. Thus, one possible explanation for variations among proteasome granule sensitivity to cycloheximide is that granule formation requires a specific factor that is stable under abrupt glucose starvation but must be actively synthesized under mild starvation conditions. There is also evidence that cycloheximide causes a large drop in ubiquitin levels<sup>147</sup>. Ubiquitin is a reported PSG component, so manipulating ubiquitin levels by cycloheximide treatment may also influence proteasome targeting to granules under certain starvation conditions. To establish whether or not proteasome granules induced by different conditions have unique functions, future experiments need to address granule composition, assembly mechanism, and biochemical properties.

To further characterize the role of shuttle factors in proteasome granule dynamics, we generated strains with fluorescent tags on full length shuttles as well as  $\Delta$ UBL and UBL-only truncations. Dsk2 and Rad23 both co-localize with proteasome granules under all inducing conditions. As proteins that both 1) have a role in granule formation and 2) co-localize with

proteasome granules, we conclude Rad23 and Dsk2 are PSG components. In addition, we show, under some conditions, Ddi1 localizes to granules that do not co-localize with proteasomes. Unfortunately, due to low signal intensity, the localization of shuttle factor truncations was difficult to interpret. However, we were able to show that UBL-only truncations of Rad23 and Dsk2 exhibit similar defects in granule formation as Rad23 and Dsk2 knockouts. Therefore, the C-terminal portions of Rad23 and Dsk2 are important for their functions in proteasome targeting to granules.

Unlike Rad23 and Dsk2, we show *DDI1* deletion actually promotes proteasome granule formation. Specifically, after growth in rich media, a *DDI1Δ* knockout strain exhibits a higher fraction of cells with granular localization of proteasomes (Figures 2.3 & 2.8). The increase in proteasome granules was observed when *DDI1* was deleted as well as when *DDI1* was truncated to contain only the UBL domain. The UBL-only Ddi1 truncation is capable of occupying proteasomal ubiquitin receptors so it is unlikely that competitive binding is the primary mechanism of Ddi1-mediated granule inhibition. These results also indicate Ddi1 inhibits granular localization via a mechanism which requires the C-terminal portion of the protein. Additionally, logarithmically growing *DDI1Δ* cells display granular localization of proteasomes (Figures 2.3, 2.5, 2.6, 2.8 & 3.4). However, these early granules do not resemble canonical PSGs—they are much smaller and more abundant. Like Rad23/Dsk2-dependent PSGs, early granules observed in *DDI1Δ* cells are sensitive to cycloheximide and do not co-localize with stress granules or P bodies (data not shown). The mechanism of proteasome granule inhibition by Ddi1 is still unclear.

Here, we offer three models for signaling events involved in Rad23/Dsk2-dependent proteasome granule formation. In addition, we expand on the distinguishing properties of Ddi1 as a noncanonical shuttle factor as well as present preliminary data expanding on its role as a granule inhibitor.

## **Potential Models**

### **Delivery model**

Within one model, proteasomes are directly transported to granules by shuttle factors, namely, Dsk2 and Rad23. Specifically, the N-terminal UBL domain interacts with proteasomes, while the C-terminal UBA domain is responsible for granular targeting (Figure 3.1). To test this

hypothesis, we generated strains with fluorescent tags on full length shuttle factors as well as UBL and  $\Delta$ UBL truncations. Although we were able to conclude that Dsk2 and Rad23 do, in fact, co-localize with proteasome granules, we were unable to draw conclusions about truncation localization due to undetectable signal intensity. Thus, our results are consistent with our hypothesis—as direct transporters of proteasomes to granules, we would expect Dsk2 and Rad23 to co-localize with proteasome granules. However, more work is necessary to determine the exact role of Dsk2 and Rad23 in proteasome granule formation. In other words, although we can conclude 1) they are important for granule formation under certain conditions and 2) they co-localize with proteasome granules, we cannot conclude or exclude that the mechanism of PSG assembly involves direct transport of proteasomes by Rad23 or Dsk2.

### **Future experiments**

Within this model, we would expect Rad23/Dsk2-proteasome co-localization throughout the granule assembly process. To test this hypothesis, fluorescent tags on both the proteasome as well as Dsk2/Rad23 (like the strains used in this study) can be used to monitor protein localization. The fluorescence microscopy approach used in this work is limited—variables such as temperature, pH, oxygen availability, etc. cannot be controlled. Actually, under some of the imaging conditions used, a timely measurement is crucial as some granules tend to dissipate within 15 min. Thus, time-lapse imaging with a confocal microscope that allows control of such variables while analyzing a fixed field of cells is needed. With such a set-up, Dsk2/Rad23 and proteasome localization can be monitored over the course of granule induction. Within the model proposed above, we would expect Dsk2 and Rad23 to co-localize with proteasomes as they exit the nucleus, travel through the cytoplasm, and eventually form granules.

In addition to localization experiments, biochemical experiments can also be used to test a direct delivery model. Within a direct delivery model, under granule inducing conditions, Rad23 and Dsk2 switch from polyubiquitinated substrate transporters to proteasome transporters. In logarithmically growing cells, we would expect a large portion of proteasomes to be bound by Rad23, Dsk2, and polyubiquitinated substrates. However, as granule formation is induced, and Rad23 and Dsk2 function as proteasome transporters, we would expect a decrease in polyubiquitin interaction with proteasome-Rad23/Dsk2 complexes. Co-IP experiments can be used to monitor the amount of polyubiquitin as well as Dsk2/Rad23 bound to proteasomes as granules form. Within

the model proposed above, we would expect a decrease in polyubiquitin interaction with proteasomes-Rad23/Dsk2 complexes as cells proliferate and PSG assembly is induced.

A third possible experiment to test direct delivery of proteasomes to granules by Dsk2 and Rad23 involves introduction of nuclear localization sequences (NLSs) on Dsk2 and Rad23. Importin proteins directly bind NLSs and transport proteins from the cytoplasm, through nuclear pore complexes, and into the nucleus<sup>151</sup>. Although Dsk2 and Rad23 exhibit nuclear localization in logarithmically growing cells, it has been reported Rad23 contains no putative NLS sites<sup>152</sup>. Like Rad23, NLS predictive software (final score cutoff = 0.86) revealed Dsk2 also does not contain any NLS sequences<sup>153</sup>. Thus, nuclear targeting of shuttle factors is largely unknown; however, some speculate nuclear localization of Rad23 is mediated by interaction with NLS-containing binding partner, Rad4<sup>152</sup>. We expect addition of integral NLS sequences on Rad23 and Dsk2 to effectively “trap” both proteins in the nucleus. If Rad23 and Dsk2 are involved in proteasome transport to cytoplasmic granules, we predict nuclear retention of both shuttles via introduction of NLS sequences to prevent proteasome re-localization to granules under mild carbon starvation conditions.

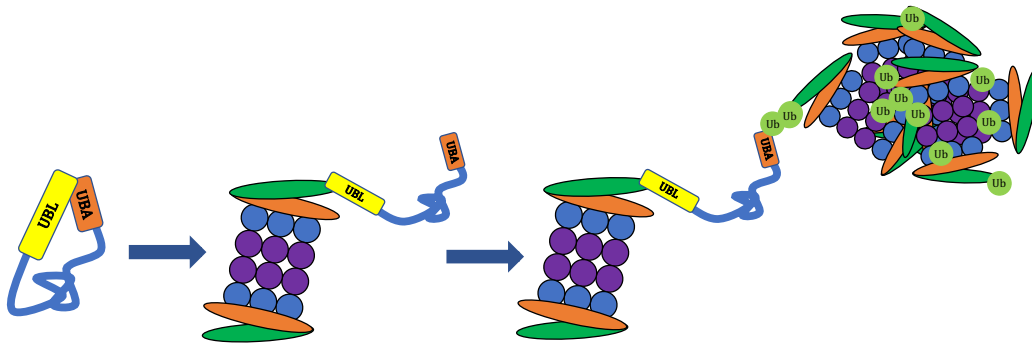


**Figure 3-1. Delivery model.**

*Within this model, proteasomes are directly transported to granules by Dsk2 and Rad23. Specifically, the UBL domains mediate proteasome binding while UBA domains are responsible for granular targeting.*

### **Degradation signal model**

As opposed to directly transporting proteasomes to granules, in a second model, Dsk2 and Rad23 are required for the degradation of a specific substrate or set of substrates that signals granular targeting of proteasomes (Figure 3.2). Within this model, the stability of factor(s) X

influences proteasome localization. Under nutrient rich conditions, factor X is stable, and proteasomes are nuclear. However, as nutrients are depleted, factor X is ubiquitinated, delivered to proteasomes by Dsk2 and Rad23, and degraded. The degradation of factor X acts as a signal for proteasome re-localization from the nucleus to cytoplasmic granules. Thus, the deletion of Rad23/Dsk2 would stabilize factor X and proteasomes would remain nuclear even after granule induction. Within this model, single knockouts show a delay in granule formation because factor X degradation is not completely abrogated; however, in a double knockout, factor X is even more stable, and therefore, granules are almost completely prevented. Factor X could serve as a proteasomal nuclear retention factor or an inhibitor of nuclear export—upon degradation, proteasomes are prone to nuclear-to-cytoplasmic targeting. Although some substrates of Dsk2 and Rad23 have been identified, a comprehensive list of specific substrates for each shuttle factor has yet to be reported.

### **Future experiments**

Within this model, factor X is delivered to proteasomes by Rad23 and/or Dsk2. Therefore, one way to narrow the list of potential factor X candidates is to identify Rad23/Dsk2 specific substrates. Mayor et al. used LTQ linear ion trap mass spectrometry to generate a list of UPS substrates<sup>154</sup>. In short, ubiquitinated protein profiles in proteasome-inhibitor treated cells were compared to non-treated cells, and proteins that accumulated in the presence of inhibitor were defined as UPS substrates. Using the same technique, the authors tested for protein accumulation in a RPN10 knockout strain. Rpn10 is a proteasomal subunit that binds polyubiquitinated substrates. Thus, ubiquitinated proteins that accumulate in a *RPN10Δ* strain were defined as Rpn10-specific substrates<sup>154</sup>. Using *RAD23Δ*, *DSK2Δ*, and *RAD23ΔDSK2Δ* strains, the same approach can be used to identify Rad23 and Dsk2-specific substrates.

Once Rad23 and Dsk2 specific substrates are identified, factors X candidates can be tested for involvement in proteasome granule formation using knockout and overexpressing strains. Within these strains, a fluorescent tag on the proteasome can be used to monitor proteasome localization and granule formation. In the proposed model, we expect overexpression of factor X, similar to a Dsk2/Rad23 knockout, to prevent proteasome re-localization to granules after prolonged growth and azide treatment. Factor X deletion, on the other hand, would cause proteasome granule formation even in the absence of inducing conditions.

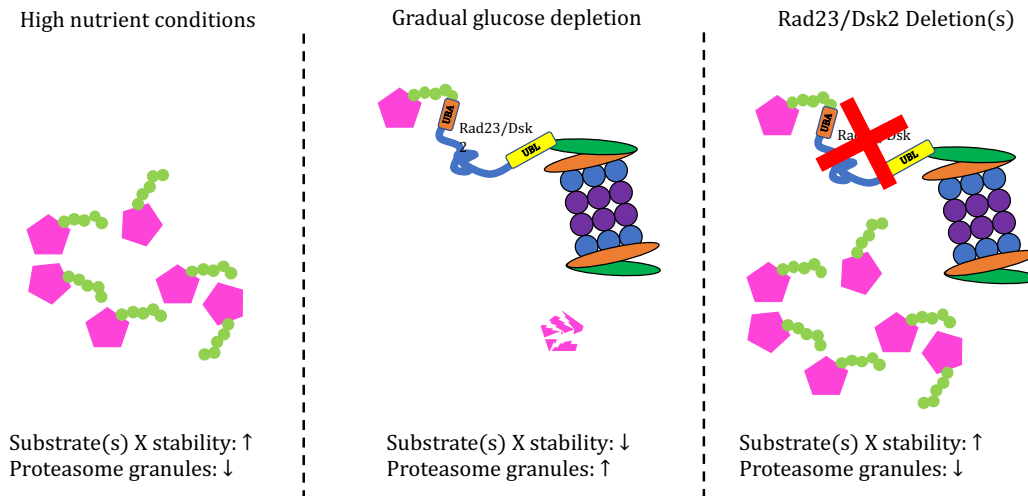


**Figure 3-2. Degradation signal model.**

*Within this model, proteasome localization is mediated by stability of a specific substrate (or set of substrates). Stabilization of such a substrate would be sensitive to changes in carbon availability: high nutrient conditions would stabilize the unidentified substrate (denoted X) causing nuclear retention of proteasomes. The degradation of substrate X upon glucose depletion, conversely, would signal proteasome granule formation. Within this model, substrate X is a Rad23/Dsk2 specific substrate; deletion of these proteins causes a defect in proteasome localization to granules via substrate X stabilization.*

### Ubiquitin pool model

In a third potential model, a shift in the ratio of free ubiquitin to polyubiquitin signals proteasome re-localization from the nucleus to cytoplasmic granules (Figure 3.3). When cells are growing logarithmically, there is a large turnover of nuclear proteins and a high demand for proteasomal degradation. Consequently, ubiquitin molecules mainly exist as polyubiquitin chains bound to substrates. We speculate that over time, as nutrients are depleted, cellular processes slow, the demand for proteasomal degradation decreases, and the ratio of free ubiquitin to polyubiquitin increases. A decrease in polyubiquitinated substrates as cells proliferate is shown in Figure 2.4a. We predict that shuttle factors, under this condition, as opposed to binding polyubiquitinated substrates, bind free ubiquitin via the UBA domain and this association is important for proteasome granules. In other words, shuttle factors act as ubiquitin pool sensors that mediate proteasome localization. When shuttle factors deliver polyubiquitinated substrates, proteasomes remain nuclear. However, when shuttle factors link proteasomes to free ubiquitin, proteasomes are targeted to granules.

Some evidence suggests Dsk2 is sensitive to changing ubiquitin pools. Specifically, 1) the UBA domain of Dsk2 does not exhibit preferential binding to specific ubiquitin linkages and 2) polyubiquitination of Dsk2 promotes substrate delivery to proteasomes<sup>65,76</sup>. Together, these data suggest a model in which Dsk2 shuttling capacity is sensitive to ubiquitin levels—when polyubiquitin is abundant, Dsk2 is ubiquitinated and delivers proteasomal substrates; however, when polyubiquitin is low, Dsk2 associates with other ubiquitin species. Within the proposed model, Dsk2 association with free ubiquitin promotes PSG formation. Consistently, using mass spectrometry, Enenkel et al. found free ubiquitin as opposed to polyubiquitin as a major PSG component<sup>16</sup>. Within the same work, deletion of *UBP6*, a deubiquitinating enzyme, was shown to prevent granule formation. Deletion of a DUB like Ubp6 causes inefficient disassembly of polyubiquitin chains and thus influences the ratio of ubiquitin pools. Additionally, cycloheximide treatment both decreases free ubiquitin levels as well as prevents granules under mild starvation conditions<sup>147</sup>.

The data presented in this work shows that, in the absence of functional Rad23 or Dsk2, cells are defective in proteasome granule formation. Within our ubiquitin pool model, Rad23/Dsk2 deletion(s) prevent the clearance of polyubiquitinated substrates and, thus, prevent the increase in free ubiquitin level required for granule targeting of proteasomes. Additionally, this work also describes a role for Ddi1 as a proteasome granule inhibitor. Within this model, Ddi1 could inhibit proteasome granule formation by sequestration of free ubiquitin; unlike other shuttle proteins, both UBL and UBA domains of Ddi1 bind ubiquitin<sup>55,155</sup>.

The ubiquitin Western blot in Figure 2.4a shows a similar level of polyubiquitinated material in Rad23 and Dsk2 mutants which contradicts this model; however, the blot does not show free ubiquitin levels and thus, we cannot draw conclusions about the ratio of polyubiquitin to free ubiquitin over time. Additionally, the ratio shift may occur specifically in the nucleus and, thus, be undetectable by Western blot. In fact, a nuclear specific change in ubiquitin populations may be required for nuclear export of proteasomes, a precursor of granular localization.

### **Future experiments**

To test for a correlation between changing ubiquitin pools and granule formation, free ubiquitin and conjugated ubiquitin can be monitored under granule inducing conditions using a ubiquitin Western blot. If a correlation is observed, then free ubiquitin level can be directly

manipulated by overexpressing a non-conjugatable form of ubiquitin. Deletion of two C-terminal glycines on ubiquitin prevents its conjugation to substrates as well as other ubiquitin molecules but does not influence the binding surface required for interaction with ubiquitin receptors<sup>156,157</sup>. Thus, overexpression of ubiquitin $\Delta$ GG would increase the pool of free ubiquitin in the cell without interfering with Rad23/Dsk2-ubiquitin interactions. Within this strain, proteasome granule formation can be visualized using fluorescence microscopy. Within the model hypothesized above, we would expect overexpression of non-conjugatable ubiquitin to increase the free ubiquitin pool, increase monoubiquitin bound to Rad23 and Dsk2 UBA domains, and induce proteasome granule formation in the absence of starvation conditions.

In an inverse experiment, deletion of the *UBI4* gene which encodes four ubiquitin molecules would decrease ubiquitin levels. Thus, we would expect a *UBI4* deletion to prevent proteasome re-localization to granules after prolonged growth or azide treatment. Enenkel et al. found *UBI4* deletion does, in fact, reduce proteasome localization to granules after cells are grown to quiescence<sup>16</sup>. However, quiescence induces large-scale changes in cellular processes: metabolic rate decreases, autophagy is upregulated, and transcription and translation rates decrease several-fold, which can all affect ubiquitin pools as well as proteasome localization<sup>158–160</sup>. Therefore, to test the proposed model, future experiments need to analyze *UBI4* $\Delta$  cells under pre-quiescent conditions as well as confirm a change in free ubiquitin level.

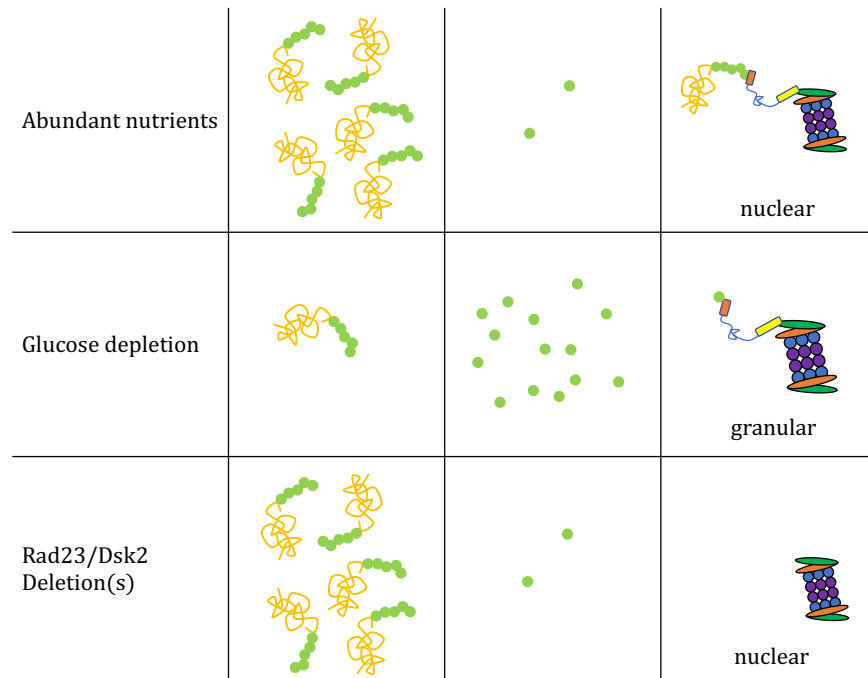


**Figure 3-3. Ubiquitin pool model.**

Within this model, proteasome localization to granules is facilitated by an increase in the ratio of free ubiquitin to conjugated ubiquitin. This table shows schematic representations of predicted ubiquitin ratios and resulting complexes under different conditions. Within this model, *RAD23* and *DSK2* deletion(s) cause a defect in proteasome granule formation due to impaired clearance of polyubiquitinated substrates.

### **Ddi1: a nonconical shuttle factor**

Consistent with previous reports, this work distinguishes Ddi1 from Dsk2 and Rad23. Structurally, Ddi1 is different from other shuttles: 1) it has a distinct and conserved RVP domain, 2) dimerization occurs via RVP domains as opposed to UBA domains, 3) Ddi1 UBL binds ubiquitin, and 4) the UBA domain is not conserved in mammalian homologs<sup>55,82,161</sup>. Functionally, Ddi1 has been shown to serve a proteolytic role like Rad23 and Dsk2; however, it is also involved in unique cellular processes like exocytosis and anterograde protein sorting where its function does not depend on delivery of proteasomal substrates<sup>82,100,109</sup>.

Here, we distinguish Ddi1 from other shuttle factors for its impact on proteasome localization in rich media. Specifically, while *RAD23* and *DSK2* deletions prevent PSG formation, the deletion of *DDI1* actually promotes granular localization of proteasomes (Figure 2.3). Additionally, *DDI1Δ* cells exhibit proteasome granules even in the absence of starvation (i.e. log phase) (Figures 2.3, 2.5, 2.6, 2.8 & 3.4). Thus, Ddi1 inhibits proteasome granules when glucose is abundant. We

hypothesized Ddi1 may inhibit granule formation by competing with Rad23 and Dsk2, factors important for proteasome re-localization to granules, for proteasome binding. However, UBL-only truncated Ddi1, a proteasomal interactor, had the same effect on granules as a *DDI1* deletion (Figure 2.17c). Thus, Ddi1 inhibits granular localization of proteasomes through an unidentified mechanism. One possible explanation is that Ddi1 protease activity is important for granule inhibition—both a *DDI1* knockout as well as UBL-only truncation lack the conserved RVP domain. However, to date, no substrates for Ddi1 protease activity have been identified<sup>155</sup>.

In a separate project, the map kinase, Mpk1, was found to be important for proteasome granule formation upon carbon starvation after cells are grown in a non-fermentable carbon source. Specifically, deletion of *MPK1* prevents proteasome localization to granules when cells are grown in YPR (Raffinose) and either transferred to carbon starvation media or allowed to grow for 48 hr. (Figure 3.4). Interestingly, in preliminary experiments, *DDI1* deletion rescued the granule defect observed in *MPK1*Δ cells (Figure 3.5). We predict Ddi1 and Mpk1 exert opposite effects on the stability of a protein that is important for proteasome granule signaling. A strong candidate is Sic1, a cyclin-dependent kinase inhibitor important for cell cycle progression from G1 phase to S phase. Turnover of both Sic1 and Ufo1, a Ddi1-specific substrate, require ubiquitination by a specific E3 ligase complex<sup>95</sup>. Deletion of *DDI1* stabilizes Ufo1, which increases competition for the E3 ligase, and indirectly, stabilizes Sic1<sup>95</sup>. Mpk1, on the other hand, directly phosphorylates Sic1, which acts as a stabilizing signal<sup>162</sup>. In brief, Ddi1 and Mpk1 have opposing roles in Sic1 turnover. In an *MPK1* knockout, Sic1 loses stability and, under specific conditions, proteasome granules do not form. Deletion of *DDI1* in an *MPK1*Δ strain presumably re-stabilizes Sic1 and rescues granule formation. To test if there is a correlation between Sic1 stability and proteasome localization, future experiments will analyze the effect of *SIC1* deletion on proteasome granules. Within our model, we expect *SIC1* deletion to prevent proteasome re-localization to granules under the same conditions as observed *MPK1*Δ defects.

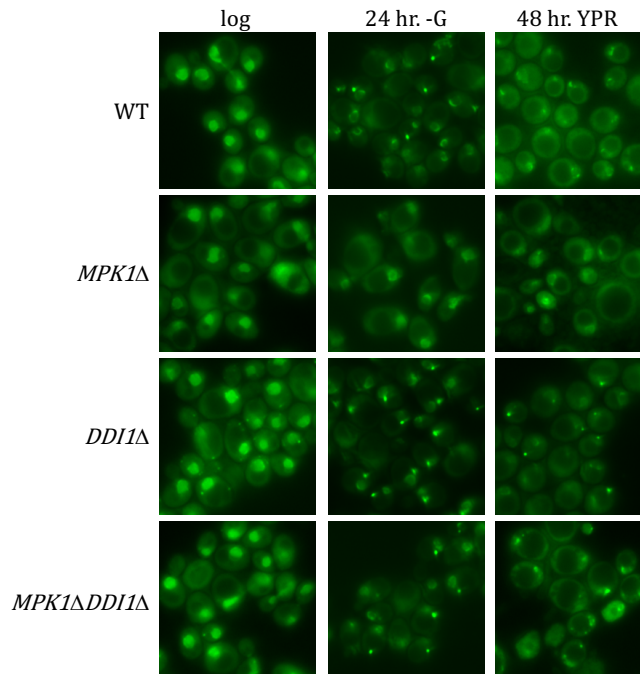


**Figure 3-4. Deletion of *DDI1* rescues defects in proteasome granule formation in *MPK1Δ* cells.**

*Indicated Rpn1-GFP strains were grown in YPR and either transferred to SD -G media or allowed to continue growing. Proteasome localization was visualized in live cells using fluorescence microscopy at indicated time points. In MPK1Δ cells, proteasome granules were largely reduced under both conditions compared to WT. However, in MPK1Δ DDI1Δ cells, granule formation was similar to WT. Thus, deletion of DDI1 rescues the defect in proteasome granule formation caused by MPK1 deletion.*

Consistent with this work, the rescued proteasome granule formation upon *DDI1* deletion in these experiments indicates a role for Ddi1 in proteasome granule inhibition. However, it is unclear whether or not the proteasome granules observed in these preliminary experiments are the same as the Dsk2/Rad23-dependent granules. As opposed to experiments addressing Dsk2 and Rad23 which used YPD, the preliminary experiments presented here used media with raffinose, a non-fermentable carbon source. When cells are grown in a fermentable carbon source before starvation, *MPK1Δ* cells exhibit efficient granular targeting of proteasomes. Thus, availability of specific carbon sources (fermentable vs. non-fermentable) influences which factors are important for proteasome granules to form. Consequently, carbon source specificity and Mpk1 requirement offer two additional properties to distinguish among proteasome granules in addition to the properties identified in this study (Rad23/Dsk2 dependence, cycloheximide sensitivity, and rate of carbon depletion). In sum, preliminary experiments further characterize Ddi1 as a proteasome granule

inhibitor and suggest a model in which granule inhibition may involve Ddi1-mediated turnover of a specific factor.

## References

1. Glick, D., Barth, S. & Macleod, K. F. Autophagy: Cellular and molecular mechanisms. *Journal of Pathology* (2010). doi:10.1002/path.2697
2. Finley, D., Ulrich, H. D., Sommer, T. & Kaiser, P. The ubiquitin-proteasome system of *Saccharomyces cerevisiae*. *Genetics* (2012). doi:10.1534/genetics.112.140467
3. Metzger, M. B., Hristova, V. A. & Weissman, A. M. HECT and RING finger families of E3 ubiquitin ligases at a glance. *J. Cell Sci.* (2012). doi:10.1242/jcs.091777
4. Hanna, J., Guerra-Moreno, A., Ang, J. & Micoogullari, Y. Protein Degradation and the Pathologic Basis of Disease. *American Journal of Pathology* (2019). doi:10.1016/j.ajpath.2018.09.004
5. Gorman, A. M. Neuronal cell death in neurodegenerative diseases: Recurring themes around protein handling: Apoptosis Review Series. *J. Cell. Mol. Med.* (2008). doi:10.1111/j.1582-4934.2008.00402.x
6. Luan, B. *et al.* Structure of an endogenous yeast 26S proteasome reveals two major conformational states. *Proc. Natl. Acad. Sci.* (2016). doi:10.1073/pnas.1601561113
7. Unverdorben, P. *et al.* Deep classification of a large cryo-EM dataset defines the conformational landscape of the 26S proteasome. *Proc. Natl. Acad. Sci.* (2014). doi:10.1073/pnas.1403409111
8. Matyskiela, M. E., Lander, G. C. & Martin, A. Conformational switching of the 26S proteasome enables substrate degradation. *Nat. Struct. Mol. Biol.* (2013). doi:10.1038/nsmb.2616
9. Dong, Y. *et al.* Cryo-EM structures and dynamics of substrate-engaged human 26S proteasome. *Nature* (2019). doi:10.1038/s41586-018-0736-4
10. Enenkel, C., Lehmann, A. & Kloetzel, P. M. Subcellular distribution of proteasomes implicates a major location of protein degradation in the nuclear envelope-ER network in yeast. *EMBO J.* (1998). doi:10.1093/emboj/17.21.6144
11. Matiuhin, Y. *et al.* Extraproteasomal Rpn10 Restricts Access of the Polyubiquitin-Binding Protein Dsk2 to Proteasome. *Mol. Cell* (2008). doi:10.1016/j.molcel.2008.10.011
12. Russell, S. J., Steger, K. A. & Johnston, S. A. Subcellular localization, stoichiometry, and protein levels of 26 S proteasome subunits in yeast. *J. Biol. Chem.* (1999).

- doi:10.1074/jbc.274.31.21943
13. Tanaka, K. The proteasome: overview of structure and functions. *Proc. Jpn. Acad. Ser. B. Phys. Biol. Sci.* (2009).
  14. Pines, J. & Lindon, C. Proteolysis: Anytime, any place, anywhere? *Nat. Cell Biol.* (2005). doi:10.1038/ncb0805-731
  15. Laporte, D., Salin, B., Daignan-Fornier, B. & Sagot, I. Reversible cytoplasmic localization of the proteasome in quiescent yeast cells. *J. Cell Biol.* (2008). doi:10.1083/jcb.200711154
  16. Enenkel, C. *et al.* Ubiquitin orchestrates proteasome dynamics between proliferation and quiescence in yeast. *Mol. Biol. Cell* (2017). doi:10.1091/mbc.e17-03-0162
  17. Hoeller, D. & Dikic, I. How the proteasome is degraded. *Proc. Natl. Acad. Sci.* (2016). doi:10.1073/pnas.1616535113
  18. Marshall, R. S., Li, F., Gemperline, D. C., Book, A. J. & Vierstra, R. D. Autophagic Degradation of the 26S Proteasome Is Mediated by the Dual ATG8/Ubiquitin Receptor RPN10 in Arabidopsis. *Mol. Cell* (2015). doi:10.1016/j.molcel.2015.04.023
  19. Marshall, R. S., McLoughlin, F. & Vierstra, R. D. Autophagic Turnover of Inactive 26S Proteasomes in Yeast Is Directed by the Ubiquitin Receptor Cue5 and the Hsp42 Chaperone. *Cell Rep.* (2016). doi:10.1016/j.celrep.2016.07.015
  20. Cohen-Kaplan, V. *et al.* p62- and ubiquitin-dependent stress-induced autophagy of the mammalian 26S proteasome. *Proc. Natl. Acad. Sci.* (2016). doi:10.1073/pnas.1615455113
  21. Murata, S., Yashiroda, H. & Tanaka, K. Molecular mechanisms of proteasome assembly. *Nature Reviews Molecular Cell Biology* (2009). doi:10.1038/nrm2630
  22. Marques, A. J., Glanemann, C., Ramos, P. C. & Dohmen, R. J. The C-terminal extension of the  $\beta$ 7 subunit and activator complexes stabilize nascent 20 S proteasomes and promote their maturation. *J. Biol. Chem.* (2007). doi:10.1074/jbc.M705836200
  23. Hirano, Y. *et al.* Dissecting  $\beta$ -ring assembly pathway of the mammalian 20S proteasome. *EMBO J.* (2008). doi:10.1038/emboj.2008.148
  24. Lehmann, A., Janek, K., Braun, B., Kloetzel, P. M. & Enenkel, C. 20 S proteasomes are imported as precursor complexes into the nucleus of yeast. *J. Mol. Biol.* (2002). doi:10.1006/jmbi.2002.5443
  25. Wendler, P., Lehmann, A., Janek, K., Baumgart, S. & Enenkel, C. The bipartite nuclear localization sequence of Rpn2 is required for nuclear import of proteasomal base complexes

- via karyopherin  $\alpha\beta$  and proteasome functions. *J. Biol. Chem.* (2004). doi:10.1074/jbc.M403551200
26. Chen, L. *et al.* Sts1 plays a key role in targeting proteasomes to the nucleus. *J. Biol. Chem.* (2011). doi:10.1074/jbc.M110.135863
  27. van Deventer, S., Menendez-Benito, V., van Leeuwen, F. & Neefjes, J. N-terminal acetylation and replicative age affect proteasome localization and cell fitness during aging. *J. Cell Sci.* (2014). doi:10.1242/jcs.157354
  28. Niepel, M. *et al.* The nuclear basket proteins Mlp1p and Mlp2p are part of a dynamic interactome including Esc1p and the proteasome. *Mol. Biol. Cell* (2013). doi:10.1091/mbc.e13-07-0412
  29. Strambio-De-Castillia, C., Niepel, M. & Rout, M. P. The nuclear pore complex: Bridging nuclear transport and gene regulation. *Nature Reviews Molecular Cell Biology* (2010). doi:10.1038/nrm2928
  30. Kimura, A., Kato, Y. & Hirano, H. N-myristoylation of the Rpt2 subunit regulates intracellular localization of the yeast 26s proteasome. *Biochemistry* (2012). doi:10.1021/bi3007862
  31. Hirano, H., Kimura, Y. & Kimura, A. Biological significance of co- and post-translational modifications of the yeast 26S proteasome. *Journal of Proteomics* (2016). doi:10.1016/j.jprot.2015.11.016
  32. Bajorek, M., Finley, D. & Glickman, M. H. Proteasome disassembly and downregulation is correlated with viability during stationary phase. *Curr. Biol.* (2003). doi:10.1016/S0960-9822(03)00417-2
  33. Marshall, R. S. & Vierstra, R. D. Proteasome storage granules protect proteasomes from autophagic degradation upon carbon starvation. *Elife* (2018). doi:10.7554/elife.34532
  34. Peters Lee Zeev, Z., Hazan, R., Breker, M., Schuldiner, M. & Ben-Aroya, S. Formation and dissociation of proteasome storage granules are regulated by cytosolic pH. *J. Cell Biol.* (2013). doi:10.1083/jcb.201211146
  35. Weberruss, M. H. *et al.* Blm10 facilitates nuclear import of proteasome core particles. *EMBO J.* (2013). doi:10.1038/emboj.2013.192
  36. Kaganovich, D., Kopito, R. & Frydman, J. Misfolded proteins partition between two distinct quality control compartments. *Nature* (2008). doi:10.1038/nature07195

37. Kumar, R., Nawroth, P. P. & Tyedmers, J. Prion Aggregates Are Recruited to the Insoluble Protein Deposit (IPOD) via Myosin 2-Based Vesicular Transport. *PLoS Genet.* (2016). doi:10.1371/journal.pgen.1006324
38. Peters, L. Z., Karmon, O., Miodownik, S. & Ben-Aroya, S. Proteasome storage granules are transiently associated with the insoluble protein deposit in *Saccharomyces cerevisiae*. *J. Cell Sci.* (2016). doi:10.1242/jcs.179648
39. Kumar, R., Neuser, N. & Tyedmers, J. Hitchhiking vesicular transport routes to the vacuole: Amyloid recruitment to the Insoluble Protein Deposit (IPOD). *Prion* (2017). doi:10.1080/19336896.2017.1293226
40. Specht, S., Miller, S. B. M., Mogk, A. & Bukau, B. Hsp42 is required for sequestration of protein aggregates into deposition sites in *Saccharomyces cerevisiae*. *J. Cell Biol.* (2011). doi:10.1083/jcb.201106037
41. Buchan, J. R., Muhrad, D. & Parker, R. P bodies promote stress granule assembly in *Saccharomyces cerevisiae*. *J. Cell Biol.* (2008). doi:10.1083/jcb.200807043
42. Brangwynne, C. P. *et al.* Germline P granules are liquid droplets that localize by controlled dissolution/condensation. *Science* (80-. ). (2009). doi:10.1126/science.1172046
43. Wippich, F. *et al.* Dual specificity kinase DYRK3 couples stress granule condensation/dissolution to mTORC1 signaling. *Cell* (2013). doi:10.1016/j.cell.2013.01.033
44. Sheth, U. & Parker, R. Decapping and decay of messenger RNA occur in cytoplasmic processing bodies. *Science* (80-. ). (2003). doi:10.1126/science.1082320
45. Mollet, S. *et al.* Translationally Repressed mRNA Transiently Cycles through Stress Granules during Stress. *Mol. Biol. Cell* (2008). doi:10.1091/mbc.e08-05-0499
46. Narayanaswamy, R. *et al.* Widespread reorganization of metabolic enzymes into reversible assemblies upon nutrient starvation. *Proc. Natl. Acad. Sci.* (2009). doi:10.1073/pnas.0812771106
47. Schaubert, C. *et al.* Rad23 links DNA repair to the ubiquitin/proteasome pathway. *Nature* (1998). doi:10.1038/35661
48. Zhu, Y. & Xiao, W. Two alternative cell cycle checkpoint pathways differentially control DNA damage-dependent induction of MAG1 and DDI1 expression in yeast. *Mol. Genet. Genomics* (2001). doi:10.1007/s004380100538
49. Biggins, S., Ivanovska, I. & Rose, M. D. Yeast ubiquitin-like genes are involved in

- duplication of the microtubule organizing center. *J. Cell Biol.* (1996). doi:10.1083/jcb.133.6.1331
50. Tsuchiya, H. *et al.* In Vivo Ubiquitin Linkage-type Analysis Reveals that the Cdc48-Rad23/Dsk2 Axis Contributes to K48-Linked Chain Specificity of the Proteasome. *Mol. Cell* (2017). doi:10.1016/j.molcel.2017.04.024
  51. Lowe, E. D. *et al.* Structures of the Dsk2 UBL and UBA domains and their complex. *Acta Crystallogr. Sect. D Biol. Crystallogr.* (2006). doi:10.1107/S0907444905037777
  52. Chuang, K.-H., Liang, F., Higgins, R. & Wang, Y. Ubiquilin/Dsk2 promotes inclusion body formation and vacuole (lysosome)-mediated disposal of mutated huntingtin. *Mol. Biol. Cell* (2016). doi:10.1091/mbc.e16-01-0026
  53. Heessen, S., Masucci, M. G. & Dantuma, N. P. The UBA2 domain functions as an intrinsic stabilization signal that protects rad23 from proteasomal degradation. *Mol. Cell* (2005). doi:10.1016/j.molcel.2005.03.015
  54. Ortolan, T. G., Chen, L., Tongaonkar, P. & Madura, K. Rad23 stabilizes Rad4 from degradation by the Ub/proteasome pathway. *Nucleic Acids Res.* (2004). doi:10.1093/nar/gkh987
  55. Nowicka, U. *et al.* DNA-damage-inducible 1 protein (Ddi1) contains an uncharacteristic ubiquitin-like domain that binds ubiquitin. *Structure* (2015). doi:10.1016/j.str.2015.01.010
  56. Sirkis, R., Gerst, J. E. & Fass, D. Ddi1, a Eukaryotic Protein With the Retroviral Protease Fold. *J. Mol. Biol.* (2006). doi:10.1016/j.jmb.2006.08.086
  57. Shi, Y. *et al.* Rpn1 provides adjacent receptor sites for substrate binding and deubiquitination by the proteasome. *Science* (80-. ). (2016). doi:10.1126/science.aad9421
  58. Riedinger, C. *et al.* Structure of Rpn10 and its interactions with polyubiquitin chains and the proteasome subunit Rpn12. *J. Biol. Chem.* (2010). doi:10.1074/jbc.M110.134510
  59. Schreiner, P. *et al.* Ubiquitin docking at the proteasome through a novel pleckstrin-homology domain interaction. *Nature* (2008). doi:10.1038/nature06924
  60. Husnjak, K. *et al.* Proteasome subunit Rpn13 is a novel ubiquitin receptor. *Nature* (2008). doi:10.1038/nature06926
  61. Mueller, T. D. & Feigon, J. Solution structures of UBA domains reveal a conserved hydrophobic surface for protein-protein interactions. *J. Mol. Biol.* (2002). doi:10.1016/S0022-2836(02)00302-9

62. Mueller, T. D., Kamionka, M. & Feigon, J. Specificity of the Interaction between Ubiquitin-associated Domains and Ubiquitin. *J. Biol. Chem.* (2004). doi:10.1074/jbc.M312865200
63. Ohno, A. *et al.* Structure of the UBA domain of Dsk2p in complex with ubiquitin: Molecular determinants for ubiquitin recognition. *Structure* (2005). doi:10.1016/j.str.2005.01.011
64. Ryu, K. S. *et al.* Binding surface mapping of intra- and interdomain interactions among hHR23B, ubiquitin, and polyubiquitin binding site 2 of S5a. *J. Biol. Chem.* (2003). doi:10.1074/jbc.M304628200
65. Raasi, S., Varadan, R., Fushman, D. & Pickart, C. M. Diverse polyubiquitin interaction properties of ubiquitin-associated domains. *Nat. Struct. Mol. Biol.* (2005). doi:10.1038/nsmb962
66. Heinen, C., Ács, K., Hoogstraten, D. & Dantuma, N. P. C-terminal UBA domains protect ubiquitin receptors by preventing initiation of protein degradation. *Nat. Commun.* (2011). doi:10.1038/ncomms1179
67. Elsasser, S. *et al.* Proteasome subunit Rpn1 binds ubiquitin-like protein domains. *Nat. Cell Biol.* (2002). doi:10.1038/ncb845
68. Gomez, T. A., Kolawa, N., Gee, M., Sweredoski, M. J. & Deshaies, R. J. Identification of a functional docking site in the Rpn1 LRR domain for the UBA-UBL domain protein Ddi1. *BMC Biol.* (2011). doi:10.1186/1741-7007-9-33
69. Hiyama, H. *et al.* Interaction of hHR23 with S5a. The ubiquitin-like domain of hHR23 mediates interaction with S5a subunit of 26 S proteasome. *J. Biol. Chem.* (1999). doi:10.1074/jbc.274.39.28019
70. Fu, H. *et al.* Multiubiquitin chain binding and protein degradation are mediated by distinct domains within the 26 S proteasome subunit Mcb1. *J. Biol. Chem.* (1998). doi:10.1074/jbc.273.4.1970
71. Zuin, A. *et al.* Rpn10 monoubiquitination orchestrates the association of the ubiquitin-type DSK2 receptor with the proteasome. *Biochem. J.* (2015). doi:10.1042/bj20150609
72. Chen, X. *et al.* Structures of Rpn1 T1:Rad23 and hRpn13:hPLIC2 Reveal Distinct Binding Mechanisms between Substrate Receptors and Shuttle Factors of the Proteasome. *Structure* (2016). doi:10.1016/j.str.2016.05.018
73. Yu, H., Kago, G., Yellman, C. M. & Matouschek, A. Ubiquitin-like domains can target to the proteasome but proteolysis requires a disordered region. *EMBO J.* (2016).

- doi:10.15252/embj.201593147
74. Rosenzweig, R., Bronner, V., Zhang, D., Fushman, D. & Glickman, M. H. Rpn1 and Rpn2 coordinate ubiquitin processing factors at proteasome. *J. Biol. Chem.* (2012). doi:10.1074/jbc.M111.316323
  75. Liang, R. Y. *et al.* Rad23 interaction with the proteasome is regulated by phosphorylation of its ubiquitin-like (Ubl) domain. *J. Mol. Biol.* (2014). doi:10.1016/j.jmb.2014.10.004
  76. Sekiguchi, T. *et al.* Ubiquitin chains in the Dsk2 UBL domain mediate Dsk2 stability and protein degradation in yeast. *Biochem. Biophys. Res. Commun.* (2011). doi:10.1016/j.bbrc.2011.06.183
  77. Chandra, A., Chen, L., Liang, H. & Madura, K. Proteasome assembly influences interaction with ubiquitinated proteins and shuttle factors. *J. Biol. Chem.* (2010). doi:10.1074/jbc.M109.076786
  78. Kang, Y. *et al.* UBL/UBA ubiquitin receptor proteins bind a common tetraubiquitin chain. *J. Mol. Biol.* (2006). doi:10.1016/j.jmb.2005.12.001
  79. Bertolaet, B. L. *et al.* UBA domains mediate protein-protein interactions between two DNA damage-inducible proteins. *J. Mol. Biol.* (2001). doi:10.1006/jmbi.2001.5105
  80. Sasaki, T., Funakoshi, M., Endicott, J. A. & Kobayashi, H. Budding yeast Dsk2 protein forms a homodimer via its C-terminal UBA domain. *Biochem. Biophys. Res. Commun.* (2005). doi:10.1016/j.bbrc.2005.08.126
  81. Ford, D. L. & Monteiro, M. J. Dimerization of ubiquilin is dependent upon the central region of the protein: evidence that the monomer, but not the dimer, is involved in binding presenilins. *Biochem. J.* (2006). doi:10.1042/bj20060441
  82. Gabriely, G., Kama, R., Gelin-Licht, R. & Gerst, J. E. Different Domains of the UBL-UBA Ubiquitin Receptor, Ddi1/Vsm1, Are Involved in Its Multiple Cellular Roles. *Mol. Biol. Cell* (2008). doi:10.1091/mbc.e07-05-0462
  83. Kang, Y., Zhang, N., Koepp, D. M. & Walters, K. J. Ubiquitin Receptor Proteins hHR23a and hPLIC2 Interact. *J. Mol. Biol.* (2007). doi:10.1016/j.jmb.2006.10.056
  84. Rao, H. & Sastry, A. Recognition of specific ubiquitin conjugates is important for the proteolytic functions of the ubiquitin-associated domain proteins Dsk2 and Rad23. *J. Biol. Chem.* (2002). doi:10.1074/jbc.M200245200
  85. Funakoshi, M., Sasaki, T., Nishimoto, T. & Kobayashi, H. Budding yeast Dsk2p is a

- polyubiquitin-binding protein that can interact with the proteasome. *Proc. Natl. Acad. Sci.* (2002). doi:10.1073/pnas.012585199
86. Chen, L. & Madura, K. Rad23 promotes the targeting of proteolytic substrates to the proteasome. *Mol. Cell. Biol.* (2002).
  87. Kaplun, L. *et al.* The DNA Damage-Inducible UbL-UbA Protein Ddi1 Participates in Mec1-Mediated Degradation of Ho Endonuclease. *Mol. Cell. Biol.* (2005). doi:10.1128/mcb.25.13.5355-5362.2005
  88. Liu, C., van Dyk, D., Li, Y., Andrews, B. & Rao, H. A genome-wide synthetic dosage lethality screen reveals multiple pathways that require the functioning of ubiquitin-binding proteins Rad23 and Dsk2. *BMC Biol.* (2009). doi:10.1186/1741-7007-7-75
  89. Verma, R., Oania, R., Graumann, J. & Deshaies, R. J. Multiubiquitin chain receptors define a layer of substrate selectivity in the ubiquitin-proteasome system. *Cell* (2004). doi:10.1016/j.cell.2004.06.014
  90. Chen, L., Shinde, U., Ortolan, T. G. & Madura, K. Ubiquitin-associated (UBA) domains in Rad23 bind ubiquitin and promote inhibition of multi-ubiquitin chain assembly. *EMBO Rep.* (2001). doi:10.1093/embo-reports/kve203
  91. Hwang, G.-W. Overexpression of Rad23 Confers Resistance to Methylmercury in *Saccharomyces cerevisiae* via Inhibition of the Degradation of Ubiquitinated Proteins. *Mol. Pharmacol.* (2005). doi:10.1124/mol.105.013516
  92. Hartmann-Petersen, R., Hendil, K. B., Gordon, C. & Kutay, U. Ubiquitin binding proteins protect ubiquitin conjugates from disassembly. in *FEBS Letters* (2003). doi:10.1016/S0014-5793(02)03874-7
  93. Kim, I. Multiple Interactions of Rad23 Suggest a Mechanism for Ubiquitylated Substrate Delivery Important in Proteolysis. *Mol. Biol. Cell* (2004). doi:10.1091/mbc.e03-11-0835
  94. Hänzelmann, P., Stingle, J., Hofmann, K., Schindelin, H. & Raasi, S. The yeast E4 ubiquitin ligase Ufd2 interacts with the ubiquitin-like domains of Rad23 and Dsk2 via a novel and distinct ubiquitin-like binding domain. *J. Biol. Chem.* (2010). doi:10.1074/jbc.M110.112532
  95. Ivantsiv, Y., Kaplun, L., Tzirkin-Goldin, R., Shabek, N. & Raveh, D. Unique Role for the UbL-UbA Protein Ddi1 in Turnover of SCFUfo1 Complexes. *Mol. Cell. Biol.* (2006). doi:10.1128/mcb.26.5.1579-1588.2006

96. Voloshin, O., Bakhrat, A., Herrmann, S. & Raveh, D. Transfer of HO endonuclease and Ufo1 to the proteasome by the UbL-UbA shuttle protein, Ddi1, analysed by complex formation in vitro. *PLoS One* (2012). doi:10.1371/journal.pone.0039210
97. Bohm, S., Lamberti, G., Fernandez-Saiz, V., Stapf, C. & Buchberger, A. Cellular Functions of Ufd2 and Ufd3 in Proteasomal Protein Degradation Depend on Cdc48 Binding. *Mol. Cell. Biol.* (2011). doi:10.1128/mcb.00962-10
98. Kim, I. *et al.* The Png1-Rad23 complex regulates glycoprotein turnover. *J. Cell Biol.* (2006). doi:10.1083/jcb.200507149
99. Baek, G. H., Kim, I. & Rao, H. The Cdc48 ATPase modulates the interaction between two proteolytic factors Ufd2 and Rad23. *Proc. Natl. Acad. Sci.* (2011). doi:10.1073/pnas.1104051108
100. Kama, R., Gabriely, G., Kanneganti, V. & Gerst, J. E. Cdc48 and ubiquilins confer selective anterograde protein sorting and entry into the multivesicular body in yeast. *Mol. Biol. Cell* (2018). doi:10.1091/mbc.e17-11-0652
101. Díaz-Martínez, L. A., Kang, Y., Walters, K. J. & Clarke, D. J. Yeast UBL-UBA proteins have partially redundant functions in cell cycle control. *Cell Div.* (2006). doi:10.1186/1747-1028-1-28
102. Clarke, D. J. *et al.* Dosage Suppressors of pds1 Implicate Ubiquitin-Associated Domains in Checkpoint Control. *Mol. Cell. Biol.* (2002). doi:10.1128/mcb.21.6.1997-2007.2001
103. Min, J. H. & Pavletich, N. P. Recognition of DNA damage by the Rad4 nucleotide excision repair protein. *Nature* (2007). doi:10.1038/nature06155
104. Xie, Z., Liu, S., Zhang, Y. & Wang, Z. Roles of Rad23 protein in yeast nucleotide excision repair. *Nucleic Acids Res.* (2004). doi:10.1093/nar/gkh934
105. Zhou, Z. *et al.* UV induced ubiquitination of the yeast Rad4-Rad23 complex promotes survival by regulating cellular dNTP pools. *Nucleic Acids Res.* (2015). doi:10.1093/nar/gkv680
106. Gillette, T. G. *et al.* The 19S complex of the proteasome regulates nucleotide excision repair in yeast. *Genes Dev.* (2001). doi:10.1101/gad.869601
107. Lommel, L. The 26S proteasome negatively regulates the level of overall genomic nucleotide excision repair. *Nucleic Acids Res.* (2002). doi:10.1093/nar/28.24.4839
108. Liu, Y. & Xiao, W. Bidirectional regulation of two DNA-damage-inducible genes, MAG1

- and DDI1, from *Saccharomyces cerevisiae*. *Mol. Microbiol.* (1997). doi:10.1046/j.1365-2958.1997.2701631.x
109. Lustgarten, V. & Gerst, J. E. Yeast VSM1 Encodes a v-SNARE Binding Protein That May Act as a Negative Regulator of Constitutive Exocytosis . *Mol. Cell. Biol.* (2015). doi:10.1128/mcb.19.6.4480
  110. Sugasawa, K. *et al.* Two human homologs of Rad23 are functionally interchangeable in complex formation and stimulation of XPC repair activity. *Mol. Cell. Biol.* (2015). doi:10.1128/mcb.17.12.6924
  111. Boutet, S. C., Disatnik, M. H., Chan, L. S., Iori, K. & Rando, T. A. Regulation of Pax3 by Proteasomal Degradation of Monoubiquitinated Protein in Skeletal Muscle Progenitors. *Cell* (2007). doi:10.1016/j.cell.2007.05.044
  112. Bergink, S. *et al.* Erythropoietic Defect Associated with Reduced Cell Proliferation in Mice Lacking the 26S Proteasome Shuttling Factor Rad23b. *Mol. Cell. Biol.* (2013). doi:10.1128/mcb.05772-11
  113. Ng, J. M. Y. *et al.* Developmental Defects and Male Sterility in Mice Lacking the Ubiquitin-Like DNA Repair Gene mHR23B. *Mol. Cell. Biol.* (2002). doi:10.1128/mcb.22.4.1233-1245.2002
  114. Ng, J. M. Y. *et al.* A novel regulation mechanism of DNA repair by damage-induced and RAD23-dependent stabilization of xeroderma pigmentosum group C protein. *Genes Dev.* (2003). doi:10.1101/gad.260003
  115. Brignone, C., Bradley, K. E., Kisselev, A. F. & Grossman, S. R. A post-ubiquitination role for MDM2 and hHR23A in the p53 degradation pathway. *Oncogene* (2004). doi:10.1038/sj.onc.1207540
  116. Glockzin, S., Ogi, F.-X., Hengstermann, A., Scheffner, M. & Blattner, C. Involvement of the DNA Repair Protein hHR23 in p53 Degradation. *Mol. Cell. Biol.* (2003). doi:10.1128/mcb.23.24.8960-8969.2003
  117. Kaur, M., Pop, M., Shi, D., Brignone, C. & Grossman, S. R. hHR23B is required for genotoxic-specific activation of p53 and apoptosis. *Oncogene* (2007). doi:10.1038/sj.onc.1209865
  118. Bacopulos, S. *et al.* Effects of partner proteins on BCA2 RING ligase activity. *BMC Cancer* (2012). doi:10.1186/1471-2407-12-63

119. Linge, A. *et al.* Identification and functional validation of rad23b as a potential protein in human breast cancer progression. *J. Proteome Res.* (2014). doi:10.1021/pr4012156
120. Chen, L. & Madura, K. Evidence for distinct functions for human DNA repair factors hHR23A and hHR23B. *FEBS Lett.* (2006). doi:10.1016/j.febslet.2006.05.012
121. Blount, J. R. *et al.* Ubiquitin-binding site 2 of ataxin-3 prevents its proteasomal degradation by interacting with Rad23. *Nat. Commun.* (2014). doi:10.1038/ncomms5638
122. Kurlawala, Z. & Beverly, L. Ubiquilin Proteins Are Critical Adaptors that Regulate Proteostasis. *J. Cell Signal.* (2018). doi:10.4172/2576-1471.1000145
123. Wang, H. & Monteiro, M. J. Ubiquilin interacts and enhances the degradation of expanded-polyglutamine proteins. *Biochem. Biophys. Res. Commun.* (2007). doi:10.1016/j.bbrc.2007.06.097
124. Heir, R. *et al.* The UBL domain of PLIC-1 regulates aggresome formation. *EMBO Rep.* (2006). doi:10.1038/sj.embor.7400823
125. Osaka, M., Ito, D., Yagi, T., Nihei, Y. & Suzuki, N. Evidence of a link between ubiquilin 2 and optineurin in amyotrophic lateral sclerosis. *Hum. Mol. Genet.* (2015). doi:10.1093/hmg/ddu575
126. Rothenberg, C. *et al.* Ubiquilin functions in autophagy and is degraded by chaperone-mediated autophagy. *Hum. Mol. Genet.* (2010). doi:10.1093/hmg/ddq231
127. Hjerpe, R. *et al.* UBQLN2 Mediates Autophagy-Independent Protein Aggregate Clearance by the Proteasome. *Cell* (2016). doi:10.1016/j.cell.2016.07.001
128. González-Pérez, P. *et al.* Association of UBQLN1 mutation with Brown-Vialetto-Van Laere syndrome but not typical ALS. *Neurobiol. Dis.* (2012). doi:10.1016/j.nbd.2012.06.018
129. Deng, H. X. *et al.* Mutations in UBQLN2 cause dominant X-linked juvenile and adult-onset ALS and ALS/dementia. *Nature* (2011). doi:10.1038/nature10353
130. Kim, S. H. *et al.* Mutation-dependent aggregation and toxicity in a Drosophila model for UBQLN2-associated ALS. *Hum. Mol. Genet.* (2018). doi:10.1093/hmg/ddx403
131. Sivá, M. *et al.* Human DNA-Damage-Inducible 2 Protein Is Structurally and Functionally Distinct from Its Yeast Ortholog. *Sci. Rep.* (2016). doi:10.1038/srep30443
132. Kottemann, M. C., Conti, B. A., Lach, F. P. & Smogorzewska, A. Removal of RTF2 from Stalled Replisomes Promotes Maintenance of Genome Integrity. *Mol. Cell* (2018).

doi:10.1016/j.molcel.2017.11.035

133. Lehrbach, N. J. & Ruvkun, G. Proteasome dysfunction triggers activation of SKN-1A/Nrf1 by the aspartic protease DDI-1. *Elife* (2016). doi:10.7554/elife.17721
134. Ramirez, J. *et al.* Quantitative proteomics reveals neuronal ubiquitination of Rngo/Ddi1 and several proteasomal subunits by Ube3a, accounting for the complexity of Angelman syndrome. *Hum. Mol. Genet.* (2018). doi:10.1093/hmg/ddy103
135. Myeku, N. & Figueiredo-Pereira, M. E. Dynamics of the degradation of ubiquitinated proteins by proteasomes and autophagy: Association with sequestosome 1/p62. *J. Biol. Chem.* (2011). doi:10.1074/jbc.M110.149252
136. Dao, T. P. *et al.* Ubiquitin Modulates Liquid-Liquid Phase Separation of UBQLN2 via Disruption of Multivalent Interactions. *Mol. Cell* (2018). doi:10.1016/j.molcel.2018.02.004
137. Lee, D. H. Proteasome inhibitors: Valuable new tools for cell biologists. *Trends in Cell Biology* (1998). doi:10.1016/S0962-8924(98)01346-4
138. Saeki, Y., Saitoh, A., Toh-e, A. & Yokosawa, H. Ubiquitin-like proteins and Rpn10 play cooperative roles in ubiquitin-dependent proteolysis. *Biochem. Biophys. Res. Commun.* (2002). doi:10.1016/S0006-291X(02)00340-6
139. Goldstein, A. L. & McCusker, J. H. Three new dominant drug resistance cassettes for gene disruption in *Saccharomyces cerevisiae*. *Yeast* (1999). doi:10.1002/(SICI)1097-0061(199910)15:14<1541::AID-YEA476>3.0.CO;2-K
140. Janke, C. *et al.* A versatile toolbox for PCR-based tagging of yeast genes: New fluorescent proteins, more markers and promoter substitution cassettes. *Yeast* (2004). doi:10.1002/yea.1142
141. Schindelin, J. *et al.* Fiji: an open-source platform for biological-image analysis. *Nat. Methods* (2012). doi:10.1038/nmeth.2019
142. Bankhead, P. Analyzing fluorescence microscopy images with ImageJ. *ImageJ* (2014). doi:10.1109/NER.2015.7146654
143. Kushnirov, V. V. Rapid and reliable protein extraction from yeast. *Yeast* (2000). doi:10.1002/1097-0061(20000630)16:9<857::AID-YEA561>3.0.CO;2-B
144. Winzeler, E. A. *et al.* Functional characterization of the *S. cerevisiae* genome by gene deletion and parallel analysis. *Science* (80-. ). (1999). doi:10.1126/science.285.5429.901
145. N'Diaye, E. N. *et al.* PLIC proteins or ubiquilins regulate autophagy-dependent cell survival

- during nutrient starvation. *EMBO Rep.* (2009). doi:10.1038/embor.2008.238
146. Pack, C. G. *et al.* Quantitative live-cell imaging reveals spatio-temporal dynamics and cytoplasmic assembly of the 26S proteasome. *Nat. Commun.* (2014). doi:10.1038/ncomms4396
  147. Hanna, J., Leggett, D. S. & Finley, D. Ubiquitin Depletion as a Key Mediator of Toxicity by Translational Inhibitors. *Mol. Cell. Biol.* (2003). doi:10.1128/mcb.23.24.9251-9261.2003
  148. Huh, W. K. *et al.* Global analysis of protein localization in budding yeast. *Nature* (2003). doi:10.1038/nature02026
  149. Ashe, M. P., De Long, S. K. & Sachs, A. B. Glucose Depletion Rapidly Inhibits Translation Initiation in Yeast. *Mol. Biol. Cell* (2013). doi:10.1091/mbc.11.3.833
  150. Orij, R., Postmus, J., Beek, A. Ter, Brul, S. & Smits, G. J. In vivo measurement of cytosolic and mitochondrial pH using a pH-sensitive GFP derivative in *Saccharomyces cerevisiae* reveals a relation between intracellular pH and growth. *Microbiology* (2009). doi:10.1099/mic.0.022038-0
  151. Cautain, B., Hill, R., De Pedro, N. & Link, W. Components and regulation of nuclear transport processes. *FEBS Journal* (2015). doi:10.1111/febs.13163
  152. Boulikas, T. Nuclear import of DNA repair proteins. *Anticancer Res.* (1997).
  153. Lin, J. rong & Hu, J. SeqNLS: nuclear localization signal prediction based on frequent pattern mining and linear motif scoring. *PLoS One* (2013). doi:10.1371/journal.pone.0076864
  154. Mayor, T., Graumann, J., Bryan, J., MacCoss, M. J. & Deshaies, R. J. Quantitative Profiling of Ubiquitylated Proteins Reveals Proteasome Substrates and the Substrate Repertoire Influenced by the Rpn10 Receptor Pathway. *Mol. Cell. Proteomics* (2007). doi:10.1074/mcp.m700264-mcp200
  155. Trempe, J. F. *et al.* Structural studies of the yeast DNA damage-inducible protein Ddi1 reveal domain architecture of this eukaryotic protein family. *Sci. Rep.* (2016). doi:10.1038/srep33671
  156. Shabek, N., Herman-Bachinsky, Y. & Ciechanover, A. Ubiquitin degradation with its substrate, or as a monomer in a ubiquitination-independent mode, provides clues to proteasome regulation. *Proc. Natl. Acad. Sci.* (2009). doi:10.1073/pnas.0905746106

157. Aida, K., Hayashi, H., Inamura, K., Mizuno, T. & Sugiyama, Y. Differential Roles of Ubiquitination in the Degradation Mechanism of Cell Surface-Resident Bile Salt Export Pump and Multidrug Resistance-Associated Protein 2. *Mol. Pharmacol.* (2014). doi:10.1124/mol.113.091090
158. Pi~non, R. Folded chromosomes in non-cycling yeast cells: Evidence for a characteristic g0 form. *Chromosoma* (1978). doi:10.1007/BF02569039
159. Fuge, E. K., Braun, E. L. & Werner-Washburne, M. Protein synthesis in long-term stationary-phase cultures of *Saccharomyces cerevisiae*. *J. Bacteriol.* (1994). doi:10.1128/jb.176.18.5802-5813.1994
160. Choder, M. A general topoisomerase I-dependent transcriptional repression in the stationary phase in yeast. *Genes Dev.* (1991). doi:10.1101/gad.5.12a.2315
161. Generation and initial analysis of more than 15,000 full-length human and mouse cDNA sequences. *Proc. Natl. Acad. Sci.* (2002). doi:10.1073/pnas.242603899
162. Moreno-Torres, M., Jaquenoud, M., Péli-Gulli, M. P., Nicastro, R. & De Virgilio, C. TORC1 coordinates the conversion of Sic1 from a target to an inhibitor of cyclin-CDK-Cks1. *Cell Discov.* (2017). doi:10.1038/celldisc.2017.12